# A NEW NANONETWORK ARCHITECTURE USING FLAGELLATED BACTERIA AND CATALYTIC NANOMOTORS

**Maria Gregori Casas**

Advisor: Ian F. Akyildiz

Georgia Institute of Technology
Universitat Politècnica de Catalunya

July 29, 2009

To my parents, Pere and Anna, for
their love and support.

# Abstract

Molecular communication has been recently proposed for interconnected nano-scale devices as an alternative to classical communication paradigms such as electro-magnetic waves, acoustic or optical communication. In this novel approach, the information is encoded as molecules that are transported between devices using different distance based communication techniques. For short distances (nm-mm ranges) there exist *molecular motors and calcium signaling techniques* to realize the communication between the nano-devices. For long distances (mm-m ranges), pheromones are used to transport information.

In this work, the medium range is explored to cover distances from μm to mm and a molecular network architecture is proposed to realize the communication between nano-machines that can be deployed over different (short, medium and long) distances. In addition, two new communication techniques, *flagellated bacteria and catalytic nanomotors,* are introduced to cover the medium range. Both techniques are based on the transport of DNA encoded information between emitter and receiver by means of a physical carrier. A physical channel model in terms of propagation delay and packet loss probability has been developed for both techniques. Flagellated bacterium has been modeled as a two state automaton. This automaton is extended and used as the basis for the design of a novel nano-machine that is able to transport information among the nano-scale devices. Finally, a qualitative comparison of flagellated bacteria and catalytic nanomotors is carried out and some future research topics are pointed out.

# Acknowledgements

I would like to deeply thank the people who, during the several months in which this endeavor lasted, provided me with useful and helpful assistance. First of all, I would like to thank professor Ian F. Akyildiz for the opportunity he has given to me when, almost one year ago, he accepted my application to develop my master thesis under his supervision, and also for the endless number of advises, not only regarding this work but also regarding how to affront and deal with professional life.

I would also like to thank the ETSETB faculty and staff that work day after day to offer this possibility to students. I would specially like to thank Professors Josep Solé Pareta and Eduard Alarcón for their support.

This experience would not have been possible without the financial support of "Fundación Vodafone España" and "Obra Social Bancaja". I greatly appreciate their support.

I would also like to thank all the people in the BWN lab from who I have learned something new every day. Especially, I would like to thank the nano-people: Lluís Parcerisa Giné, Josep Miquel Jornet Montaña and Massimiliano Pierobon. I also thank Dario Pompili, Berk Canberk and Xavier Gelabert for their helpful remarks and feedback on this work. I also thank Kaushik Roy Chowdhury and Won Yeol Lee for their endless help in the lab.

I greatly appreciate the biology lessons of Laia Simó Riudalbas who helped me a great deal to understand the biological concepts required for this work.

Last but not least, I will be eternally thankful to my family because without their support, love and help, none of this would have been possible.

# Table of Contents

# List of Figures

# List of Tables

# Chapter 1

# Introduction

During the last century, the ICT community has discovered, proposed and developed many technological capabilities, from the telephone towards the internet passing through several inventions such as the radio, the television, the PC and mobile phones. An analysis of these technological achievements over several years shows an exponential growth rather than the expected linear behavior. This trend is commonly known as Moore's law, which states that the number of transistors on an integrated circuit increases exponentially, doubling every 24 months. Moore observed this exponential trend in 1965 and it has continued over half a century, indeed, it is not expected to stop almost for another decade. Actually, Moore's law of integrated circuits is not the first paradigm to show an exponential behavior but the fifth (after mechanical calculating devices, Turing's relay, vacuum tube computers, and the transistor-based machines). Ray Kurzweil's abstraction of Moore's law shows that the exponential trend, in terms of calculation per second per $1000, has been satisfied over 100 years (Figure 1.1) [28].

In the last decades, in order to keep increasing the number of computations per second with the same cost, the procedure has been to increase the number of transistors per integrated circuit, which is achieved by reducing the size of transistors. However, this procedure seems to be approaching some fundamental physical limits. First, the increase of the number of transistors per integrated circuit leads to a dramatic increase in the chip temperature. Second, the size of the gate is approaching the size of atoms. In 2000, Intel started to produce high volume transistors with lengths less than 100nm. Finally, the cost of the semiconductor fabrication plants increases with the transistor reduction.

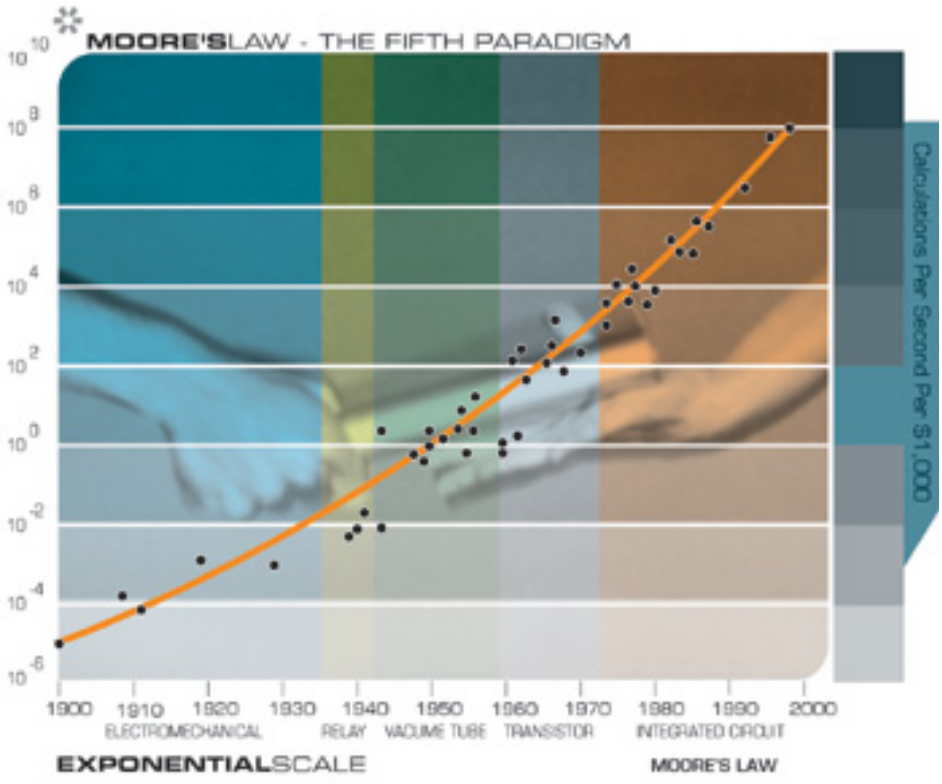


Figure 1.1: Generalization of Moore's law by Ray Kurzweil (From [28]).

In this context, several approaches have been proposed for the development of future computers. Nanotechnology is present in all of them and seems to be the basis to develop the sixth computation paradigm. Molecular electronics (also called a moletronics) is one of the nano-scale alternatives to CMOS transistors. Molecular electronics research is conducted by interdisciplinary teams that aim to use organic molecules, carbon nanotubes, biomolecules, or semiconductor nanowires in order to improve the capabilities of bulk silicon and produce effective electronic components. Molecular electronics is expected to produce circuitry a millions time denser than current microcomputers [29]. Leonard Adleman proposed DNA computing as an alternative to silicon in 1994 [1]. After that, some advances lead to the demonstration of constructible Turing machines [12]. Other alternatives have been already proposed such as the use of DNA as scaffolds in order to create Carbon Nanotube structures [22].

Eventually, nanotechnology science will enable powerful computers but also simple devices ranging some nanometers, nano-machines.

In this work, we are concerned with the interconnection and networking of these molecular level machines. In the following sections of this chapter, some formal definitions of nanotechnology, nano-machines (and the different approaches proposed to build them), NanoNetworking and the current state-of-the-art of molecular communication is explained and discussed. Finally, an overview of the entire thesis is given in Section 1.5.

## 1.1 Nanotechnology

Nanotechnology is a new multidisciplinary field based on knowledge of diverse scientific areas such as chemistry, physics, molecular biology, material science, computer science, and engineering. Nanotechnology focuses in technological developments on the nanometer scale, usually on the order of 0.1 to 100 nm. At this scale, the bulk approximations of Newtonian physics are not anymore valid, leading to quantum physics. Because of this, particles present different chemical and physical properties that can be engineered in order to develop structures and devices with powerful properties and capabilities. An example of the Nanotechnology's potential is metamaterials, which are engineered nano-structures able to produce negative index of refraction of electromagnetic waves. For instance, an invisible cloak is built in the microwave range for a two dimensional object in [46].

Scientists all over the world are starting to break the barriers among different disciplines and work together in order to allow novel materials, structures and devices. This synergy will enable a great number of improvements and socio-economic growth in the following decades.

Nanotechnology promises new solutions for applications in a broad variety of fields:

- **Medicine:** Nanotechnology enables the possibility to integrate nanomaterials with biological elements due to these nano-scale materials are in the same length scale than cellular inner structures and organelles. This provides a way to develop more powerful diagnosis devices, contrast agents, sensors, analytical tools, physical therapy applications, and drug delivery vehicles.

- **Information and Communication:** Nanotechnology will allow the improvement of the capacity of current memory storage devices, an increase of the computing capacity, and the creation of novel semiconductor and optoelectronic devices.
- **Energy:** There are also several research groups that are doing projects about energy storage, conversion, saving and the creation of enhanced renewable energy sources.
- **Industry & Consumer goods:** Nanotechnology is also bound to revolutionize different fields of the industry and consumer goods, such as the textile, automotive, aerospace and cosmetic industries.

## 1.2 Nano-machines

At nano-scale, a nano-machine can be considered as the most basic functional unit which is able to perform very simple tasks [48]. In general terms, we define a nano-machine as ‘‘a device, consisting of nano-scale components, able to perform a specific task at nano-level, such as communicating, computing, data storing, sensing and/or actuation” [4]. There are three different approaches for the development of nano-machines, namely, the Top-Down, the Bottom-up and the Bio-hybrid approaches, as shown in Figure 1.2.

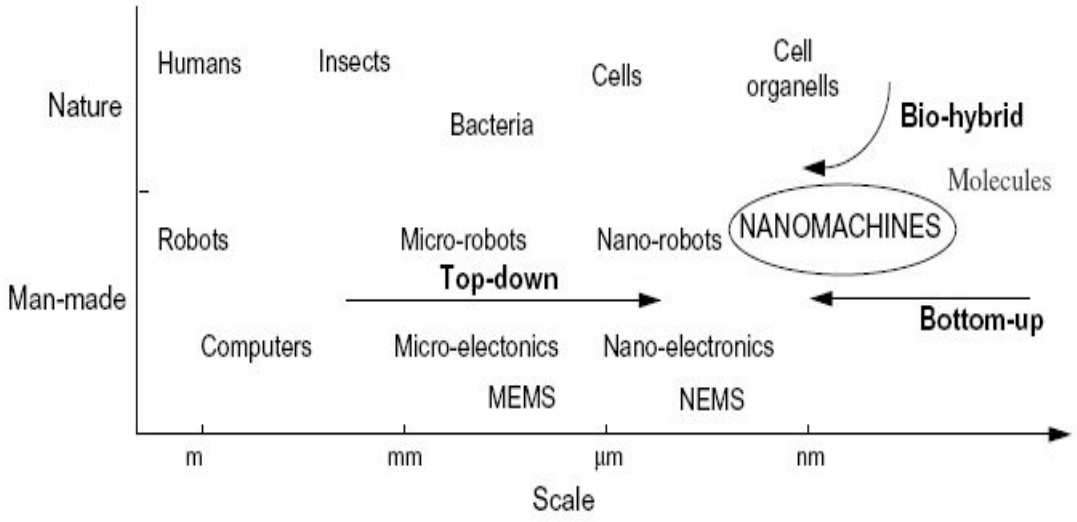


Figure 1.2: Approaches for the development of nano-machines (From [4])

## A. Top-Down Approach

In the top-down approach, nano-machines are developed by means of downscaling current microelectronic and micro-electro-mechanical devices to nano-level [20,33]. To achieve this goal, advanced manufacturing techniques, such as electron beam lithography and micro-contact printing are used. Resulting devices keep the architecture of pre-existing micro-scale components such as microelectronic devices and micro-electro-mechanical systems (MEMS). Nano-machines, such as nano-electromechanical systems (NEMS) components, are being developed using this approach [14]. However, the fabrication and assembly of these nano-machines are still at an early stage. So far, only simple mechanical structures, such as nano-gears, can be created following this approach.

## B. Bottom-Up Approach

In the bottom-up approach, nano-machines are developed using individual molecules as the building blocks [17]. Recently, many nano-machines, such as molecular differential gears and pumps, have been theoretically designed using a discrete number of molecules. Manufacturing technologies able to assemble nano-machines molecule by molecule do not exist, but once they do, nano-machines could be efficiently created by the precise and controlled arrangement of molecules. This process is called molecular manufacturing. Molecular manufacturing could be developed from current technologies in couple decades if adequate resources are invested.

## C. Bio-Inspired Approach

Nature provides a wide library of examples of nano-machines, i.e., molecular motors or cell receptors. Notice that a cell, though having micro-scale, presents a potential number of desired characteristics of future nanomachines [4]. Cells are *self-contained* due to the set of instructions that they must carry out is completely specified in the DNA contained in its nucleus (or nucleoid if we are talking about a prokaryotic cell). *Self-replication,* the ability to create new cells or machines autonomously with the same set of instructions or genome, is another of the important features of cells. Self-assembly is defined as the process in which several disordered elements form an organized structure without external intervention, as a result of local interactions between them [4]. Cells are also *self-assembled* because from one single cell, a stem cell, the human body is able to produce all the different cells required for living by means of differentiation. Some

cells, i.e., Escherichia coli (E. coli), also have different organelles such as flagellum or cilia that give them *locomotion* ability. Finally, cells are able to communicate, for instant by means of calcium signaling, and interact among each other in order to synchronize, collaborate and carry out complex tasks.

Taking into account the potentials of the already existing structures, the Bio-inspired approach focuses in the use of these biological components as building blocks to develop more complex nano-machines. Some research groups also try to re-engineer the information systems in biology in order to obtain potent features [43].

Currently, complex nano-machines cannot be built following the Top-Down approach. However, the design and development of nano-devices following the bio-inspired and bottom-up approach offers promising solutions in the near term.

## 1.3 NanoNetworking

As stated before, nano-machines are defined as small devices only able to develop simple tasks. Nanonetworks, the interconnection of different nano-machines, will expand the capabilities of single nano-machines by providing them a way to cooperate and share information. In a similar way that happens with cells, the collaboration among nano-machines will allow the fulfillment of more complex tasks.

The communication between nano-machines can be realized through nano-mechanical, acoustic, electromagnetic, chemical or molecular communication [19]. The main drawback of nano-mechanical communication is that emitter and receiver must be in direct contact. As far as acoustic and electromagnetic waves are concerned, the main inconvenience is that the acoustic transducers and radiofrequency transceivers may not be integrated at the nano-scale, due to nano-machines may not have enough power to send a signal from the nano-scale to the macro-scale. In our opinion [4], the most promising approach for nano-networking is *molecular communication* mainly because of two reasons. The first reason is the disadvantages of the above mentioned schemes. Whereas the second reason is the fact that in a near term nano-machines will be developed by following the Bio-inspired approach which will allow the use of cell receptors in a similar way that are used by cells in order to communicate among them by using molecules.

## 1.4 Molecular Communication for Nanonetworks

Molecular communication is based on the use of molecules to encode the desired information and transmit it by mimicking biological systems found in nature. Hence, molecular communication seems to be a good direction to interconnect nano-devices developed following the Bio-inspired approach. As it happens in nature, molecular communication should be tackled in different ways depending on the distance between emitters and receivers. Thus, two different approaches have been already established in [4], i.e., short-range (nm-mm) and long-range (mm-m) molecular communication, which are explained in Sections 1.4.1 and 1.4.2, respectively. For the short-range, two techniques, namely, molecular signaling and molecular motors have been proposed. Regarding the long-range, pheromones will carry out the communication among nano-machines, as shown in Figure 1.3.

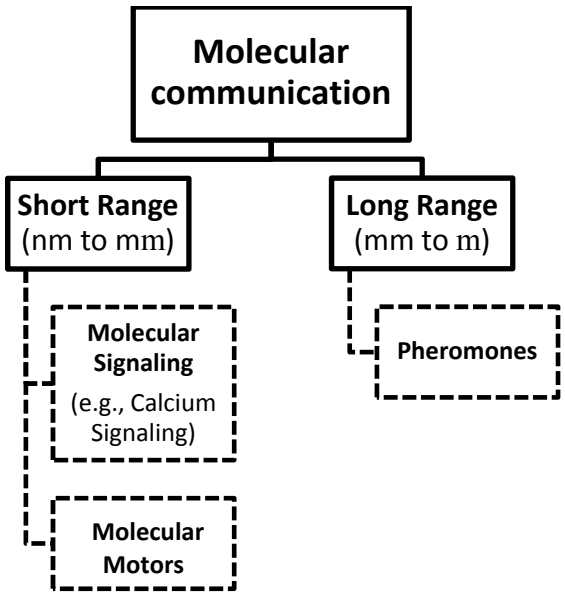


Figure 1.3: State-of-the-art of molecular communication techniques

### 1.4.1 Short-Range Molecular Communication

The term *short-range molecular communication* is used to refer to the communication techniques, such as molecular motors and molecular signaling, i.e., calcium signaling, that allow communication between nano-machines in short distances, which are ranging from 1nm to 1 mm.

## A. Molecular Motors

*Molecular motors,* e.g., kinesin, dynein and myosin, are proteins or protein complexes that are able to transform chemical energy into mechanical work in the molecular scale [33]. These motors move directionally along cytoskeletal tracks, e.g., microtubules, and also are able to transport a molecule, a macromolecule or a set of them embedded in a vesicle or container [34,49]. For instance, Kinesin motors can transport cargoes towards the plus end of microtubules, while Dynein motors move towards minus end. Hence, in this case, the information is encoded within a molecule or a macromolecule that will be literally transported usually following pre-set pathways.

## B. Molecular Signaling

*Molecular signaling* is based on transmitting the information by varying a given concentration of molecules (signals) according to the message that needs to be propagated. Drawing an analogy with the classical wireless communication scheme, the molecule concentration level is considered as the carrier. This carrier may be modulated in frequency (by changing the rate of molecules concentration) or in amplitude (by changing the number of molecules per unit volume). A natural example of this type of short-range molecular communication is the calcium signaling among cells [35]. This communication takes place in different ways depending on whether the cells are in direct contact or not.

On the one hand, when cells are not in direct contact, the $Ca^{2+}$ ions travel through the medium following Brownian diffusion laws. Calcium ions can go inside the cell's cytoplasm through gated ion channels. This produces a change in the transmembrane electrical potential of the cell which triggers a cascade of chemical reaction.

On the other hand, when cells are in direct contact, they can also communicate through gap junctions. Gap junctions are inter-cellular channels that connect the cytoplasm of adjacent cells and allow the exchange of small molecules (e.g., inorganic ions,$IP_3$, cyclic AMP or GMP)[21]. When the emitter cell is stimulated, the concentration of $Ca^{2+}$ in its cytoplasm increases, enabling inositol 1,4,5-triphospate ($IP_3$), a secondary messenger, to travel through the gap junction and leading to the release of $Ca^{2+}$ ions from the Endoplasmatic Retiliculum (ER) of the adjacent cells. This increase on the $Ca^{2+}$ ions in adjacent cells will produce the propagation of $IP_3$ through its

neighbor cells, and the $Ca^{2+}$ release from their ER and so forth. In this way, the calcium message is amplified in each cell and it is broadcasted through the medium. The calcium signal can also be directed if a network is formed by cells that express gap junctions with different permeability [35].

### 1.4.2 Long-Range Molecular Communication

Concerning the long-range molecular communication, pheromones can be considered as encoded molecular messages that are released into the medium, such as air or water. As seen in the nature, pheromones emitted by a member of a certain species can only be detected by other members of the same species [53]. Similarly, pheromones transmitted by a particular type of nano-machine may only be detected by other nano-machines equipped with the corresponding decoder [4].

## 1.5 Motivation and Overview of This Work

The short-range techniques, already proposed in the literature, were meant to cover distances up to mm. However, after analyzing in more detail both techniques, molecular motors and molecular signaling, we discovered that are inefficient for distances longer than a few μm:

- Molecular motors turn out to be an inefficient way to transport information in the entire short-range, because of several reasons, especially when distances become larger than a few micrometers. First, the velocity of molecular motors moving along cytoskeletal tracks is in the order of 500 nm per second [49]. Second, they tend to detach of the microtubule and diffuse away when they have moved distances in the order of 1 μm [42]. Moreover, since molecular motors move along cytoskeletal tracks, the development of a proper network infrastructure of microtubules is required. These microtubules will act as unidirectional wires for the communication process between nano-machines because each type of molecular motors can only go to one end of the microtubule. When bidirectional communication is required, there are two possible options, either to increase the complexity of the network topology by having two microtubules in each point-to-point link, or to wait until the communication in the other direction ends. Both of these approaches would cause severe delays in the transmission and would degrade the network capacity.

- As far as molecular signaling is concerned, several issues regarding network capacity and the maximum communication range have to be addressed. However, so far it is known that the time required for a particle to diffuse a certain distance increases with the square of the distance [39]. Hence, a degradation of the channel capacity is expected with distance increase.

The inefficiency of the short-range techniques that had been already proposed in the literature, more precisely for distances longer than a few μm, supposes a bottleneck on the capabilities of the future NanoNetworks. This problem is analyzed and solved in this thesis by defining the medium-range (μm-mm) and the discovery of two novel communication techniques, *Flagellated Bacteria* and *Catalytic Nanomotors*, to carry out the transport of information in this range. The information is encoded in DNA sequences, which we call DNA packet, and carried by the medium-range techniques to the proper receiver.

A network architecture for molecular communication is developed in order to allow the interconnection and networking of nano-machines deployed over different distances. This architecture is presented in Chapter 2 and uses different techniques to interconnect nano-machines.

The novel communication techniques proposed in this thesis for the medium range (from μm to mm), *Flagellated Bacteria* and *Catalytic Nanomotors* are presented in Chapters 3 and 4, respectively. In Chapters 5 and 6 a physical channel model in terms of propagation delay and packet loss probability is derived for flagellated bacteria and catalytic nanomotors. In Chapter 7, an automaton model of a communication nano-machine is presented. This nano-machine is based on the behavior of a flagellated bacterium. Then, a qualitative comparison of the proposed medium range techniques is given in Chapter 8. Finally, the work is concluded in Chapter 9.

# Chapter 2

# NanoNetwork Architecture for Molecular Communication

Since the existing short-range molecular communication methods do not seem to be effective for distances longer than a few μm, we define the medium-range that encloses distances from μm to mm, and the two new communication mechanisms for this range, i.e., *flagellated bacteria and catalytic nanomotor*. Hence, Figure 2.1 shows the general scheme of the different molecular communication techniques. It is similar to Figure 1.3 but now it includes the medium-range communication techniques proposed in this work.

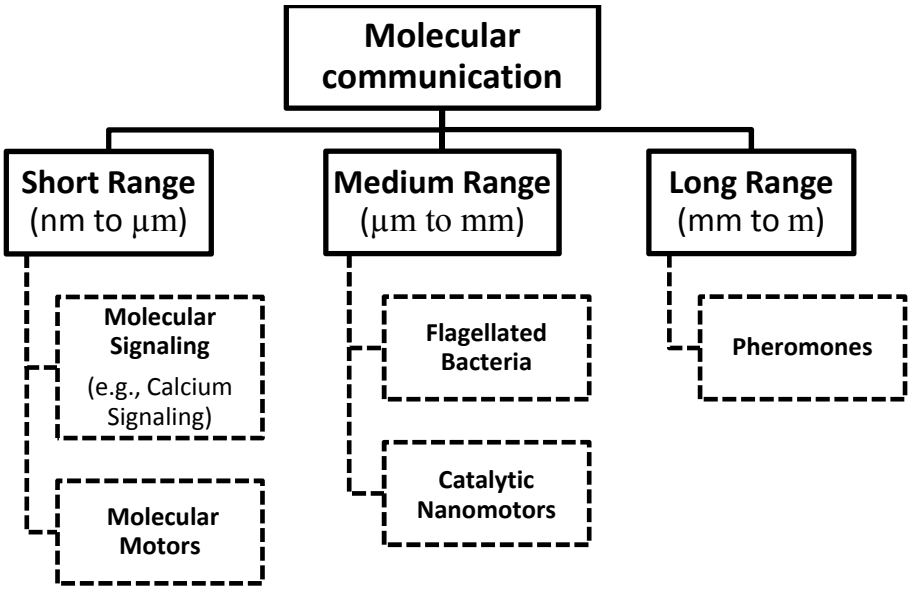


Figure 2.1: Distance-dependent techniques for molecular communication

Nano-machines may only be able to send messages using short-range methods mainly because of, as stated in Section 1.2, nano-machines are tiny and simple devices that will not be able to carry out complex tasks. Moreover, flagellated bacteria and catalytic nanomotors are around 2 μm long. Hence, the medium-range techniques will not be able to reach nano-machines that measure a few nm.

However, nano-machines should be able to communicate with other nano-machines independently of the distance that separates them. For this reason, a network architecture for molecular communication is required and presented in this chapter.

## 2.1 NanoNetwork Architecture

The proposed architecture is shown in Figure 2.2. All nano-machines are represented as dark dots and are connected with a point-to-point link to its specific gateway (gateways are also nano-devices), which are represented as squares. In this point-to-point link, the communication is done by means of short-range techniques. Hence, taking into account the techniques already proposed, this link can be either wired, when molecular motors are used, or wireless, when the communication is realized by means of molecular signaling.

Gateways (G1, G2, G3 and G4) are not only able to switch from short-range mechanisms to medium or long-range techniques, but also to multiplex information of different nano-machines that have the same destination gateway. The address of each gateway is specified by a unique chemical compound, which the gateway is constantly releasing to the medium. Interconnection of gateways is realized by means of medium-range techniques, which are able to follow positive gradients of a given attractant particle. Once the information is in the gateway, this will identify which is the receiver's gateway. If the destination nano-machine is connected to itself (for instance communication between nano-machines A and B in Figure 2.2), the gateway will relay the DNA packet using the point-to-point link to the receiver nano-machine. Otherwise, the gateway will multiplex the information and will send it, by means of medium range communication techniques, to the receiver's gateway, for example communication between nano-machines C and D.

Finally, in the receiver's gateway, the DNA packet is demultiplexed and the different messages are routed to the proper receiver nano-machines by means of short-range techniques.

Moreover, there exist gateways that are able to transmit and receive information using long-range techniques, e.g., gateways G2 and G4 in Figure 2.2. Hence, the communication between nano-machines D and E can be performed as follows. First, D transmits the packet to its gateway (G3) using short-range techniques. Second, the gateway relays the information to the nearest node that is able to carry out the transduction to long-range communication techniques (G2). Finally, the molecular packet is sent by using long-range communication techniques to the receiver's gateway (G4) that will relay the information to the proper receiver nano-machine (E).

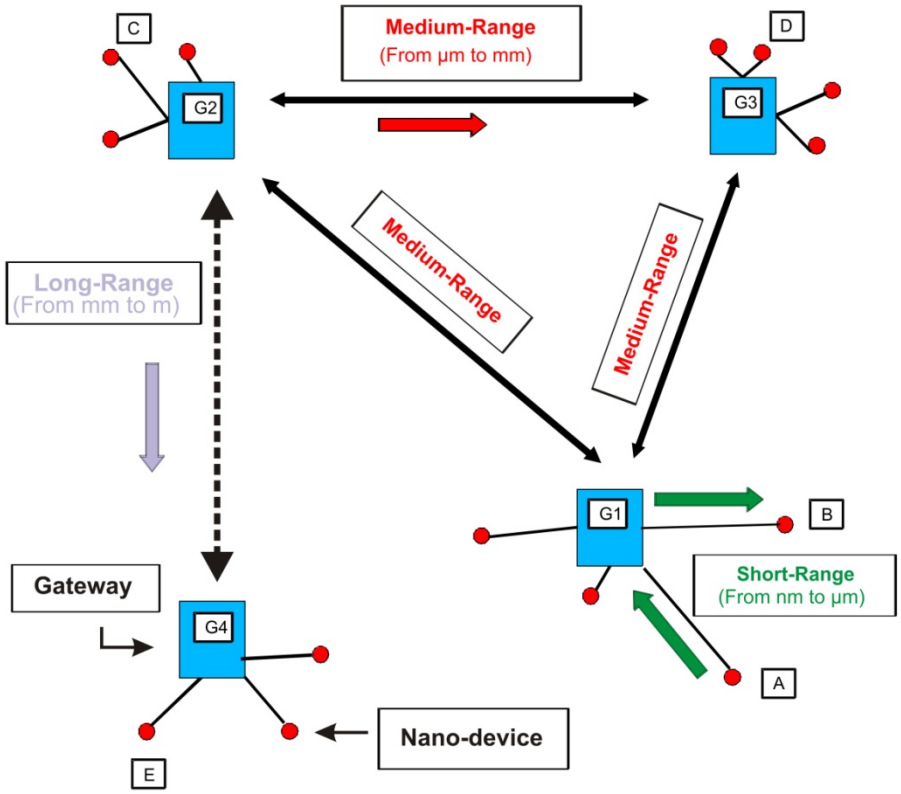


Figure 2.2: Molecular network architecture.

Gateways are the key elements of the proposed architecture. So far the creation of such nodes is not feasible, however researchers around the world are working on the design and development of DNA nano-machines [5] and DNA computers [32]. Hence, we assume that progress in these research areas will allow the creation of such nodes. In the next two chapters, we define the two

medium-range communication techniques, *flagellated bacteria* and *catalytic nanomotors* that will allow the interconnection of gateways.

# Chapter 3

# Medium-Range Molecular Communication based on Flagellated Bacteria

Bacteria have spent several billion years developing skills and efficient machinery, as cilia and flagellum that allow them to convert chemical energy into motion. For instance, *Escherichia coli* (*E. coli*), which is shown in Figure 3.1, has between 4 and 10 flagella, which are moved by rotary motors, placed at the cell membrane, fuelled by chemical compounds. *E. coli* also has several *pili* distributed around its outer membrane that give the bacterium the ability to cohere other cells in order to exchange genetic material, this is done following a cellular process called *bacterial conjugation.*

Among all possible flagellated bacteria we will focus on *E. coli* because it is the most studied prokaryotic cell, and his complete genome sequence is well known [10]. *E. coli* is approximately 2 μm long and 1 μm in diameter and it is usually an inoffensive bacterium that lives in the human intestinal tract. Its nucleoid[1] contains only one circular DNA molecule and in its cytoplasm there are some smaller DNA sequences arranged in a circular way, these DNA circles are called *plasmids* [36]. *Plasmids* can give the bacteria resistance to some antibiotics in the environment, but they are also used in genetics engineering in order to conduct genetic manipulation experiments [26].

[1] The nucleoid is a region within the prokaryote cells where the genetic material of the cell is localized without a nuclear membrane

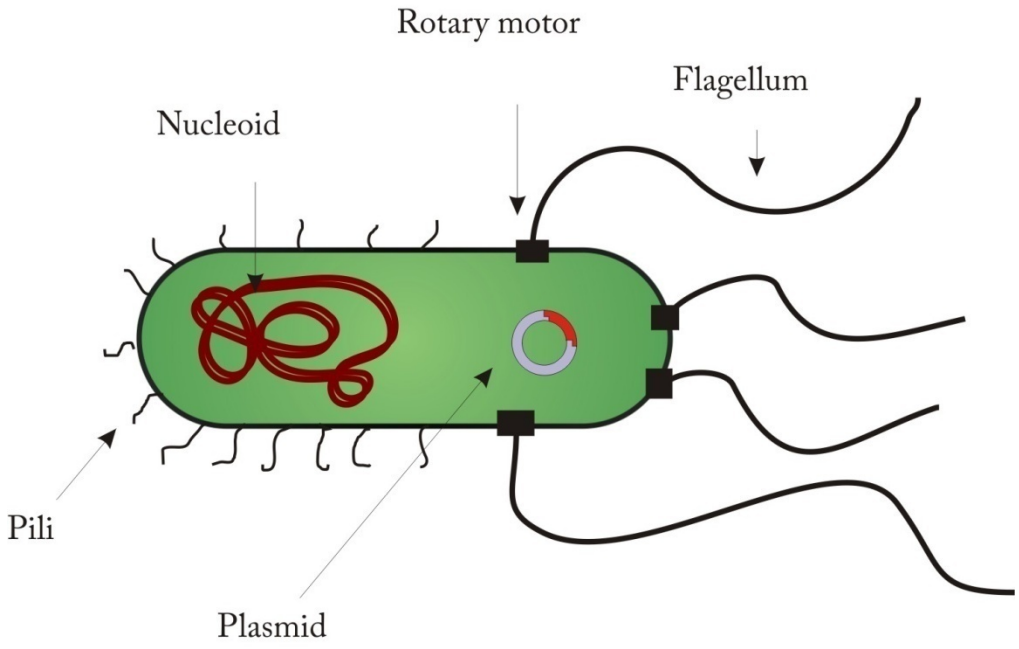


Figure 3.1: Flagellated Bacteria

In this work, we propose to use flagellated bacteria [18], i.e., *E. coli*, to carry DNA messages to the proper receivers. First, a specific mutant of the bacteria that only responds to a specific set of attractants is chosen [23]. Second, the DNA message is introduced inside the bacterium cytoplasm. Then, the bacterium is released to the environment and it will follow his natural instincts and will propel itself to the proper receiver, which is continuously releasing attractant particles to the environment. The next section explains how the communication process is accomplished. Whereas, in Section 3.2 some open issues and research challenges are pointed out.

## 3.1 Communication Process

In this section, we qualitatively explain how the exchange of information between to nodes of the network is done. As shown in Figure 3.2, the communication process is enclosed in the following five steps: Encoding, transmission, propagation, reception and decoding.


Figure 3.2: Communication Process

### 3.1.1 Encoding

Instead of working with the common binary alphabet as all computers, nano-machines will be able to work with a quaternary alphabet composed by the DNA nucleotides *Adenine, Thymine, cytosine* and *Guanine* (A, T, C and G) [32]. Thus, the information that the emitter nano-machine wants to send is expressed as a set of DNA base pairs, i.e., the *DNA packet*.

The encoding is the process by which the *DNA packet* is inserted inside bacteria's cytoplasm[2]. The introduction of DNA inside the bacteria is done by means of different genetic engineering procedures, as *plasmids*, *bacteriophages* or *Bacterial Artificial Chromosomes* (BACs). All of these techniques are well-known and widely used in fields like biology or pharmacy. These techniques consist in:

- *Plasmids* are circular sequences of DNA [31], with length between 5.000 and 400.000 base pairs. Plasmids can be inserted inside bacterial cells by transformation or electroporation [36]. Two types of enzymes[3] are required for encoding the *DNA packet* inside the plasmid, restriction endonucleases and DNA ligase. *Restriction endonucleases* are enzymes that cleave DNA in specific DNA sequences called *restriction sites*[4], whereas, the *DNA ligase* is able to link DNA strands that have single strand breaks.

  Therefore, the encoding of the DNA packet in the plasmid will follow three steps, which are shown in Figure 3.3. First, the plasmid is cleaved in the restriction sites by restriction endonucleases. Second, the *DNA packet* containing the desired information is added and

[2] The cytoplasm is the inner part of the cell which is enclosed within the cell membrane. It is composed by a viscous substance called cytosol and contains various organelles.
[3] Enzymes are biomolecules able to catalyze chemical reactions.
[4] Restrictions sites are specific sequences of nucleotides that are recognized by restriction endonucleases, which will cut the DNA sequence between two nucleotides within its restriction site.

linked to the plasmid by means of the *DNA ligase.* Finally, the plasmid is inserted inside bacteria's cytoplasm using *transformation* or *electroporation* techniques.

- *Bacteriophages* are a type of viruses, which are much smaller than bacteria (Bacteriophages range between the 20 and 200 nm while *E. coli* bacteria are a few μm long), and are able to infect bacteria with its genetic material. For instance, Bacteriophage λ vectors have been developed and can be easily cleaved into three pieces, using *restriction endonucleases.* Two of the pieces contain the essential genes of the phage, but the other one is called "filler", and can be discarded and replaced with the target DNA. The bacteriophage with the DNA packet in its genome will infect the bacteria, so the molecular information will be encoded inside the bacteria.

- *Bacterial Artificial Chromosomes* (BACs) are artificial plasmids designed for cloning long segments, up to 300.000 base pairs of DNA. The procedure used to encode the message inside the BAC is the same than the one used for plasmids, as shown in Figure 3.3. However, in this case, the host bacteria must be genetically modified in order to allow the entrance of the long BAC vector through the membrane.

The maximum packet size depends on the method used for encoding the information inside bacteria. It was reported in [36] that with plasmids it is difficult to clone (in our case, encode) sequences longer than about 15.000 base pairs whereas, bacteriophage λ vectors enable the cloning of 23.000 base pairs. However, the most effective method is BACs because it enables to encode packets inside bacteria of up to 300.000 base pairs.

The network capacity will depend on the number of base pairs that can be encoded inside each bacterium, and also on the time that the bacteria needs to reach the proper receiver by chemotaxis, which has been estimated in the Chapter 5.

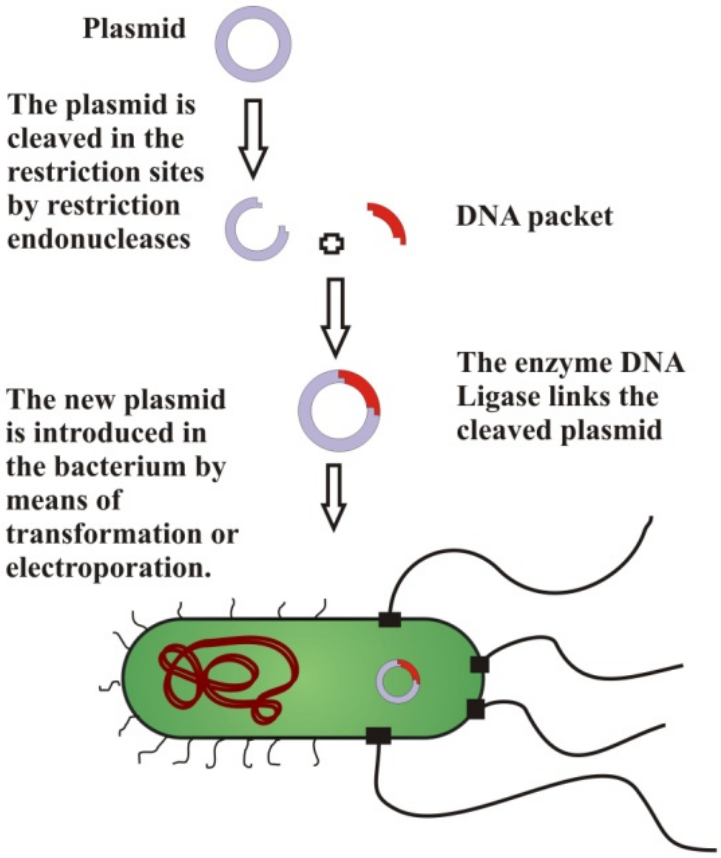


Figure 3.3: Encoding of the DNA packet using plasmids.

### 3.1.2 Transmission

In order to transmit the desired bacteria to the medium, one option could be the creation of E. coli libraries, where each E. coli will have different encoded information, so different DNA packets. These bacteria could be stored in the gateway node, in a kind of *warehouse*. The gateway can release the desired bacteria, which will contain the desired DNA information, to the medium when it is necessary. Since E. coli, as all bacteria, are able to reproduce, so create a new bacteria with the same genome, new bacteria are constantly created, this ensures that the warehouse will never be empty.

### 3.1.3 Propagation

Bacteria have a great number of chemical receptors around his membrane that allow them to sense the environment for the presence of attractant particles and move towards the direction it finds the best living conditions, this process is called *chemotaxis*. Bacterial chemotaxis is a nature marvel example of signal transduction and it is being widely studied [3,9].

*E. coli* moves in series of "*runs*" and "*tumbles*" [8]. In each run, the flagella motors spin counterclockwise, and the bacterium swims approximately in straight line. Whereas, a tumble is a small period of time where the bacterium moves erratically in the same place due to one or more filaments are spinning clockwise. During a running period, bacteria sense the amount of nutrients (sugars, amino acids, dipeptides) in the environment several times, using cell membrane's chemoreceptors [2]. Comparing the obtained results, the bacterium is able to decide whether the nutrient concentration is increasing or decreasing. If the concentration is increasing, the running time will be longer, so the rotary motor will spin in counterclockwise longer. This bias in the running time enables cells to find the places where the environment is better.

In recent decades, an exhaustive research has been conducted in understanding how the flagellar motor of bacteria works. Its structure, parts, and how these parts are assembled are well known [8]. Information regarding the fuel that it uses, the torque that it can generate at different speeds and what controls the likelihood of the direction changes are also well documented in the literature. However, it is still unknown what makes the bacterium run or tumble and what makes the motor change from one state to another. For this reason, bacterial mobility still has a small random component that is being widely studied in [6,9,47]. This random component has to be modeled in order to find out the time required for the bacteria to move from the emitter to the receiver. In Chapter 5, we have developed a simulation tool able to characterize how bacteria move in a point to point communication and estimate the required propagation time.

### 3.1.4 Reception

The reception of the DNA packet may be done following a natural cellular process called Bacterial Conjugation that is defined as the exchange of genetic material among bacteria cells [31]. For the exchange of these circular sequences of genetic material, *plasmids*, direct contact between cells is necessary. This contact is achieved by means of the bacterial appendage called

pilus. Hence, the donor bacterium localizes the receiver cell, which in our case is the receiver's gateway, and attaches to it using the pilus. Then the bacteria retract the pilus in order to have direct contact with the receiver. This contact makes both membranes to fuse together, in a kind of bridge by which the donor bacterium transfers a single strand of the plasmid DNA. When both, donor and recipient, cells have a single strand of the plasmid, DNA synthesis must be done, by both of them, in order to recover the whole plasmid.

### 3.1.5 Decoding

Once the plasmid is in the receiver, the DNA packet must be extracted from the plasmid. This is done by *restriction endonucleases* enzymes that cleave the plasmid in *restriction sites,* as shown in Figure 3.4 . When the plasmid has been cleaved, the receiver nano-machine is able to use and process the DNA packet. If the receiver machine is a gateway, the message can be demultiplexed and routed to other nano-machines, not only by means of medium-range mechanism but also by means of long or short-range techniques.

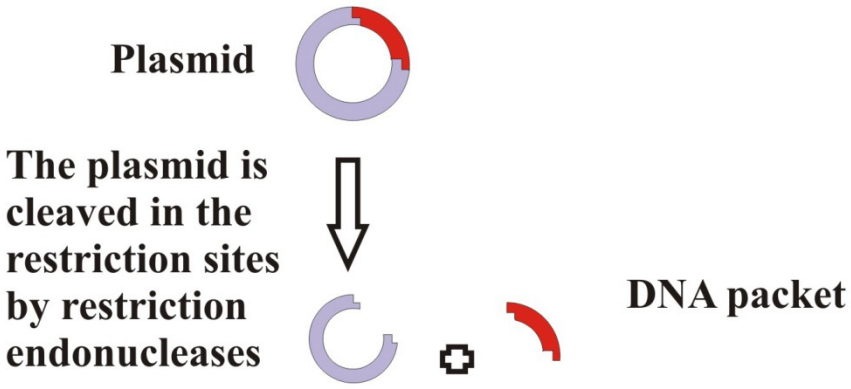


Figure 3.4: Decoding of the DNA packet

## 3.2 Open Issues and Research Challenges

In this section, we want to point out some of the issues that must be solved in order to use Flagellated Bacteria as communication mechanism in the medium-range.

We think that the first step is to know if the Flagellated Bacteria are able to reach the receiver following chemotaxis, and, if they are, how much time the bacteria will require to reach a receiver that is placed a certain distance $d$ from the transmitter. Moreover, it is interesting to know the rate of times the Flagellated Bacteria are able to reach the receiver in less than a certain maximum time $t_{max}$. If a bacterium needs more than $t_{max}$ to arrive to the receiver we assume that the Bacterium and the packet are lost. All of this is modeled in Chapter 5 where we obtain a physical channel model in terms of propagation delay and packets loss probability for a point to point communication between two nodes.

Another issue that should be studied is Selective Breeding or Artificial Selection. Selective breeding is the process of breeding plants and animals for particular genetic traits. Regarding Flagellated Bacteria, i.e., E. coli, Selective Breeding can be used to generate faster bacteria. The process would be as follows. First, several bacteria are placed in an environment where there is a source of attractant particles. The bacterium that arrives first to the source is selected and bred. The same process is done with the offspring of this bacterium. Then the faster bacterium among the offspring is selected and so forth. The final result is a strain of the bacterium that is able to move efficiently to the source of attractant particles.

Another issue that must be studied is how the mutation rate affects to the information that must be transmitted. Mutations are permanent changes in the genome of a certain organism produced by copying errors during cell division process. Hence, the symbol error probability is proportional with the mutation rate that in bacteria cells is around $10^{-8}$ errors per base pair per generation [16].

Finally, it may be possible to encode several plasmids inside the bacteria. This must be also studied because it is directly related with the amount of information that can be encoded inside a single bacterium.

# Chapter 4

# Medium-Range Molecular Communication based on Catalytic Nanomotors

Catalytic nanomotors are defined as particles that are able to propel themselves, and small objects, by means of self-generated gradients that are produced by catalyzing the free chemical energy present in the environment. One of the most common types of catalytic nanomotors is platinum (Pt) and gold (Au) nanorods, which are 370 nm in diameter and 2 μm long (1 μm of gold and 1 μm of platinum). These nanorods are able to propel themselves, approximately in a unidirectional way, in an aqueous hydrogen peroxide ($H_2O_2$) solution by catalyzing the formation of oxygen at the Pt end (See Figure 4.1 (a)) [38].

Some experimental results about the velocity and directionality that the platinum and gold nanorods can achieve have been presented in [37]. It was found that the rate at which the oxygen is produced is limited by the surface area of the platinum. For instance, when a 2 μm rod is introduced in a solution composed of 3.3% of hydrogen peroxide, they observe that the rod is able to move with a speed of 7.9 μm per second and with a directionality of 0.75 (Directionality is defined in Section 6.2). Nanorods speed is in the same order of magnitude of swimming velocity of flagellated bacteria, between 2 and 10 body lengths per second [37]. One of the main drawbacks of Pt/Au nanorods is the lack of a complete control over the direction of the movement, although they show an important improvement in comparison with the movement of particles in the nano-scale, which follows Brownian diffusion laws. This directionality can be improved by adding nickel (*Ni*) segments, which length is shorter than the diameter of the rod. The Au/Ni/Au/Ni/Pt striped nanorods are 1.3 μm long (With respective segment sizes of 350, 100, 200, 100 and 550 nm) and 400 nm on diameter, and can be externally directed by applying

magnetic fields, as shown in Figure 4.1 (b). This can be done because of the nickel segments introduced drive the rods to align in the perpendicular direction of the magnetic field, thus mimicking the movement of magnetotactic bacteria [30].

Bacterial chemotaxis, as seen in Figure 4.1 (c), might also be achieved by means of building rafts of nanorods. The main concept beyond this is that the raft is immersed in a solution with inhibitor particles. These particles bind to several receptors placed on the rods surface, and make the nanorods move slightly slower. Since the concentration gradient of the inhibitor between one corner of the raft and the other, the corner of the raft that is closer to the inhibitor source will move slower than the corner of the raft that is further. This fact makes the raft to steer and move towards the inhibitor source (S). The main drawback is that the velocity of the raft will decrease as it approaches to the source [38].

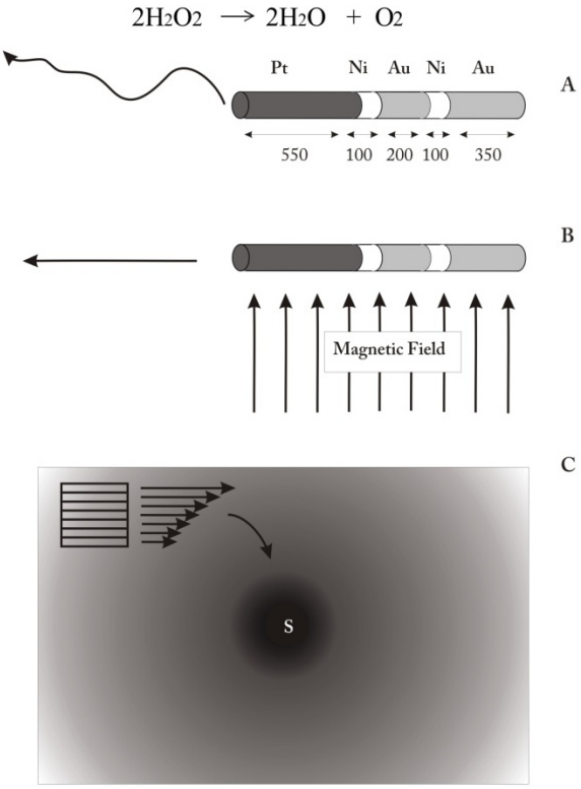


Figure 4.1: The movement of Pt-Ni-Au-Ni-Au rods in aqueous hydrogen peroxide solution without a magnetic field applied (A) and with an applied field (B). (C) Chemotactic response of a raft made of nanorods. Lengths of segments are expressed in nanometers.

Taking into account all the possibilities that catalytic nanomotors offer when working in the nano-scale, we propose to use them as a carrier to transport the DNA information among nano-machines. This communication process is explained in Section 4.1. Moreover, some open issues and research challenges are given in Section 4.2.

## 4.1 Communication Process

In this section, we qualitatively explain how the exchange of information between to nodes of the network is done using catalytic nanomotors. As shown in Figure 3.2, the communication process is enclosed in the following five steps: Encoding, transmission, propagation, reception and decoding.

### 4.1.1 Encoding

Nanorods are being widely studied in biomedicine because they offer new applications such as sensing and, drug and gene delivery. We are concerned mainly with the gene delivery application because we want to carry out the transport of DNA information. In [45] it was reported how to load DNA plasmids of up to 6.400 bases in an Au/Ni nanorod and use it as a gene delivery system. This nanorod is 100 nm in diameter and 200 nm long (100 nm of Au and 100 nm Ni). In order to attach the plasmids to the nanorod, this must be introduced in a solution of 3-[(2-aminoethyl)dithio] propionic acid (AEDP). The carboxylic acid terminus of the AEDP binds with the Nickel. Then the plasmids, which are conjugated with the AEDP, attach in the free amines placed in the nickel surface. They obtained a plasmid concentration on the nickel surface of 4 x $10^{12}$ molecules$\cdot$cm$^{-2}$. This number gives us a reference of the amount of information that may be encoded in a nanorod. After that, the nanorods are introduced in a $CaCl_2$ solution in order to compress and immobilize the plasmid. On the other hand, transferrin protein is bound in the gold segment of the rod by means of a thiolate linkage [45]. The transferrin is a protein used in order to ease the receptor-mediated endocytosis, in other words, it helps the uptake of the rod by means of the cell receptors placed in the cellular membrane.

Hence, the desired information is encoded as DNA nucleotides forming plasmids, which must be conjugated to AEDP. Then, these plasmids are attached to the Au/Ni/Au/Ni/Pt nanorods following the previous procedure, which is shown in Figure 4.2.

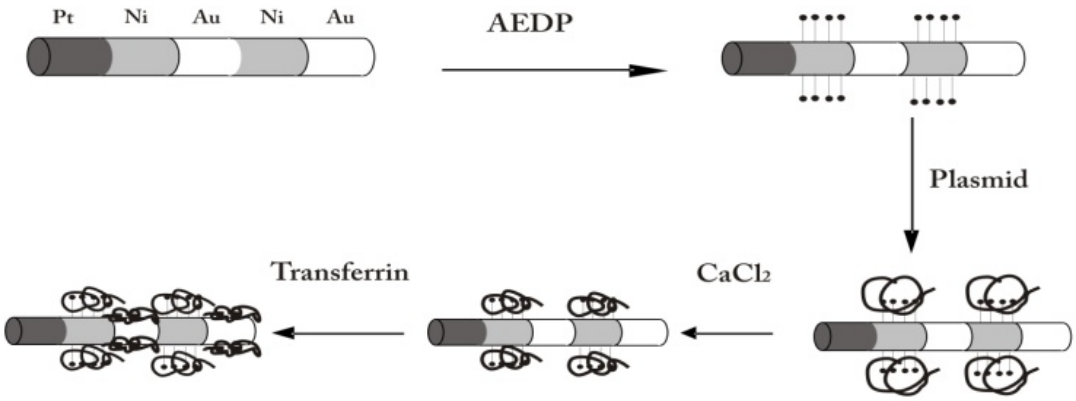


Figure 4.2: Encoding of the plasmids in the Au/Ni/Au/Ni/Pt nanorods.

### 4.1.2 Transmission

As in the medium-range communication using bacteria, the transmission of the nanorods with the encoded information is highly bound to the gateway design. Hence, further research is required on this topic.

### 4.1.3 Propagation

There are two different alternatives in order to make the plasmid reach the proper receiver. The first option relies on the possibility to direct and guide the nanorods using pre-established magnetic paths from the emitter to the receiver. The second option is to build a raft by means of joining several nanorods together and take advantage of the chemotactic process.

The main drawback of the first option is that a magnetic field must be applied and controlled, and taking into account the scale it might not be feasible to handle when there are lots of different communication channels. If it is possible, the propagation time will be notably improved. Concerning to the chemotactic raft of nanorods, there exist also some drawbacks, the first of them is that the velocity of the raft decreases as the raft approaches to the inhibitor source. The second inconvenience is that the dimensions of the raft are bigger than the dimension of a single nanorod, however, this could be used in order to transmit much more information at the same time.

### 4.1.4 Reception

As we have mentioned in the encoding subsection, the nanorod has not only the plasmid attached but also has the transferrin protein bound to the gold segment of the rod. The transferrin is a protein used for the transport and delivery of iron ions around the body. This protein is able to go inside cells by means of binding to the transferrin receptors placed at the cellular membrane. Hence, the receiver device must include transferrin receptors in order to carry out the uptake of the nanorods. This has been done with the gene delivery Au/Ni nanorods [45], however it is not certain that the uptake of Au/Ni/Au/Ni/Pt nanorods is feasible because of the size of these rods is bigger. In this case, other alternative could be applied on the reception process.

### 4.1.5 Decoding

Once the plasmid is in the receiver, it can be cleaved using *restriction endonucleases* enzymes in order to recover the molecular packet encoded inside the plasmid, as shown in Figure 3.4. Then, the receiver device is able to process the DNA information as the application requires.

## 4.2 Open Issues and Research Challenges

In this section, we want to point out some of the issues that must be solved in order to use Catalytic Nanomotors as communication mechanism in the medium-range.

We think that the first step is to know if the Catalytic Nanomotors are able to reach the receiver and, if they are, how much time will be required in order to reach a receiver that is placed a certain distance $d$ from the transmitter. Moreover, it is interesting to know the rate of times the Catalytic Nanomotors are able to reach the receiver in less than a certain maximum time $t_{max}$. If a nanorod needs more than $t_{max}$ to arrive to the receiver we assume that the nanorod, and thus the packet, is lost. All of this is modeled in Chapter 6 where we obtain a physical channel model in terms of propagation delay and packet loss probability for a point to point communication between two nodes.

Further research regarding the design of the gateway node is also required. It is necessary to determine if the node will be able to carry out the different processes required for the communication.

Finally, the creation of a proper magnetic field, which drives the nanorod from the transmitter to the receiver, must be studied. Ideally, the magnetic field will not require any external control because it may not be feasible to control the large amount of different communication channels that will exist in the nano-scale. An insight of this is given in Chapter 6, where two autonomous alternatives are given in order to create the magnetic field.

# Chapter 5

# Physical Channel Model for Flagellated Bacteria

In this chapter, we aim to develop the physical channel model in terms of propagation delay and packet loss probability for a point-to-point communication by using a flagellated bacterium as information carrier. As shown in Figure 5.1, the communication system is formed by a transmitter, a receiver and the channel. The channel is an aqueous environment where there is a gradient of attractant concentration (In Figure 5.1 the level of concentration is proportional to the background color). Both transmitter and receiver are assumed to be in a fixed position in the space. The communication process is developed as follows:

- The transmitter releases a bacterium that is carrying the desired DNA information to the environment.
- The receiver is constantly releasing a fixed attractant concentration that diffuses away following Fick's Laws to the environment.
- The bacterium swims following positive gradients of attractant particles to the receiver. Bacterium movement can be modeled with a *biased random walk*.

Hence, in order to obtain a physical channel model, namely, the propagation time and the packet loss probability, we need to analyze several parameters that constrain the bacterium movement in the environment:

- The forces sensed by micro-scale objects, i.e., bacteria, trying to move in a fluid are completely different that the forces sensed by macro-scale objects. In the micro-scale, viscous forces domain versus inertial forces. An insight of this is given in Section 5.1.

- In section 5.2 , we analyze how bacteria manage to overcome the viscous forces, hence, how they are able to generate the required force to propel itself and swim forward.
- The diffusion of attractants must be modeled because the concentration sensed by the bacterium in every time instant determines its movement in the environment. The diffusion of attractants is studied in Section 5.3 using Fick's Laws of diffusion.
- The parameters that govern the biased random walk of the bacterium, namely, rotational diffusion, run and tumbling lengths, changes in direction and the bacterial impulse response, are modeled in Section 5.4.

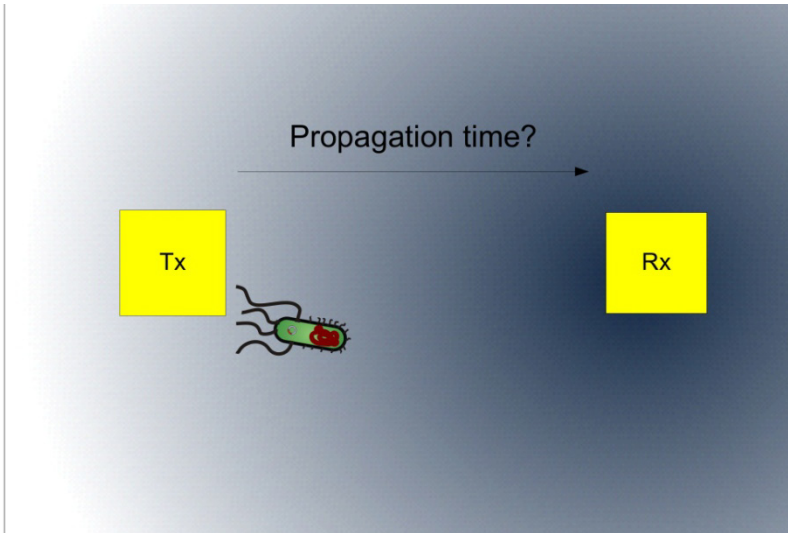


Figure 5.1: Point to point communication using flagellated bacteria

With all of this information, we have developed a simulation tool that is able to model the biased random walk of a bacterium from the transmitter to the receiver. This tool computes the propagation delay, the time required from the bacterium to swim from the transmitter to the receiver, and the packet loss probability, the rate of packets that not arrive to the receiver in a certain time $t_{max}$. Finally, by averaging the results obtained in several simulations, we have obtained a physical channel model in terms of propagation delay and packet loss probability for a point-to-point communication.

## 5.1 Low Reynolds Number

The Reynolds number [44] is a dimensionless number that expresses a ratio between inertial and viscous forces of a given object:

$$\mathrm{R} = \frac{\text{Inertial forces}}{\text{Viscous forces}} \tag{5.1}$$

Bacteria movement is governed by a set of forces completely different from the forces that govern motion of objects in the macro scale. From the E. coli bacteria point of view, water is a granulated substance through which it has to swim, hence, bacterial movement is not constrained by inertial forces but by viscous forces. For this reason it is said that bacteria move in low Reynolds numbers [41].

For a swimming organism, the Reynolds Number is given by:

$$\mathrm{R} = \frac{\mathrm{l}\nu\rho}{\eta} \tag{5.2}$$

where $l$ is the size of the organism, $v$ its velocity and, $\rho$ and $\eta$ are the density and viscosity of the medium respectively [41].

For instance, an E. coli bacterium swimming fast in water has a Reynolds coefficient of $R = 10^{-5}$, whereas, a human paddling in a pool experiences a Reynolds coefficient of $R = 10^{5}$. In order to understand the forces acting upon a swimming bacterium, it is proposed in [41], to imagine yourself trying to move in a swimming pool that is full of molasses, and that you are not allowed to move the parts of your body faster than the hands of a clock. Then it is pointed out that "If under those ground rules you are able to move a few meters in a couple of weeks, you may qualify as a low Reynolds number swimmer".

## 5.2 Flagellar Motor and Flagellar Propulsion

Natural selection has driven microorganisms to develop efficient machinery and tools that allow them to propel themselves in low Reynolds numbers environments. E. coli bacteria have developed complex rotary motors that are powered by protons or sodium ions ($Na^{+}$) flux [6]. These motors are able to produce a rotary movement of the flagellum either in a clockwise or counterclockwise way.

When an E. coli is swimming in constant velocity the rotary motors spin counterclockwise and the cell body spins clockwise, as shown in Figure 5.2. Since the velocity is constant, the net force experienced by the bacterium must be zero. Otherwise, it would either accelerate or decelerate. Then, the torque generated by rotation of the filaments is balanced by viscous drag due to counter-rotation of the body of the cell, and thrust generated by rotation of the filaments is balanced by viscous drag due to translation of the body of the cell.

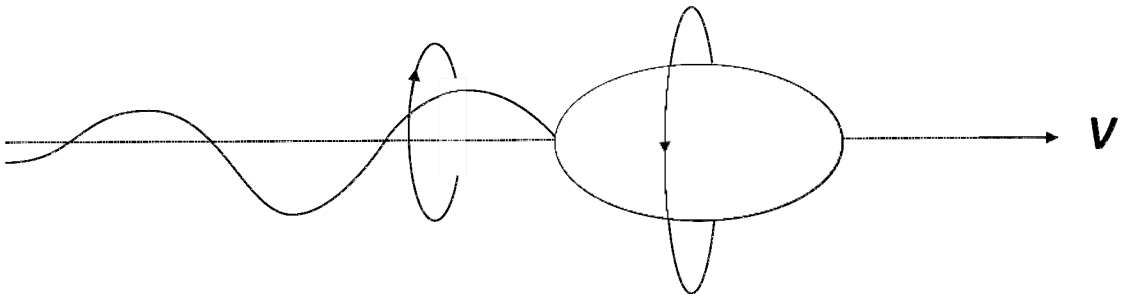


Figure 5.2: Bacterium swimming in constant velocity $v$

In order to understand which forces make the bacterium being able to move forward in a low Reynolds numbers environment, we analyze the viscous drag in two points of the flagellum, which are in counter-phase. The force analysis is presented in Figure 5.3, the velocity of the flagellum $v$ can be decomposed in normal and parallel components, $v_n$ and $v_p$. Hence, the frictional drag forces, $F_n$ and $F_p$, act in the opposite direction of $v_n$ and $v_p$. These forces can be decomposed in the normal and parallel directions of the bacteria movement, $F_\Omega$ and $F_v$. Hence, $F_\Omega$ and $F_\Omega{}'$ act in opposites directions and contribute on the generation of the torque in the cell body, where $F_v$ and $F_v{}'$ act in the same directions and are the forces that push the bacterium forward [7].

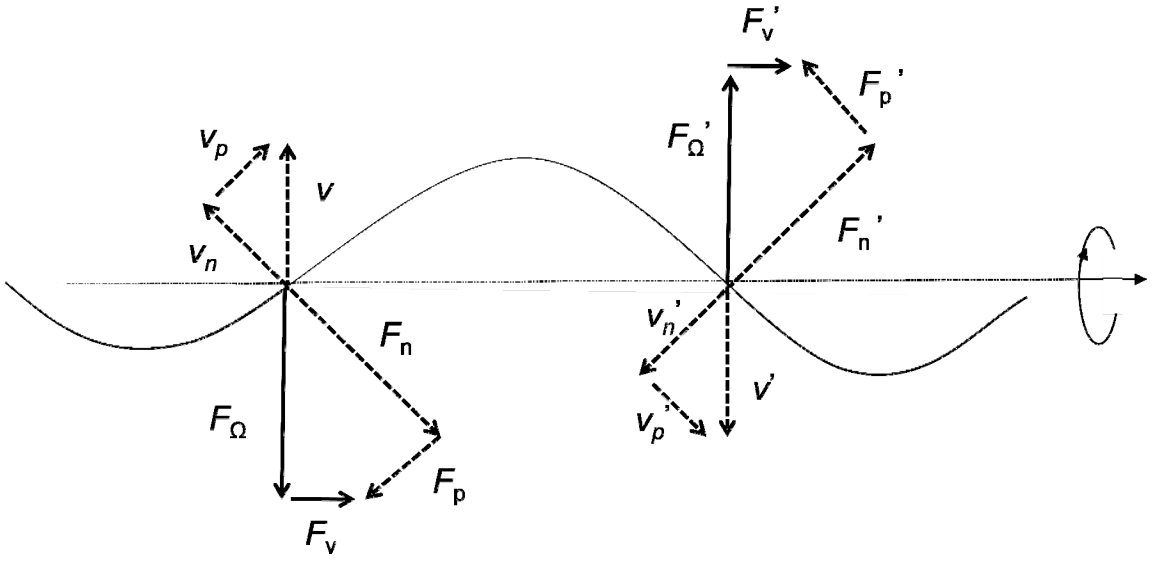


Figure 5.3: Force analysis of a bacterium swimming in constant velocity $v$

## 5.3 Diffusion of Particles

As was stated in Chapter 3, the receiver gateway is constantly releasing particles to the environment. These particles will diffuse away generating concentration gradients, which will be sensed and followed by bacteria. In order to model the time required for a bacterium to reach the receiver, the first thing that must be modeled is the attractants diffusion through the environment.

### 5.3.1 Fick's Laws of Diffusion

When in a certain environment there exist a non-uniform distribution of particles, these tend to diffuse away in order to reach a uniform concentration through all the space [39]. The flux of particles is obtained with the Fick's first equation, given in (5.3), that states that the net flux of particles in a certain position and time is equal to the spatial gradient of the particle concentration $\mathrm{c}(\bar{\mathrm{x}}, \mathrm{t})$ multiplied by the diffusion coefficient, D.

$$\bar{\mathrm{J}}(\bar{\mathrm{x}}, \mathrm{t}) = -\mathrm{D}\,\nabla \mathrm{c}(\bar{\mathrm{x}}, \mathrm{t}) \tag{5.3}$$

where $\nabla \mathrm{c}(\bar{\mathrm{x}}, \mathrm{t}) = \left( \frac{\partial\, \mathrm{c}(\bar{\mathrm{x}},\mathrm{t})}{\partial \mathrm{x}_1} \frac{\partial \mathrm{c}(\bar{\mathrm{x}},\mathrm{t})}{\partial \mathrm{x}_2} \quad \ldots \quad \frac{\partial \mathrm{c}(\bar{\mathrm{x}},\mathrm{t})}{\partial \mathrm{x}_\mathrm{n}} \right)$ is a vector that have the same dimension that $\bar{\mathrm{x}}$ and $\bar{J}$.

The diffusion coefficient (D) for spherical particles moving in low Reynolds numbers fluids is expressed as follows:

$$D = \frac{K_b T}{6\pi\eta r} \tag{5.4}$$

where r is the radius of the particle, η and T are the viscosity and temperature of the medium respectively and $K_b$ is the Boltzmann constant.

The continuity principle (5.5) states that particles cannot be created or destroyed, thus, the number of particles entering and leaving the system must be the same. The principle states that the time derivative of the particle concentration $\frac{\partial c(\bar{x},t)}{\partial t}$ at location $\bar{x}$ and time t is equal to the opposite of the particle concentration flux $\bar{J}(\bar{x},t)$ at location $\bar{x}$ and time t.

$$\frac{\partial c(\bar{x},t)}{\partial t} = -\nabla \bar{J}(\bar{x},t) \tag{5.5}$$

The second Fick's law (5.6), is obtained by substituting the first Fick's law (5.3) into the continuity principle (5.5):

$$\frac{\partial c(\bar{x},t)}{\partial t} = D\,\nabla^2 c(\bar{x},t) \tag{5.6}$$

where $\nabla^2$ (or $\Delta$) is the Laplace operator that expresses the divergence of the gradient, hence, $\nabla^2 c(\bar{x},t) = \frac{\partial^2 c(\bar{x},t)}{\partial^2 x_1} + \frac{\partial^2 c(\bar{x},t)}{\partial^2 x_2} + \cdots + \frac{\partial^2 c(\bar{x},t)}{\partial^2 x_n}$.

The second Fick's equation in two or more dimensions is analogous to the heat equation, which expresses the heat distribution as a function of the space and the time [39,40].

### 5.3.2 Finite Differences Fick's Laws

The receiver is constantly adding particles in the environment, hence, the concentration is always increasing and then the continuity principle is not satisfied. Under this constrain, we are not allowed to use the second Fick's equation (5.6).

In order to satisfy the continuity principle, we sample the concentration in the environment in small periods of time, $\Delta t$. If $\Delta t$ is small enough, we can assume that, in this time interval, the

number of particles in the overall system is constant, and therefore, the continuity principle is fulfilled.

Hence, we can express the second Fick's Law using the finite differences method in a discrete environment:

$$\frac{c(\bar{x}, t + \Delta t) - c(\bar{x}, t)}{\Delta t} = D \frac{c(\bar{x} - \Delta\bar{x}, t) - 2c(\bar{x}, t) + c(\bar{x} + \Delta\bar{x}, t)}{(\Delta\bar{x})^2} \quad (5.7)$$

In order to use the finite differences scheme we must verify that the system is stable. The stability equation (5.8) states that the time interval, $\Delta t$, must be smaller than the length interval, $\Delta\bar{x}$, divided by two times the diffusion coefficient.

$$\Delta t \leq \frac{(\Delta\bar{x})^2}{2D} \quad (5.8)$$

### 5.3.3 Simulation Attractant Particle Diffusion

We are now able to compute, by using using (5.7) and choosing the parameter correctly to satisfy (5.8), how the attractant particles that the receiver is releasing diffuse through the environment, thus, the concentration that a bacterium senses when moving towards the receiver. The parameters used in our simulation are the following:

- **Diffusion Coefficient:** Bacteria have a lot of different chemoreceptors in its membrane. Each kind of chemoreceptor reacts with a different particle and present different efficiencies and sensibility [2]. Aspartate and Serine receptors present the best response and precision. For this reason, in our simulations, we have used the diffusion coefficient of Aspartate and Serine in water that is $D = 10^{-9}\ m^2/s$ [6].
- **Time and Length Intervals**: The time interval, $\Delta t$, and the length interval, $\Delta\bar{x}$, have been chosen in order to satisfy the stability equation (5.8) but taking into account that $\Delta t$ must be small enough to let the bacteria have enough resolution of attractant concentration. Hence, the values used in our simulation are $\Delta t = 10^{-2}$ s and $\Delta\bar{x} = 10^{-5}$ m.

The receiver nano-machine, which is constantly releasing attractant particles, is placed in the middle of the simulated space, hence, in the position $x = y = 2$ mm. We assume that the concentration gradient becomes stable after a certain time since turning on the receiver nano-

machine, so after starting the emission of particles. The results presented in Figure 5.4 have been taken after 10 minutes of turning on the system and it is easy to observe that the diffusion is an isotropic process that affects in a same way in all the possible directions of the space. Moreover, the concentration gradient increases when approaching to the source of attractants, the receiver nano-machine. This increase in the concentration gradient is easily sensed by bacterium's chemoreceptors allowing the organism to reach regions with high concentration of attractants.

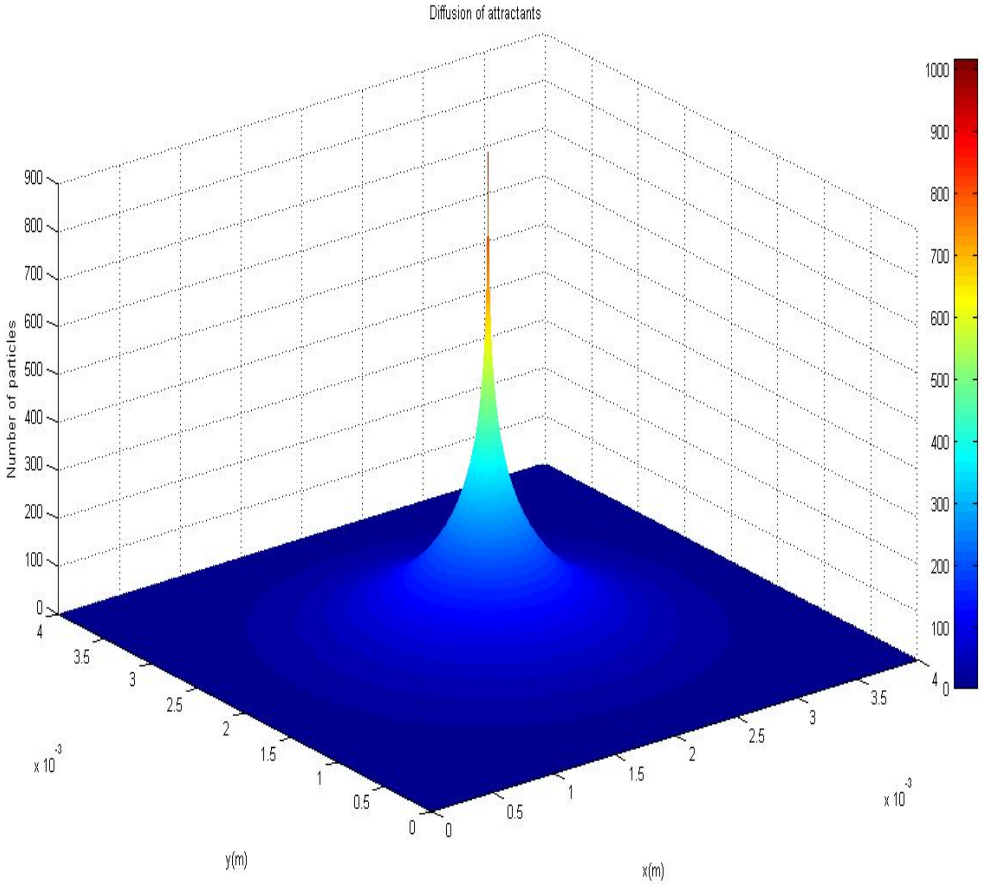


Figure 5.4: Diffusion of attractant particles

## 5.4 Biased Random Walk

When an attractant particle binds to one of the chemoreceptors placed at the cell membrane of the bacterium, it triggers a complex pathway of chemical signals that ends regulating the motion of

flagella's rotaries motors. However, we do not aim to get into detail into microbiology, chemistry or biology, more information regarding the sensory signal transduction pathway can be found in [6]. In this section, we aim to physically describe and model the overall movement of the bacterium.

Our starting point is [9], where they developed a microscope that is able to track and analyze bacteria's movement in a three dimensional environment. They developed two different experiments. In the first one, they introduced the bacteria in a homogenous environment, where the concentration is uniform. In the second experiment, they introduced gradients of attractant particles using capillary tubes. In both cases, they track bacteria's motion with the microscope and analyzed the resulting data.

From the first experiment they found out that the bacterium moves in series of running and tumbling periods. They observed that during a running period, the cell swims at a constant velocity in a nearly unidirectional direction. However, the cell drifts due to the rotational diffusion which produces small changes in direction, as a result, the cell meanders during a run. In a tumble period the bacterium slows down or stops and changes its direction with an angle $\gamma$. They observed that the probability density function of $\gamma$ was not uniform but small changes on direction where more probable. Moreover, they computed several autocorrelations of running and tumbling sequences and they discovered that the run length and tumble length times are exponentially distributed [9].

In the second experiment they observed clouds of bacteria near the mouths of the capillaries sank, hence, the result of chemotactic process. Tracking run and tumbling lengths they were able to understand how bacteria move towards places with higher concentrations. In this experiment, they observed the same behavior in terms of changes in direction and, run and tumble length time distributions, which still follow are exponentially distributed. The main difference is that the mean run length increases when the bacterium moves up the gradient, whereas when it is moving down gradients the mean run length is similar than the one observed in homogeneous solutions. This increase in the mean run length produce that the bacteria move following a random walk model but with a preferred direction, hence, a biased random walk.

In the next subsections we explain and model the parameters that govern the movement of bacteria, namely, rotational diffusion, run and tumbling lengths, changes in direction and impulse

responses in bacterial chemotaxis. By using all this information taken from biological observations, we have developed a tool that is able to model the biased random walk of a bacterium from the transmitter to the receiver. This simulation tool is explained in more detail in Section 5.5.

### 5.4.1 Rotational Diffusion

As we explained in Section 5.1, the forces required by bacteria in order to move in water are governed by low Reynolds numbers. To E. coli, water looks as a set of granulated particles that are continuously moving. When the bacterium wants to swim it has to drag these particles causing the fluid to shear.

Collisions with water molecules produce the cell to slightly drift from one place to the other following a Brownian motion model. This drift is commonly known as rotational diffusion and drives the cell to drifts off course more than 60 degrees in 10 seconds.

Rotational diffusion can be analyzed as a rotational random walk [7], hence, every $\tau$ seconds the angle with which the bacterium is moving makes a step of $\pm\phi$ degrees. This is shown in Figure 5.5, where we assume that the bacterium is moving in a two dimensional space following the x axis and that in every time interval $\tau$ the bacterium changes its direction in steps of either $\phi$ or $-\phi$ with the same probability.

Hence, the angle at which the bacterium $j$ is moving in a certain time $t = n\tau$ is given by:

$$\theta_j(n) = \theta_j(n-1) \pm \phi \tag{5.9}$$

The angle taken by different bacterium is independent, so we can compute the mean angle as:

$$< \theta(n) >= \frac{1}{N}\sum_{j=1}^{N} \theta_j(n) = \frac{1}{N}\sum_{j=1}^{N} [\theta_j(n-1) \pm \phi_j] = \frac{1}{N}\sum_{j=1}^{N} \theta_j(n-1) + \sum_{j=1}^{N} \pm \phi_j \tag{5.10}$$

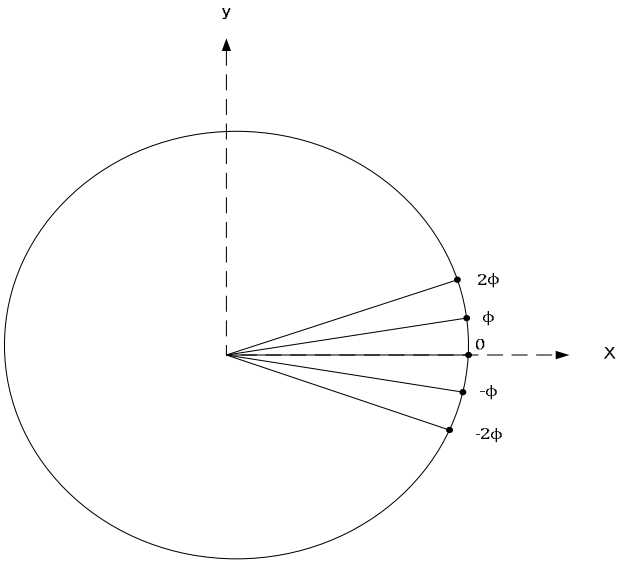


Figure 5.5: Rotational Random Walk

The second sum in (5.10) tends to zero because the sign of $\pm\phi$ is positive or negative with the same probability. As a result of this, the mean angle in the iteration $n$ is equal to the mean angle in the previous instant $n-1$. As given in (5.11), this can be extrapolated leading that the mean angle in the iteration $n$ is equal to the mean angle in instant 0, that is zero because all the bacteria are moving with an angle of 0 degrees.

$$< \theta(\mathrm{n}) >=< \theta(\mathrm{n}-1) >= \cdots =< \theta(0) >= 0 \tag{5.11}$$

The mean square angular derivation that the bacterium will suffer is given by:

$$< \theta^2(\mathrm{n}) >= \frac{1}{\mathrm{N}}\sum_{\mathrm{j}=1}^{\mathrm{N}} {\theta_\mathrm{j}}^2(\mathrm{n}) = \frac{1}{\mathrm{N}}\sum_{\mathrm{j}=1}^{\mathrm{N}} \left[{\theta_\mathrm{j}}^2(\mathrm{n}-1) \pm 2\theta_\mathrm{j}(\mathrm{n}-1)\phi + \phi^2\right] \tag{5.12}$$

As before, the second term on the sum averages to zero because half of the times it will be positive and the other half negative. Hence, the mean square angular deviation in the time interval $n$ is given by the mean square deviation in the previous time interval $(n-1)$ plus the square of the angular step:

$$< \theta^2(\mathrm{n}) >= < \theta^2(\mathrm{n}-1) > +\phi^2 \tag{5.13}$$

If we extrapolate this result we obtain:

$$< \theta^2(\mathrm{n}) >=< \theta^2(0) > + n\phi^2 = n\phi^2 \tag{5.14}$$

that taking into account that $n = t/\tau$, we obtain the mean angular deviation as:

$$< \theta^2(\mathrm{t}) >= {}^{t}/_{\tau}\, \phi^2 = 2\mathrm{D_r t} \tag{5.15}$$

where $\mathrm{D_r} = \phi^2/2\tau$ is the rotational diffusion coefficient [7].

The rotational diffusion can also be expressed by the Einstein-Smoluchowski equation as a function of the frictional drag coefficient, $f_r$. The bacterium can be approximated as a sphere of radius $a = 1\mu m$. Since the frictional drag coefficient for a sphere is $f_r = 8\pi\eta a^3$, we can obtain the rotational diffusion coefficient as follows:

$$\mathrm{D_r} = \frac{\mathrm{K_b T}}{f_r} = \frac{\mathrm{K_b T}}{8\pi\eta a^3} = 0.062\ rad^2/sec \tag{5.16}$$

where we have assumed that the bacterium is placed in an environment with temperature $T = 305\ K$ and viscosity $\eta = 0.027\ g/cm\ sec$. $\mathrm{K_b}$ is the Boltzmann constant [7].

As an example, in Figure 5.6, the probability distribution of the angular deviation of the bacterium after 10 seconds in a running period, which will be a Gaussian with mean $< \theta(\mathrm{n}) >= 0$ and root mean square displacement $< \theta^2(\mathrm{t}) >^{1/2} = 1.12\ \mathrm{rad} = 64.2\ °$, is shown in Figure 5.6.

### 5.4.2 Run and Tumbling lengths

One may wonder why E. coli tumbles. The answer is easy. E. coli is an intelligent organism that knows the physics of the medium where it is living. It knows that after ten seconds swimming in straight line, the rotational diffusion will cause a deviation on its initial course of more than 60 degrees. Hence, the bacterium does not know anymore where it is going and is not able to decide whether the concentration is increasing or decreasing. So, E. coli bacterium just stops, takes another direction and starts swimming again. Therefore, the upper limit of the running time is set by the effect of the rotational diffusion.

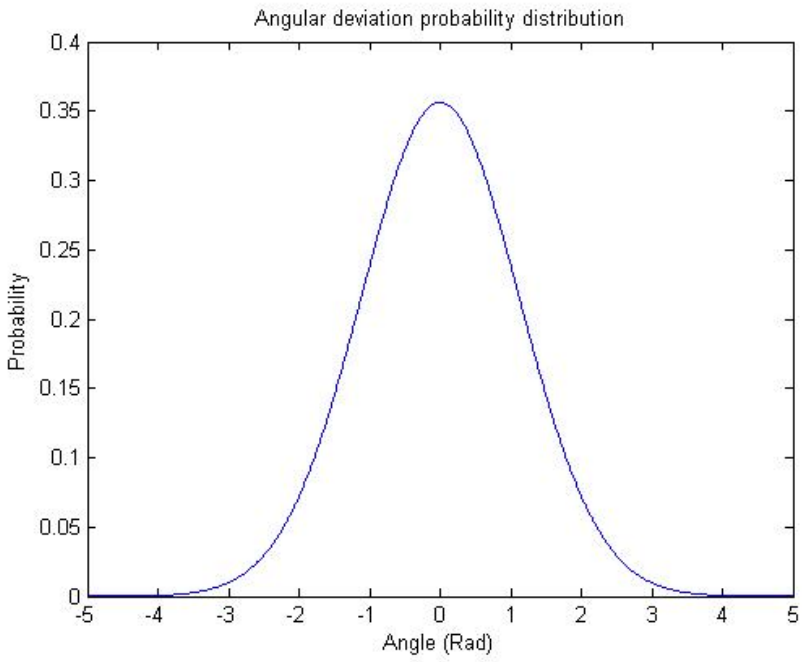


Figure 5.6: Angular deviation probability distribution

The lower limit is fixed by the time required by the bacterium to sense, count and process the information regarding the concentration of attractant and repellents in the environment. If the bacterium remains stopped in one place for a period of time $t$, it will sense the attractant particles that are diffusing that come from a distance $\sqrt{Dt}$ . When the bacterium is swimming with constant velocity $v$, if it wants to decide whether the concentration is increasing or decreasing it must outrun the diffusion of particles. This implies that $vt > \sqrt{Dt}$, thus, that the minimum time required for the bacteria to sense the concentration appropriately is :

$$t_{min} = D/v^2 \tag{5.17}$$

as we mentioned previously the diffusion coefficient of attractant particles, such as Aspartate or Serine, is $\mathrm{D} = 10^{-9}\ \mathrm{m}^2/\mathrm{s}$. If we assume that the bacterium is moving with a velocity of $v = 30\mu m/sec$, the minimum time is $t_{min} \approx 1\ sec$ .

The theoretical minimum and maximum running times presented in the previous paragraphs match with the experimental measures taken in [9]. As shown in Figure 5.7, it was observed that both running and tumbling lengths are exponentially distributed.

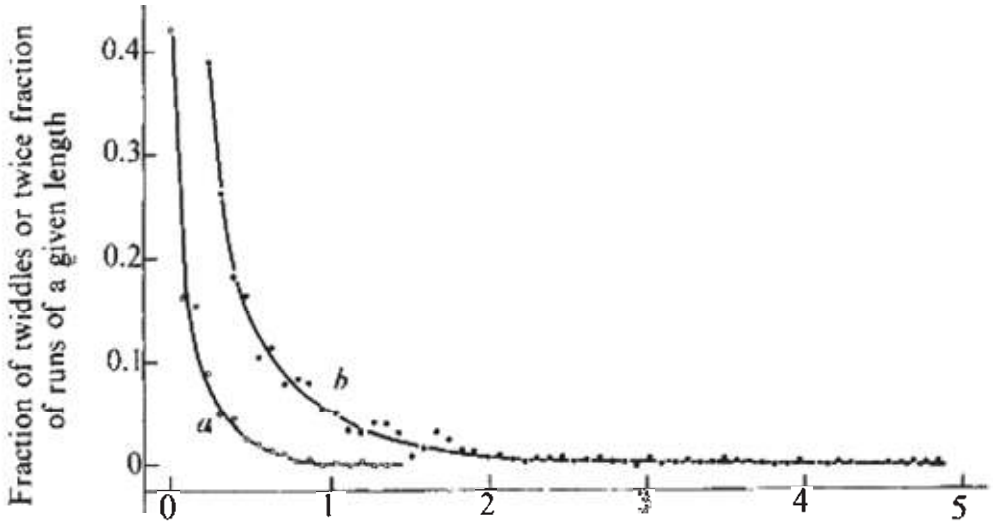


Figure 5.7: Tumble (a) and run (b) length distribution (From [9]).

**Run Length:** We consider an event as a change in the bacterium state from run to tumble. Then, the probability that the event occurs in a certain instant $t_o$, i.e., the probability of the run length is $t_o$, is given by:

$$\mathrm{P}(t_o;\lambda) = \lambda\, \mathrm{e}^{-\lambda t_o} \tag{5.18}$$

were λ is the mean run length of the bacterium.

The mean run length is the inverse of the tumbling rate, $\alpha(t)$, and depends on whether the bacterium is going in the right or wrong direction, thus, up or down the gradient of attractant particles.

$$\lambda(\mathrm{t}) = \frac{1}{\alpha(\mathrm{t})} \tag{5.19}$$

Where, if the bacterium is going down the gradient the mean run length is $\lambda = 1$ second, whereas if it is going up the gradient the mean run length is longer and can be obtained as a function of the sensed concentration $y(t) = f(c)$ [6]. The process by which the bacterium obtains $y(t)$ is explained more precisely in Section 5.4.4.

$$\alpha(\mathrm{t}) = \begin{cases} 1 - \mathrm{k}\, \mathrm{y(t)}, & y(t) > 0 \\ 1, & y(t) \leq 0 \end{cases} \tag{5.20}$$

**Tumbling Length:** In a similar way, the probability that the bacterium changes from tumble to run in a certain instant $t_o$, thus, the probability of the tumble length is $t_o$, is given by:

$$\mathrm{P}(t_o, \mu) = \mu\, \mathrm{e}^{-\mu t_o} \tag{5.21}$$

were $\mu$ is the mean tumble length of the bacterium. In this case, $\mu = 0.1$ seconds [6].

### 5.4.3 Changes in direction

Between two consecutives runs bacteria tumble, they rest for a short period of time where they wonder which direction to take in the next run period. We define $\theta_n$ and $\theta_{n+1}$ as the angles that determine the bacterium direction in two consecutives runs. The angle $\theta_{n+1}$ can be obtained as a function of the previous angle, $\theta_n$, and a random angle $\gamma$:

$$\theta_{n+1} = \theta_n + \gamma \tag{5.22}$$

For our simulation, we model the changes in direction between runs following the empirical measures of bacteria carried out in [9], where they measure the absolute variation on the angle between two runs, $\psi = |\gamma| = |\theta_{n+1} - \theta_n|$, and obtain its probability distribution, as shown in Figure 5.8. They obtain that the mean change in direction is about 62º and its standard deviation is around 26º.

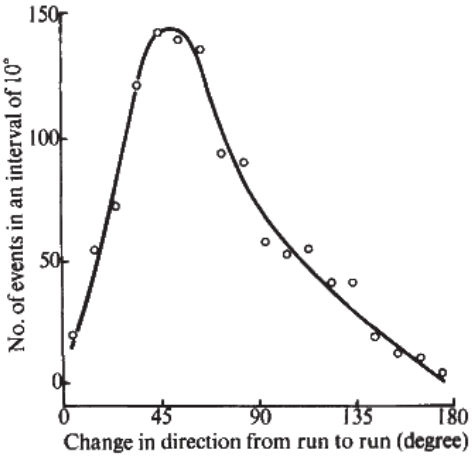


Figure 5.8: Distribution of changes in direction between runs (From [9])

In order to model the changes in directions between runs, we have approximated the probability density function $f(\psi)$ as:

$$f(\psi) = \begin{cases} \frac{1}{2}\cos(\psi/2), & \psi \leq \pi \\ 0, & \pi < \psi \leq 2\pi \end{cases} \tag{5.23}$$

This probability distribution has a mean value of 65.4º and a standard deviation of 48.88º. Note that these values are close to the ones observed in [9].

It is easy to demonstrate that equation (5.23) satisfies both equations (5.24) and (5.25), thus, that the probability distribution function of the change in the angle is correctly defined.

$$f(\psi) \geq 0, \qquad \forall\, \psi \tag{5.24}$$

$$\int_{-\infty}^{\infty} f(\psi) d\psi = 1 \tag{5.25}$$

The bacterium can turn either right or left, thus the probability density function of $f(\gamma)$ is calculated as:

$$f(\gamma) = \begin{cases} \frac{1}{4}\cos(\gamma/2), & |\gamma| \leq \pi \\ 0, & |\gamma| > \pi \end{cases} \tag{5.26}$$

where equations (5.24) and (5.25) are still satisfied.

Hence, in the simulation the angle of each running period, $\theta_{n+1}$, has been calculated using the angle in the previous run $\theta_n$ and a random number $\gamma$ generated with the distribution given by equation (5.26), which is shown in Figure 5.9

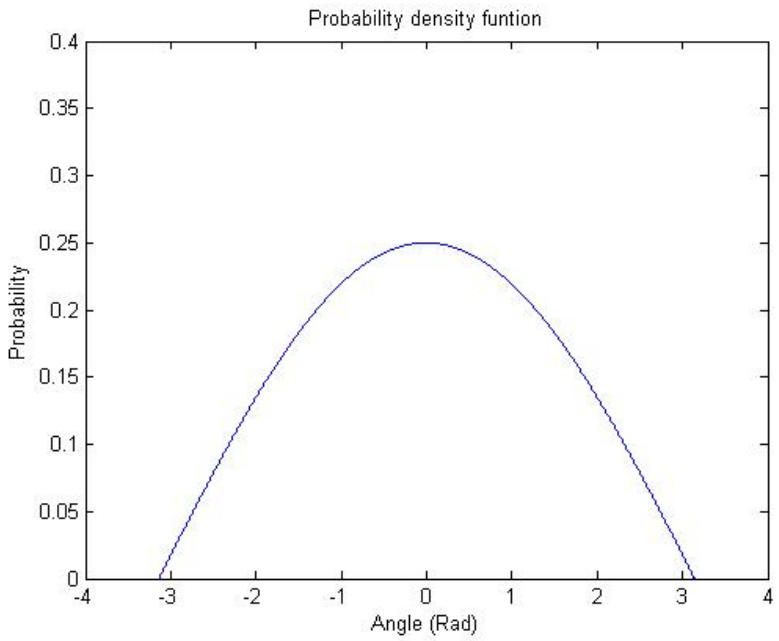


Figure 5.9: Probability density function of γ

### 5.4.4 Impulse Responses in Bacterial Chemotaxis

The response of the bacteria to brief impulses of attractants, the impulse response, has been measured in [11]. In order to obtain the bacteria's response to an attractant impulse, a flagellum of the cell is tethered to a glass surface and the response of the rotary motor can be monitored, measuring the probability that the motor spins counterclockwise, hence, the probability that the cell is running.

The first plot in Figure 5.10 shows the response of the bacteria when a stimulus of an attractant is applied, whereas, in the second plot, a repellent stimulus has been applied to the cell. Both stimuli have been applied in the time instant $t = 5\,sec$. The response of the cell appears after 0.2 seconds and it has a peak after 0.4 seconds of applying the stimulus. Then the probability goes down again crossing the baseline in time instant $t = 6\,sec$. It reaches a minimum in $t = 6.5\,sec$ and finally it returns to the initial value about 4 seconds after applying the stimulus $t = 9\,sec$.

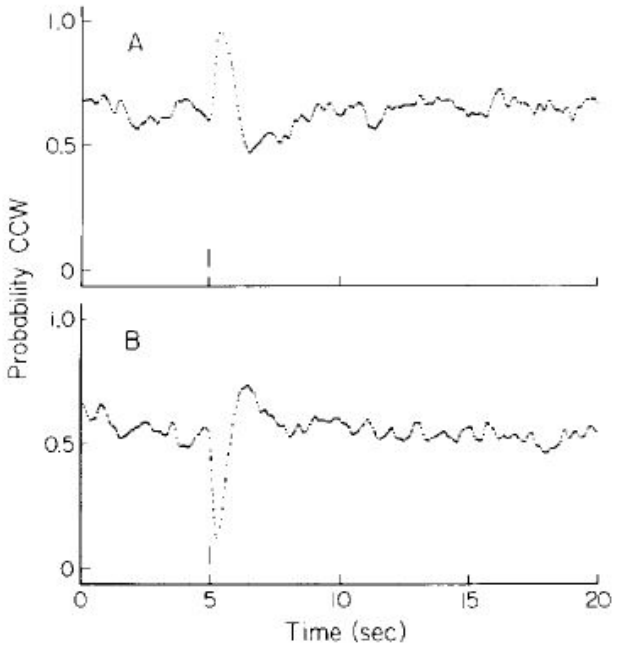


Figure 5.10: Impulse Responses of E. coli (From [11])

Notice that the response of the bacteria in front of impulses of attractants satisfies the following desirable properties of a system:

- **Linearity:** A system is linear if it satisfies both the properties of superposition and scaling. Superposition principle states the output of the sum of inputs is equal to the sum of individual outputs $y(x_1 + x_2) = y(x_1) + y(x_2)$. Whereas, the scaling principle says that if an input $x_1$ is scaled by a constant $\alpha$ and passed through the system, the output will also be scaled by $\alpha$ , thus, $y(\alpha x_1) = \alpha y(x_1)$.
- **Invariance:** A time invariant system has the property that for a certain input always generates the same output, independently of when the input was applied to the system.

Since bacteria behave as a linear and time-invariant system, it is possible to model bacteria as a system characterized by the input c$(t)$ and the impulse response $h(t)$, as shown in Figure 5.11.

The input of the system is the concentration sensed by the bacterium $c(t)$.The impulse response has been obtained from normalizing the power of the empirical observations from [11] and it is shown in Figure 5.12.

The Fourier transform of the impulse response is shown in Figure 5.13 and shows that the bacteria behave as a low pass filters of the concentration on the environment with a cut-off frequency of $f_c = 0.64\ Hz$.

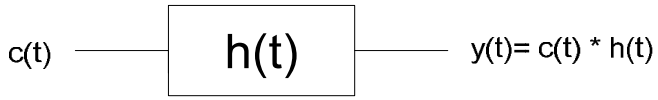


Figure 5.11: Bacteria behavior modeled as a system.

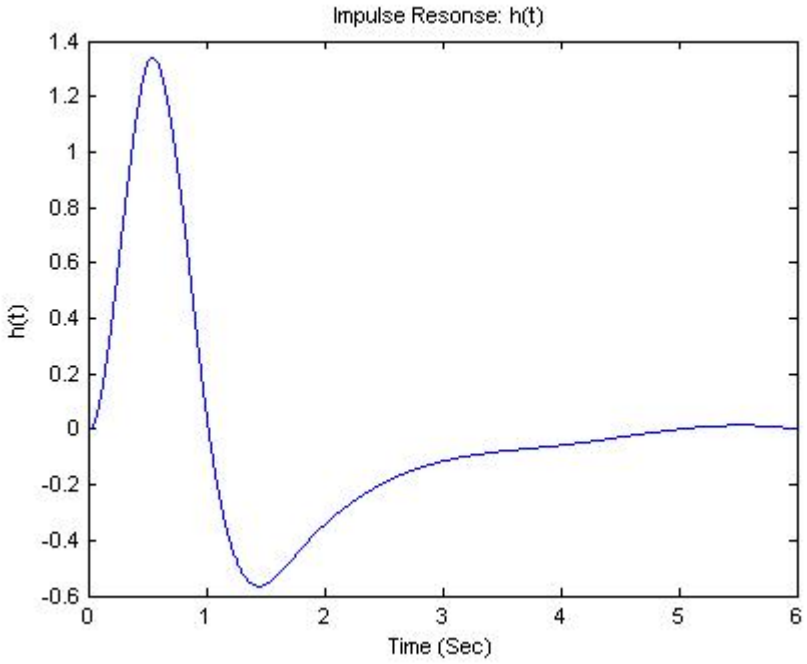


Figure 5.12: Normalized Impulse response of Flagellated Bacteria.

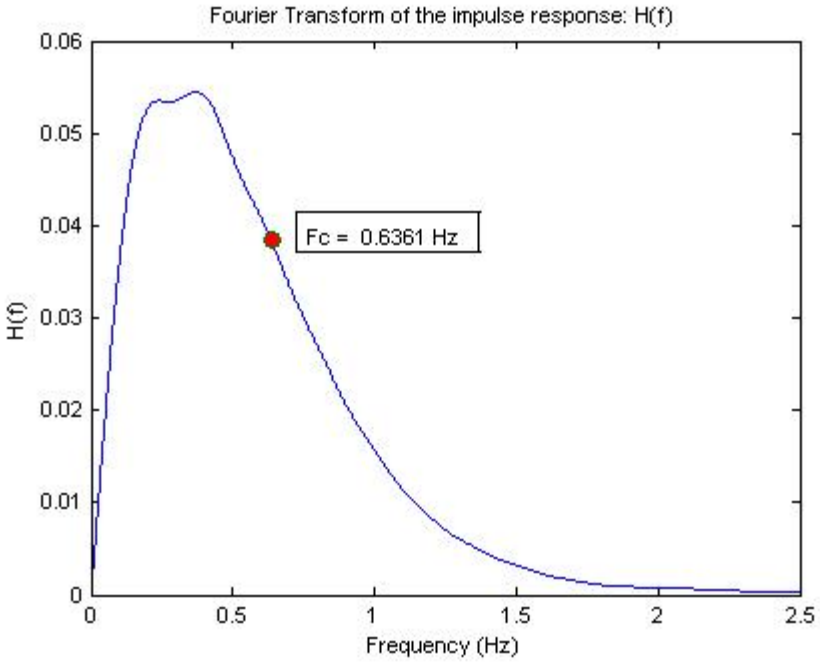


Figure 5.13: Fourier Transform of the impulse response

The output of the system is the convolution of the sensed concentration with the impulse response:

$$y(t) = c(t) * h(t) = \int_0^\infty \mathrm{h(t)c(t-\tau)d\tau} \tag{5.27}$$

This output $y(t)$ is used by the bacterium in order to determine the mean run length $\lambda(\mathrm{t})$, or its inverse, the tumbling rate $\alpha(\mathrm{t})$. Then, the tumbling rate can be obtained by substituting equation (5.27) to (5.20):

$$\alpha(\mathrm{t}) = \frac{1}{\lambda(\mathrm{t})} = \begin{cases} 1 - \mathrm{k}\int_0^\infty \mathrm{h(t)c(t-\tau)d\tau}\ , & \int_0^\infty \mathrm{h(t)c(t-\tau)d\tau} > 0 \\ 1, & \int_0^\infty \mathrm{h(t)c(t-\tau)d\tau} \le 0 \end{cases} \tag{5.28}$$

where $k$ is a constant that normalizes the energy of the output $y(t)$.

## 5.5 Simulation Modeling of Flagellated Bacteria Movement

We have developed a simulation tool that is able to simulate a point-to-point link by using a flagellated bacterium as information carrier. This simulation tool takes into account all the parameters that regulate bacteria behavior, which have been explained in the previous sections of this Chapter.

With this model, we are not only able to obtain the path that a certain bacterium follows but also the required time to reach the receiver, i.e., the propagation time. In case that the bacterium does not reach the receiver after a certain time, $t_{max}$, we will assume that the bacterium is lost, and hence, that the transmitted packet is lost. Moreover, the developed simulation tool allows us to obtain a physical channel model for communications based on flagellated bacteria.

The parameters assumed throughout the simulation are:

- The simulation space is assumed to be a 2-D squared space with a length side of 2 mm, because we want to simulate a maximum range of 1mm.
- The transmitter is always placed in the middle of the space, hence, in the position $x = y = 1\ mm$
- The receiver is placed in a distance $d$ from the transmitter. Hence, in the position $x = d + 1\ mm$ and $y = 1\ mm$.
- The bacterium is moving at a constant velocity $v = 20\ \mu m/sec$ [6].
- Initially, the bacterium is in the running state and it is released in the correct direction, so in the positive direction of the $x$ axis.
- The maximum simulation time is $t_{max} = 3000\ \text{sec} = 50\ \text{min}$. If the bacterium does not arrive at this time, we consider that the packet is lost.
- The bacterium reaches the receiver if the distance that separates them is less than 15 μm, which could be the size of a gateway node.
- All the computations are carried out periodically every 0.01 seconds.

The pseudocode of the simulation is given in Figure 5.14 (The complete code can be found in Appendix B).

The commands executed by the bacterium depend on the present state. After reading the concentration on the environment, the bacterium computes the probability to change the state and decides either to change or remain in the same state. These probabilities are computed by taking into account the mean run and tumbling lengths of the bacterium (see Section 5.4.2). In case the bacterium is running it moves 0.2 μm ($20\ {}^{\mu m}/_{sec} \cdot 0.01\ sec$) in the direction given by θ, otherwise it remains in the same position. The rotational diffusion, see Section 5.4.1, is simulated by generating a random number with the variance given by (5.15). The changes in direction between runs have been obtained by generating a random number distributed following the probability density function shown in Figure 5.9.

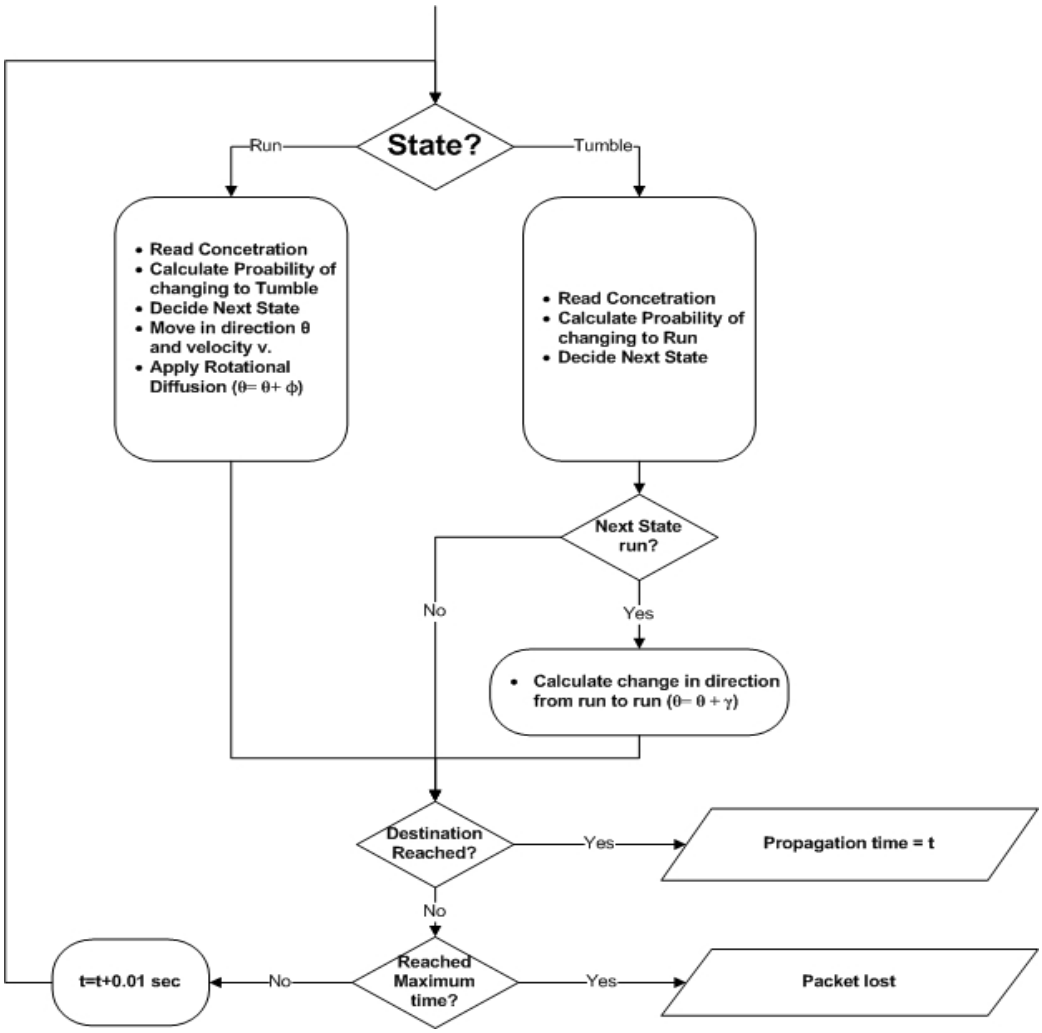


Figure 5.14: Simulation pseudocode

## 5.6 Simulation Results

The trace of a single bacterium from the transmitter (square) to the receiver (circle) is shown in Figure 5.15. We observe that the bacterium is moving by following a biased random walk model, as discussed in Section 5.4. When the bacterium is going in the correct direction, the runs are longer than when it is going far away from the receiver. Moreover, the plot shows that when the bacterium is running the direction is slightly affected by the rotational diffusion, whereas, when it tumbles there are bigger changes in the directions.

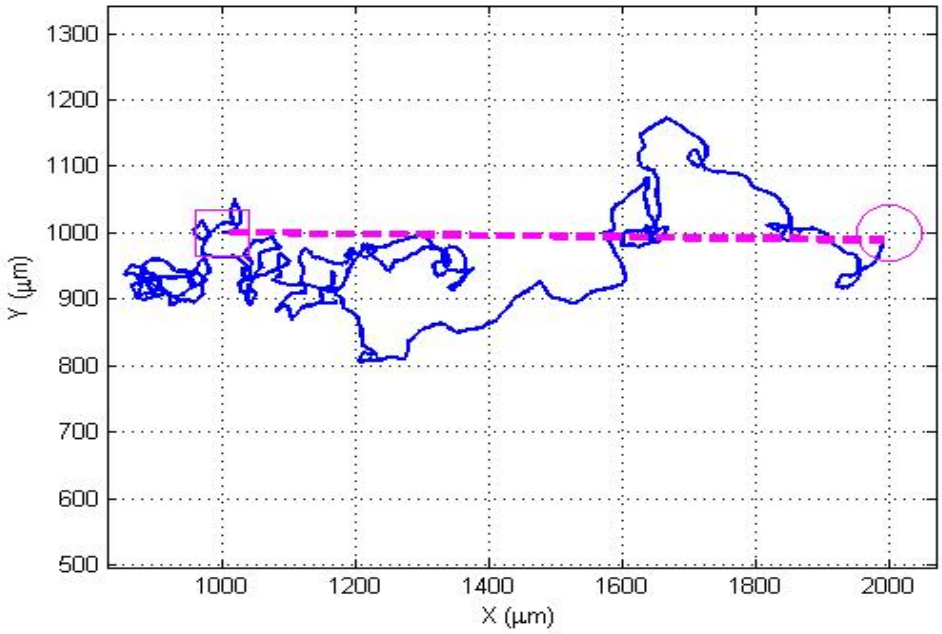


Figure 5.15: Trace of the bacterium from the transmitter (square) to the receiver (circle).

In order to check that the simulation works properly, we obtain how the Run and Tumbling lengths are distributed. If the simulation is correct the Run and Tumbling lengths distribution, which are shown in Figure 5.16 and Figure 5.17, must be equal to the distributions observed in [9] that are shown in Figure 5.7. The Figures of the Run and Tumbling lengths distributions obtained from the simulation follow an exponential distribution, where the mean is 0.1 for the tumbling length and 1.7 for the run length, as in Figure 5.7. Hence, the behavior of the bacteria in terms of Run and Tumbling lengths is correctly modeled.

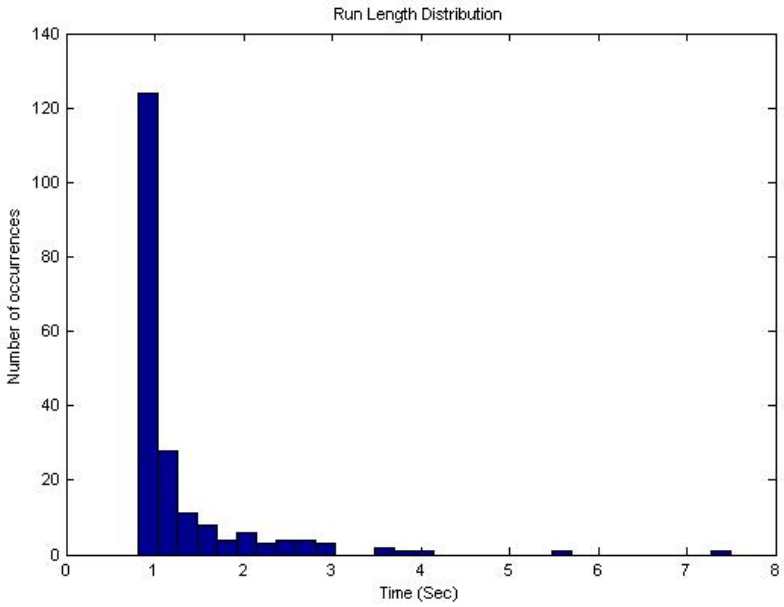


Figure 5.16: Run length distribution

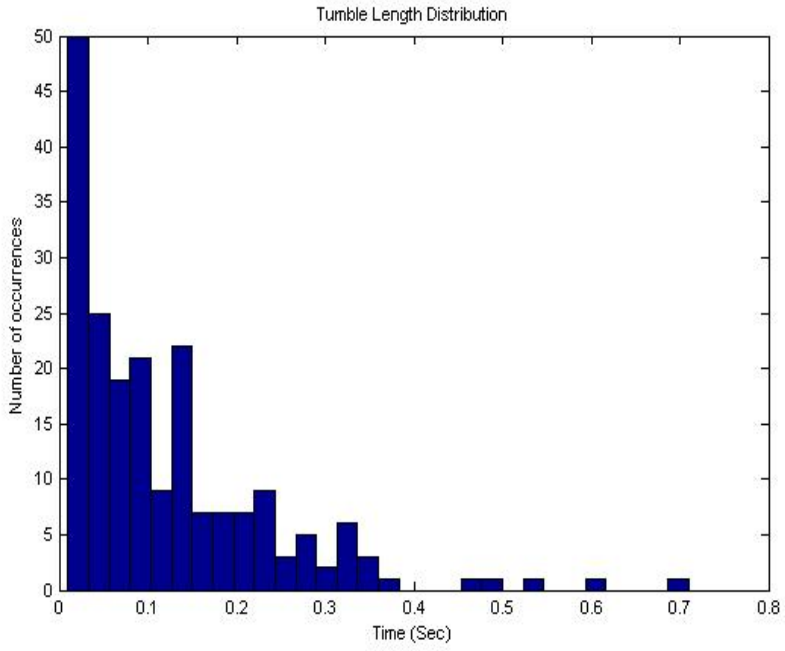


Figure 5.17: Tumble length distribution

The results in terms of the propagation time of the bacteria from the transmitter to the receiver are shown in Figure 5.18. The simulation has been launched 1000 times for different distances, starting at 50 µm until 1mm, in steps of 50 µm. By averaging the different results obtained for a given distance $d(mm)$, we obtain the mean propagation time $t_{prop}(d)$ in minutes as a function of the distance, which is shown in Figure 5.18. The squares show the times obtained through simulation, where, the solid line is an approximation of the propagation time $\hat{t}_{prop}(d)$ by a second order polynomial, which is obtained by a polynomial fitting:

$$\hat{t}_{prop}(d) = 1.82\ \mathrm{d}^2 + \ 4.49\ \mathrm{d} + \ 0.17 \tag{5.29}$$

This second order polynomial $\hat{t}_{prop}(d)$ effectively approximates the mean propagation time $t_{prop}(d)$ in minutes as a function of the distance $d$ in mm.

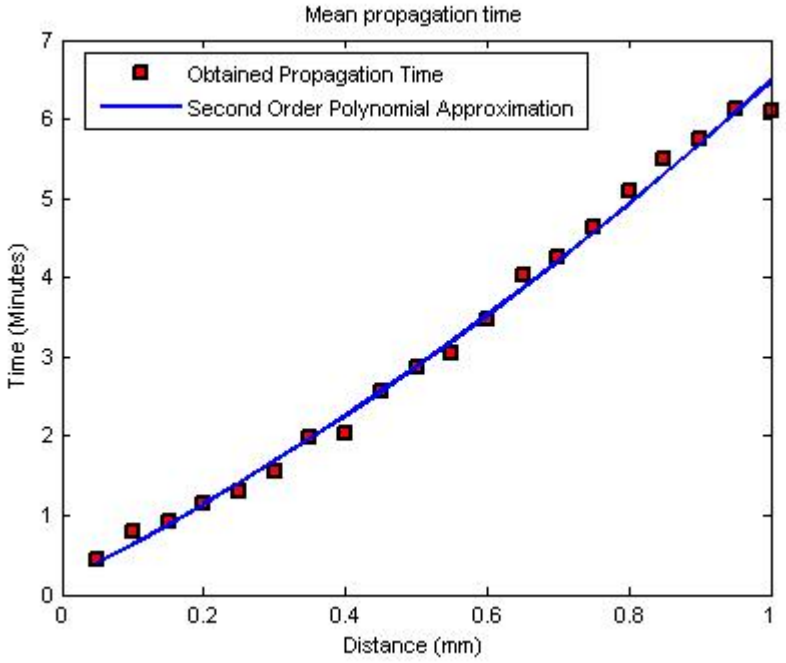


Figure 5.18: Mean Propagation Time using flagellated bacteria

Moreover, for a given distance it is possible to analyze how the arrivals are distributed as a function of the time. The results show that the propagation time of the bacteria exhibits the characteristics of a Poisson process:

$$P_k(t) = \frac{\lambda t \, e^{-\lambda t}}{k!} \tag{5.30}$$

where k is the number of arrivals in a period from 0 to t, and λ is the average arrival rate.

$$\lambda(d) = \frac{1}{t_{prop}(d)} \tag{5.31}$$

Note that the arrival rate decreases with the increase of the distance. This is because the propagation time $t_{prop}(d)$ increases, hence, the bacterium needs more time to reach the receiver. The expected values of the arrival rate λ can be calculated from the simulation values of the propagation time $t_{prop}(d)$ obtained in the simulation, which are shown in Figure 5.18:

$$\lambda(150\ \mu m) = \frac{1}{0.9224}\ \text{min}^{-1} \tag{5.32}$$

$$\lambda(500\ \mu m) = \frac{1}{2.8694}\ \text{min}^{-1} \tag{5.33}$$

$$\lambda(150\ \mu m) = \frac{1}{6.0926}\ \text{min}^{-1} \tag{5.34}$$

Notice that the propagation times of different bacteria are independent of each other, thus, the arrivals of different lengths occur at random. The statistics are Poisson, where the probability per unit time of an arrival is constant. This is demonstrated in the following three figures (Figure 5.19, Figure 5.20 andFigure 5.21) that show the number of bacteria that arrive in each time interval for distances 150, 500 and 1000 μm, respectively. Analyzing these figures it is possible to observe that the arrivals follow a Poisson distribution where the arrival rates coincide with the values in (5.32), (5.33) and (5.34), respectively.

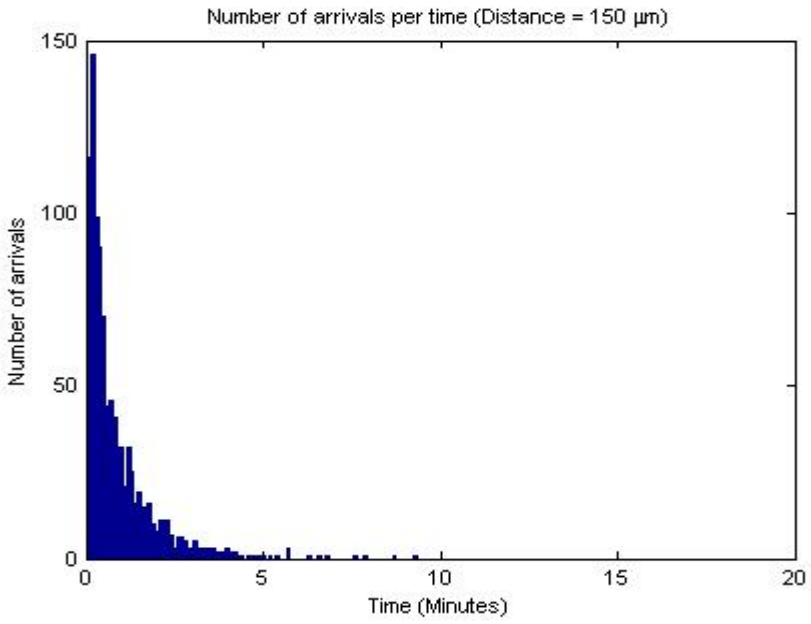


Figure 5.19: Number of arrivals per time for a distance of 150 µm

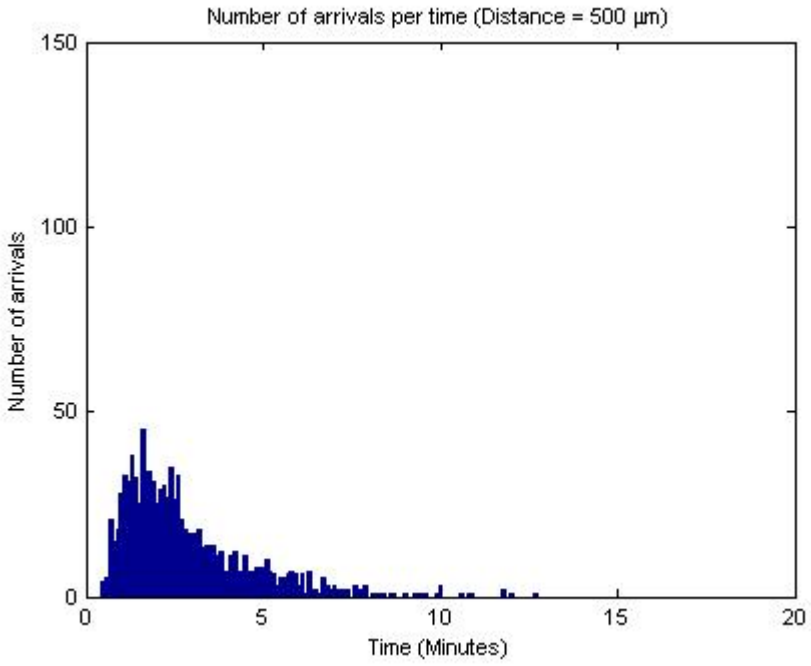


Figure 5.20: Number of arrivals per time for a distance of 500 µm

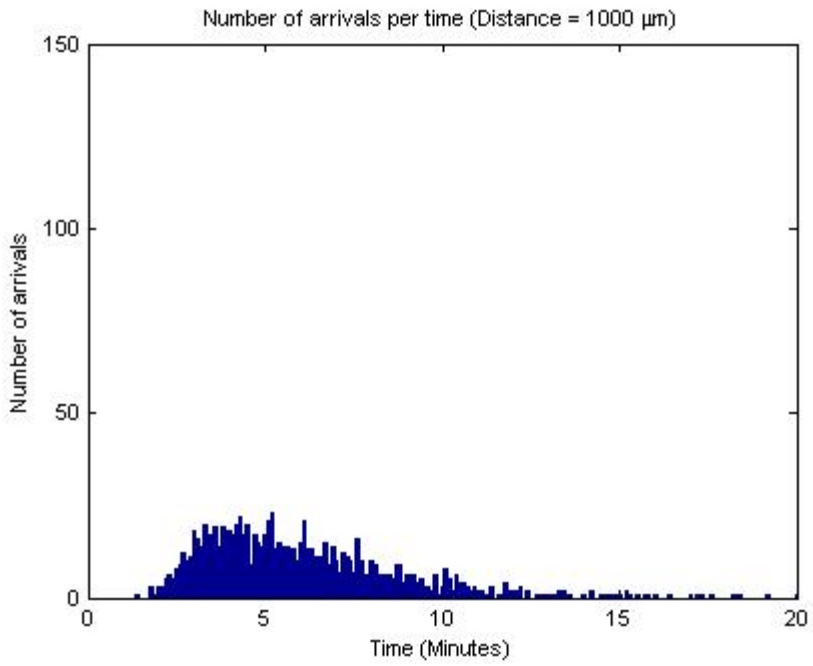


Figure 5.21: Number of arrivals per time for a distance of 1000 µm

Regarding the number of packets lost we found out that all the bacteria reached the destination, this shows us that this communication method can be used for longer distances, maybe reaching a few hundred of micrometers. However, we have not been able to analyze how bacteria behave in longer distances because high computational power and very long simulation times are required.

# Chapter 6

# Physical Channel Model for Catalytic Nanomotors

In this chapter, we aim to obtain the physical channel model in terms of propagation delay and the packet loss probability for a point-to-point communication by using catalytic nanomotors as information carriers. The communication system is formed by a transmitter, a receiver and the channel. Both transmitter and receiver are assumed to be in a fixed position in the space. The channel is composed by a uniform concentration of hydrogen peroxide ($H_2O_2$) solution in water. There exist certain paths created by means of magnetic fields that will lead the nanorod from the transmitter towards the receiver. The communication process is developed as follows:

- The transmitter encodes the desired information in the catalytic nanomotor, as explained in Chapter 4, and releases it to the environment.
- Due to the presence of the magnetic field, the catalytic nanomotor will align and move in the perpendicular direction of the field, which leads the nanorod towards the receiver.
- Finally, the nanorod arrives at the receiver which decodes and processes the information.

Catalytic nanomotors were first developed by [37] where nano-scale engines are created which are able to convert chemical energy into motion. The concept developed in [25] is downscaled which uses catalytic decomposition to power the motion of objects ranging between cm and mm. In this case, the motion is achieved by means of the recoil force of the oxygen bubbles produced in the platinum end. However, it is demonstrated in [37] that in the nano-scale this catalytic motor moves with the platinum end forward, hence, in an opposite way which was expected. This is due to the fact that the movement of nano-scale objects is governed by interfacial forces rather than inertial forces, as explained in 5.1.

Different theories have been proposed [51] in order to physically explain the motion of catalytic nanomotors in hydrogen peroxide solutions and so far there is no general agreement that justifies the energy transduction mechanism that produces the unidirectional motion of catalytic nanomotors. First, it was thought that the movement towards the platinum end was produced due to an inertial tension gradient along the nanorod. The main concept is that the generation of oxygen in the platinum end produces a disruption of the hydrogen bonding of the water molecules, hence, lowering the interfacial tension between the aqueous solution and the gas-coated nanorod [37]. In subsequent work, they proposed an electrokinetic mechanism where the disproportionation of $H_2O_2$ occurs differently in the Pt and the Au:

Platinum (Anode) $$H_2O_2(aq) \rightarrow O_2\,(g) + 2H^+(aq) + 2e^- \quad (6.1)$$

Gold (Cathode) $$H_2O_2(aq) + 2H^+(aq) + 2e^- \rightarrow 2H_2O\,(l) \quad (6.2)$$

Overall $$H_2O_2(aq) \rightarrow O_2\,(g) + 2H_2O\,(l) \quad (6.3)$$

To maintain the charge balance, protons move from the Platinum to the Gold end which results in a flow of water molecules from the Pt to the Au end. This displacement of the water molecules is equivalent to the observed motion of the rod in the opposite direction [51].

In order to obtain a physical channel model, i.e., the propagation time and the packet loss probability, we need to analyze how catalytic nanomotors move in the presence of a certain magnetic field. Taking into account that currently there is no general agreement about the physics that govern the rod movement, we use empirical observations of the directionality of the nanorod to model the propagation delay of the information.

## 6.1 Magnetic Field

Catalytic nanomotors can be aligned in a desired direction, which is perpendicular to the applied magnetic field, by adding short segments of magnetized nickel (length < diameter) in the nanorod. The nanorod orients its net magnetic moment parallel to the magnetic field, resulting in a difference of 90 degrees between the long axis of the rod and the direction of the magnetic field.

In order to interconnect two nodes of the network, a proper magnetic field must be created. If one wants to minimize the propagation delay, the most efficient way would be to control and redirect

the catalytic nanomotor in real time. As it is done in [27], catalytic nanomotors are tracked using the Scanning Electron Microscope (SEM) and the magnetic field is adjusted in order to correct the direction of the catalytic nanomotor. This would be feasible if just a few communication channels must be handled. However, if there are lots of nodes and communication channels in the network, the creation of the magnetic field must be autonomous and should not be controlled from the outside.

We propose two autonomous alternatives for the creation of the magnetic field. However, these alternatives will produce an increase of the propagation delay. The first one, shown in Figure 6.1, is to create the magnetic field, which is represented by dashed lines, by means of a solenoid or a small magnet placed in each of the nodes of the network. As shown by the solid lines, the nanorods have predefined path that joins the transmitter with the receiver. The other alternative is shown in Figure 6.2, where the magnetic field is created by means of a small dipole placed at the receiver node where a small amount of current is circulated. This dipole can be implemented by means of a carbon nanotube as presented in [13]. As shown in Figure 6.2, the magnetic field produced in a certain point is always perpendicular to the radial direction, exactly the direction in which the nanorods will align.

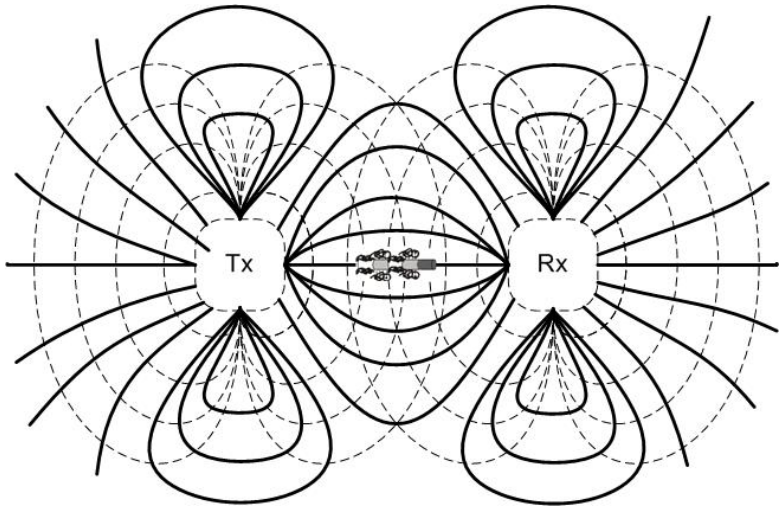


Figure 6.1: Communication scheme using a solenoid to create the magnetic field.

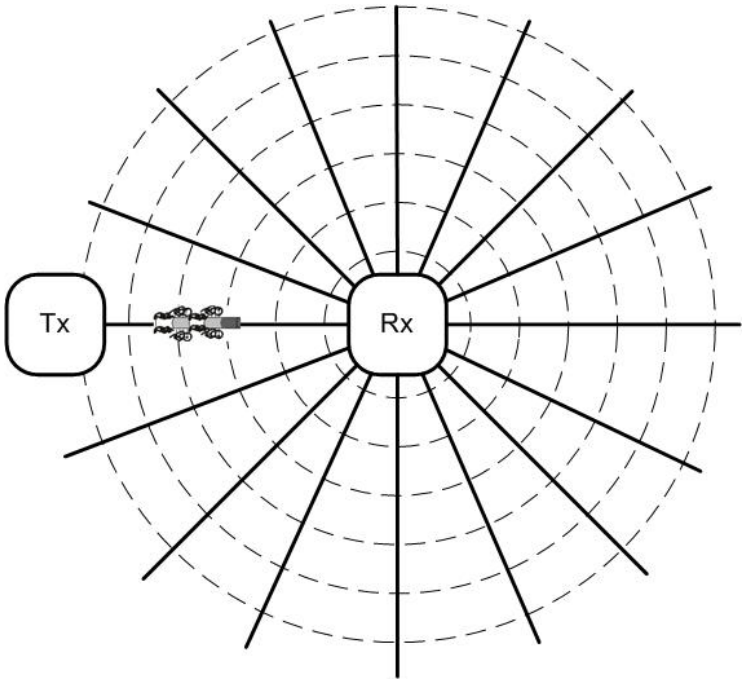


Figure 6.2: Communication scheme using a dipole to create the magnetic field

Comparing both schemes it is easy to notice that the paths created with the dipole are much more effective because they connect the actual position of the nanorod with the receiver in shortest possible direction. However, this scheme has some shortcomings. Note that if for any reason, such as the rotational diffusion or a lack of directionality, the rod turns more than 90 degrees then the rod will start moving in the contrary direction of the receiver and will keep moving away from the receiver until the rotational diffusion produces another 90 degrees of turn in the angle or until the rod arrives at the end of the space. Moreover, when the nanorod is correctly moving towards the receiver, the rotational diffusion can produce that the rod passes the receiver by some micrometers away and then it will keep the same orientation moving away from it. These problems are solved in the first scheme, where if the nanorod is deviated more than 90 degrees by the rotational diffusion it will go back to the transmitter, which will retransmit the packet. When the nanorod passes by the receiver, it will be reoriented by the magnetic field towards the receiver again.

Power consumption is another issue that must be taken into consideration due to nano-machines not having high amounts of power available. In order to avoid high power requirements, we

propose that the nano-machines just generate the magnetic field during small periods of time. Therefore, the nanorod will move freely, in a somehow unidirectional way, during time intervals where there is no magnetic field. Then, the nodes generate the magnetic field which will produce that the rods align with the path. Once aligned, the rods will start moving again in a free manner and so forth. There is a tradeoff between propagation delay and power consumption. The smaller the interval without magnetic field, the smaller is the propagation delay, but the bigger the power consumption (See the simulation results in Section 6.4 to observe a difference in the propagation time). The proposed first scheme has more power consumption than the second one because the magnetic field must be created both in the emitter and the receiver. Moreover, there must be a perfect synchronization between them in order to generate the field in the exactly same instant. The time synchronization of all the nodes in the nanonetwork can be obtained by transmitting a signal from a macro node.

## 6.2 Directionality

Catalytic nanomotors, as bacteria, are objects in the micro scale and their motion is governed by viscous forces rather than by inertial forces. Catalytic nanomotors move in low Reynolds numbers (See Section 5.1) and are affected by the rotational diffusion (See Section 5.4.1) as well as by other factors that produce small changes in the direction of the rod. As stated in the previous section, if the nanorod is significantly deviated, then, when the magnetic field is applied, it will realign with the path but in the wrong direction, producing that the rod moves away from the receiver.

The directionality is used to analyze the center-to-center displacement of the nanorod after a certain period of time $\Delta t$. The directionality $D$ is defined as the cosine of the angle between the rod axis ( $\hat{\mathrm{Z}}$ ) and the direction that it moves ( $\vec{\mathrm{D}}$ ) [37], as shown in Figure 6.3.

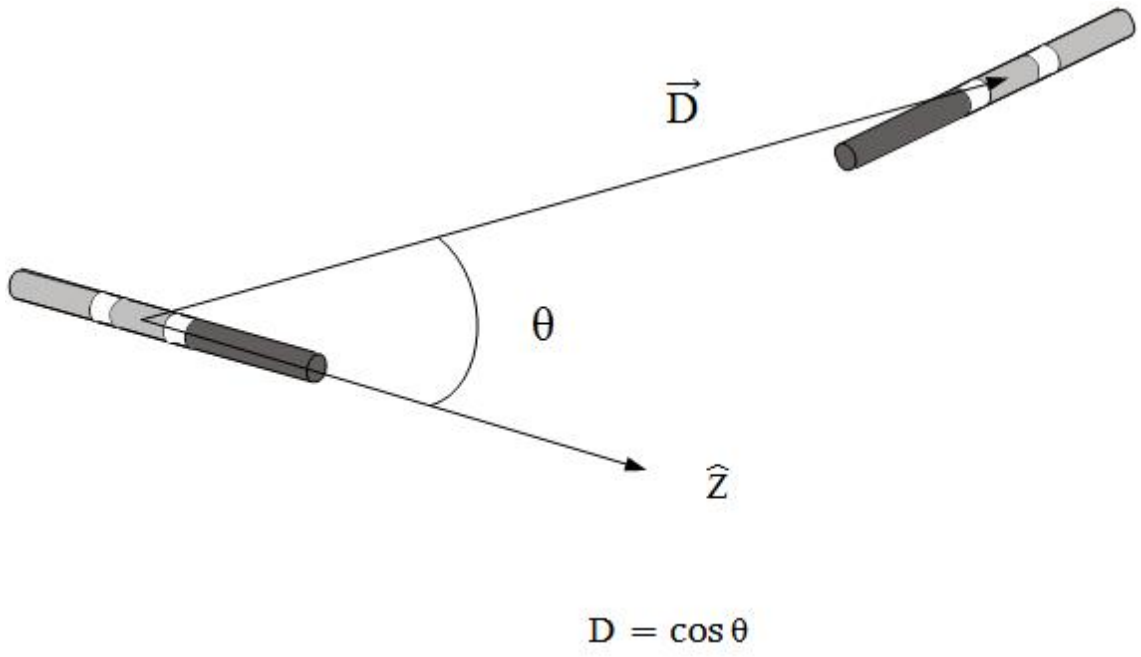


Figure 6.3: Directionality of the catalytic nanomotor

Irregularities in the direction of the rod have been observed and modeled in terms of directionality in [27]. Under a 5% concentration of $H_2O_2$ in water, the nanorods move with a directionality of 0.6 when there is no magnetic field applied [27]. However, with the effect of the magnetic field, the directionality is increased to 0.85. The data are used in order to simulate the movement of the nanorods in the medium.

## 6.3 Simulation Modeling of Catalytic Nanomotors Movement

We have developed a simulation tool that is able to simulate a point-to-point link using catalytic nanomotors as information carriers. This tool takes into account both the directionality factor of the nanorod and the magnetic field.

With this model, we are not only able to obtain the path that a certain nanorod follows but also the required time to reach the receiver, the propagation time. In case that the nanorod does not reach the receiver after a certain time, $t_{max}$, we will assume that the catalytic nanomotor is lost,

and hence, the transmitted packet is lost. Finally, the developed simulation tool allows us to obtain a physical channel model for communications based on catalytic nanomotors.

The pseudocode of the simulation is shown in Figure 6.4 (The complete code can be found in Appendix C). We use the following parameters in the simulation:

- The simulation space is assumed to be a 2-D squared space with a length side of 2 mm, in order to allow the simulation for distances ranging from 50 μm to 1.5 mm.
- The used magnetic field is given in Figure 6.2.
- The directionality factor of the nanorod is 0.6, as observed in [27].
- Different intervals (Ranging from 0.6 to 9 seconds) for the alignment of the rod with the magnetic field have been used.
- The transmitter is always placed in the position $x = 0.1\ mm$ and $y = 0.1mm$.
- The receiver is placed in a distance $d$ from the transmitter. Hence, in the position $x = d + 0.1\ mm$ and $y = 1\ mm$. We have change $d$ in order to simulate different distances.
- In [51], it was reported that catalytic nanomotors can move at velocities around 20 $\mu m/sec$. However, there are recent projects that report the fabrication of ultrafast catalytic alloy nanomotors which can move with velocities of $150\ \mu m/sec$ [15]. In order to ease the comparison with flagellated bacteria, we have used the same value of velocity, thus $v = 20\ \mu m/sec$. Note that the use alloy nanomotors may produce a significant improvement of the propagation delay.
- Initially, the catalytic nanomotor is released in the correct direction, so in the positive direction of the $x$ axis.
- The maximum simulation time is $t_{max} = 3000\ \text{sec} = 50\ \text{min}$. . If the catalytic nanomotor does not arrive at this time, we consider that the packet is lost.
- The catalytic nanomotor reaches the receiver if the distance that separates them is less than 20 μm, which could be the size of a gateway node.
- All the computations are done periodically every 0.1 seconds.

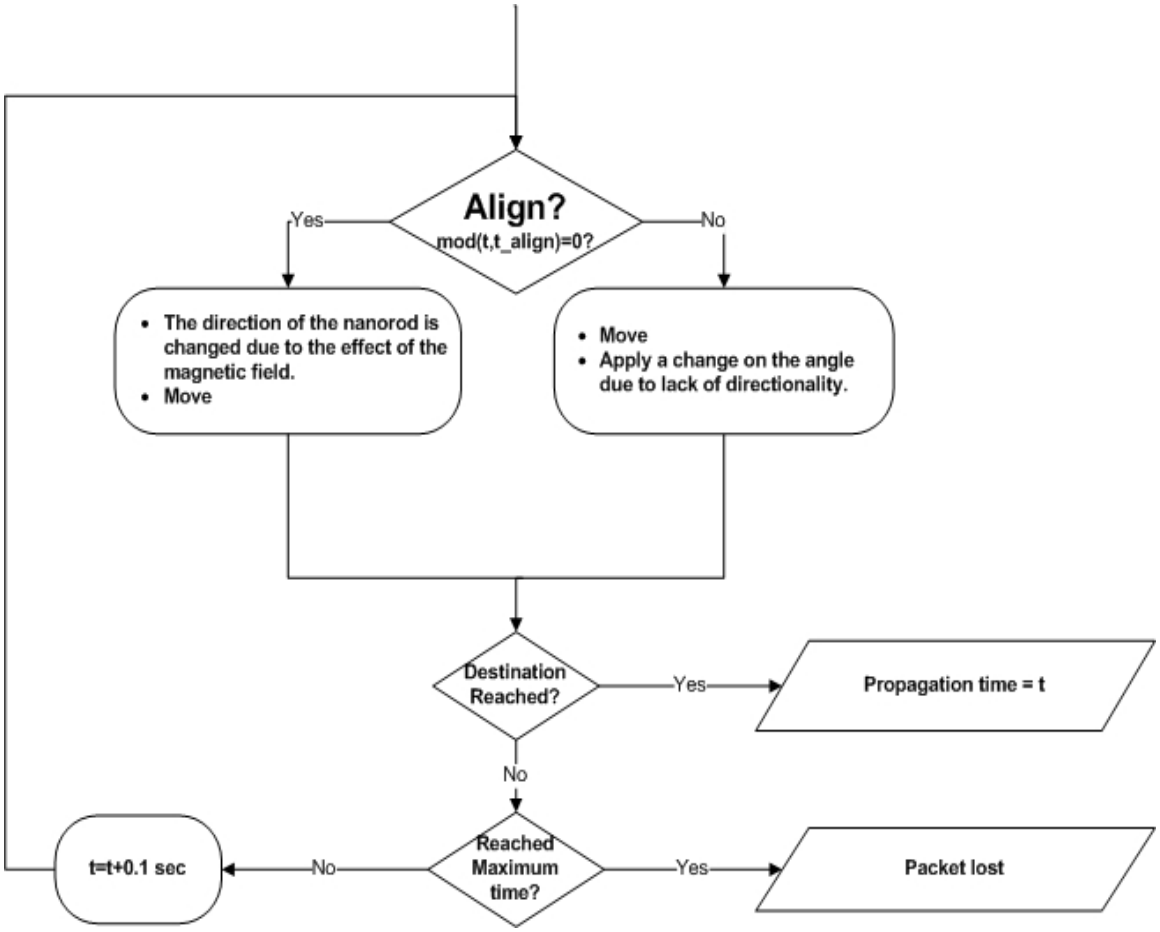


Figure 6.4: Simulation pseudocode for Catalytic Nanomotors

## 6.4 Simulation Results

The trace of a single catalytic nanomotor from the transmitter (square) to the receiver (circle), is shown in Figure 6.5. We observe that the nanorod is biased to move in the radial direction from the receiver and also that the action of the magnetic field sometimes produces that the rod orients in the wrong direction. Moreover, the lack of a complete directionality produces that the nanorod meanders. As shown in Figure 6.5, the catalytic nanomotor usually moves correctly towards the receiver, but at the last moment it passes some nanometers away of it. Then the motor keeps moving away from the receiver until it arrives to the edge of the simulated space. This produces

long delays that can be easily solved by adding a constant magnetic field of less strength. This field will only be sensed by the rod when it is close to the receiver.

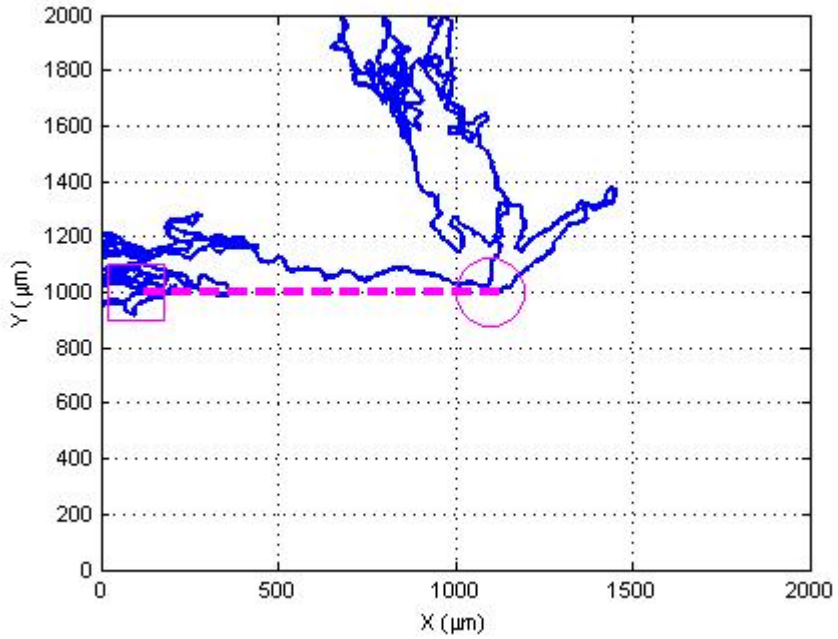


Figure 6.5: Trace of the catalytic nanomotor from the transmitter (square) to the receiver (circle).

The results in terms of propagation time $t_{prop}(d)$ of the catalytic nanomotor from the transmitter to the receiver are shown in Figure 6.6. The simulation has been launched 500 times for different distances, (starting at 50 µm until 1.5mm, in steps of 50 µm) and for different alignment intervals (3,6 and 9 seconds). By averaging the different results, we obtain the mean propagation time $t_{prop}(d)$, which is shown in Figure 6.6. The squares, circles and pentagons show the times obtained in the simulation for the different alignment intervals, three, six and nine seconds, respectively. Whereas, the solid lines are approximations of the propagation time $\hat{t}_{prop}(d)$ by a second order polynomial obtained by polynomial fitting in Matlab. These second order polynomials, which expressions are given in Table 6.1, are mathematical expressions that effectively approximates the mean propagation time in minutes as a function of the distance in mm. By using these polynomials it is possible to calculate the propagation time for the distances that have not been simulated. Note that for alignment intervals bigger than 3 seconds, the propagation delay is really high and the channel capacity is degraded.

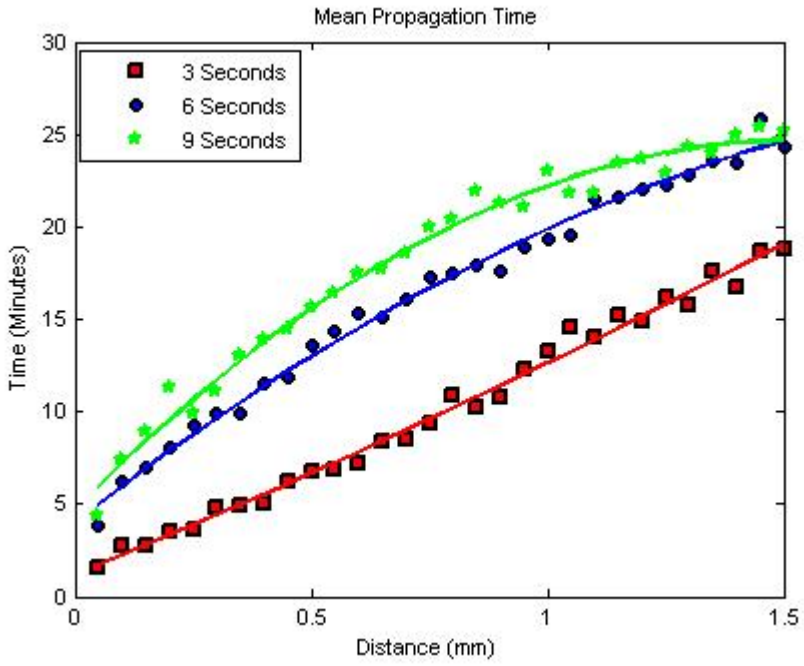


Figure 6.6: Mean Propagation Time for different alignment intervals (from 3 to 9 sec.) using Catalytic Nanomotors.

The results in terms of packet loss probability for alignment intervals of 3, 6 and 9 seconds are shown in Figure 6.7. The system presents really bad behavior because the lost packet rates are really high for the required distances. Using an alignment interval of 6 seconds and looking at a distance of 1mm more than 40 per cent of the packets do not arrive to the receiver in less than 50 minutes. Whereas, using an alignment interval of 9 seconds almost 60 per cent of the packets got lost. Using a 3 seconds alignment interval the lost rate is notably improved and it does not reach the 10 per cent.

Due to the long delays and high error rates, we have run the simulation using smaller values of alignment intervals (from 0.6 to 2.4 seconds). In this case, the propagation delay, which is shown in Figure 6.8, is significantly reduced. The approximation of the propagation times $\hat{t}_{prop}(d)$ by a second order polynomial is also given in Table 6.1 for these alignment intervals. Moreover, we observe that the lost rate drops to zero using alignment intervals smaller than 3 seconds.

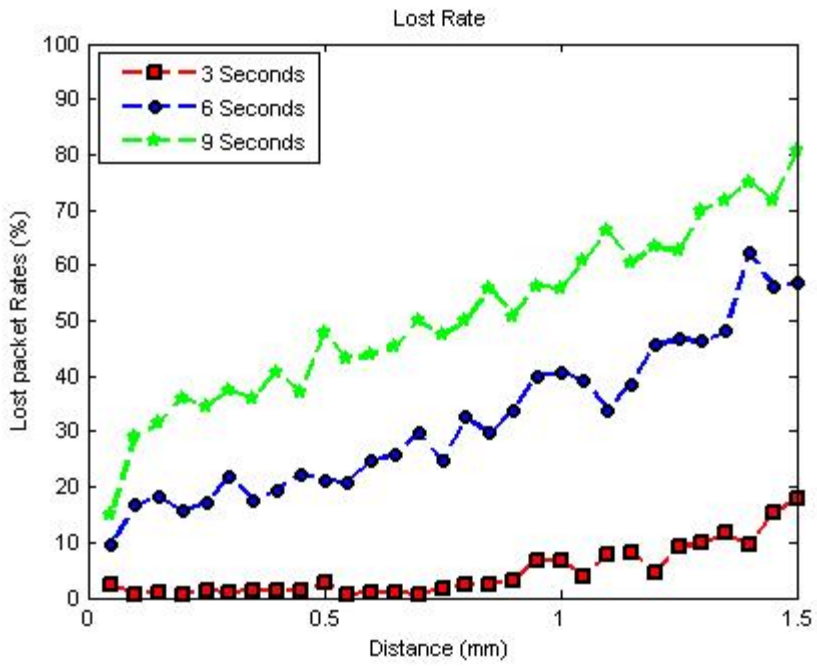


Figure 6.7: Lost Packet Rates for different alignment intervals using Catalytic Nanomotors

| ***Alignment interval*** | ***Polynomial approximation*** |
|---|---|
| 0.6 Seconds | $\hat{t}_{prop}(d) = 0.06\mathrm{d}^2 + 0.88\mathrm{d} - 0.02$ |
| 1.2 Seconds | $\hat{t}_{prop}(d) = 1.14\ \mathrm{d}^2 + 1.54\mathrm{d}$ |
| 1.8 Seconds | $\hat{t}_{prop}(d) = 2.12\ \mathrm{d}^2 + 5.60\ \mathrm{d} + 0.76$ |
| 2.4 Seconds | $\hat{t}_{prop}(d) = \ 3.28\ \mathrm{d}^2 + 6.03\ \mathrm{d} + 0.46$ |
| 3 Seconds | $\hat{t}_{prop}(d) = \ 0.94\ \mathrm{d}^2 + \ 10.53\ \mathrm{d} + \ 1.17$ |
| 6 Seconds | $\hat{t}_{prop}(d) = \ -4.17\ \mathrm{d}^2 + \ 20.03\ \mathrm{d} + \ 4.01$ |
| 9 Seconds | $\hat{t}_{prop}(d) = \ -8.41\ \mathrm{d}^2 + \ 25.95\ \mathrm{d} + \ 4.69$ |

Table 6.1: Second order polynomial approximation of the propagation time (min) as a function of the distance (mm)

One of the open research issues resulting of this work is the optimum alignment interval of the catalytic nanomotors. There exists a tradeoff between the propagation delay and the power required by the nano-machine to create the magnetic field. The smaller the alignment interval, the smaller is the propagation time. Hence, the maximum power that a nano-machine can support must be determined. We conclude that in order to achieve reasonable values of the propagation delay, nano-machines are required to have enough power to generate the magnetic field with intervals smaller than 3 seconds.

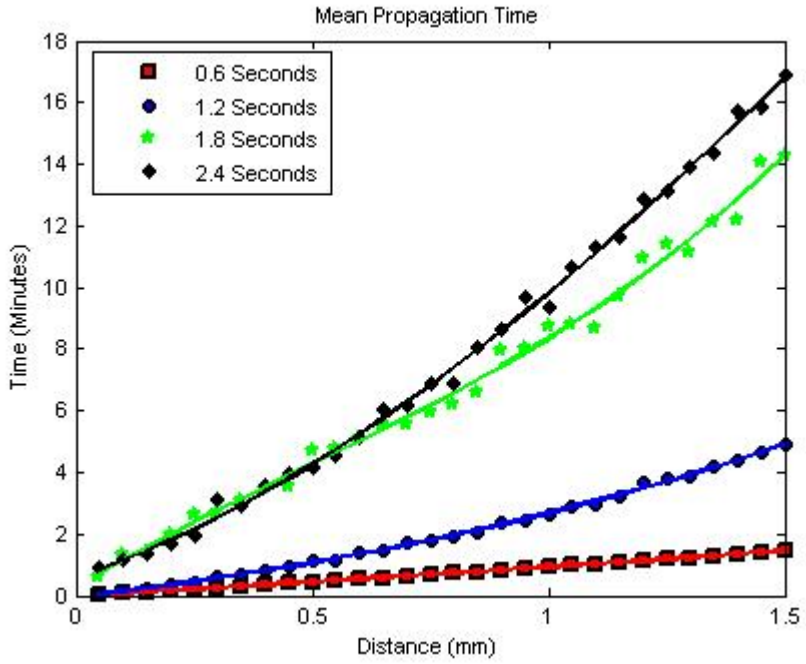


Figure 6.8: Mean Propagation Time for different alignment intervals (from 0.6 to 2.4 sec.) using Catalytic Nanomotors.

For a given distance it is possible to analyze how the arrivals are distributed as a function of the time. The propagation delay of different catalytic nanomotors are independent of each other, thus, arrivals of different lengths occur at random. As happened with bacteria (See Section 5.6), the statistics are Poisson. The probability per unit time of an arrival is constant which expression is given in (5.30). This is demonstrated in Figure 6.9, Figure 6.10 and Figure 6.11 that show the

number of catalytic nanomotors that arrive in each time interval for distances 200, 700 and 1200 μm, respectively. The difference between these figures is that the arrival rate decreases with the increase of the distance. This is because the propagation time $t_{prop}(d)$ increases, hence, the catalytic nanomotor needs more time to reach the receiver.

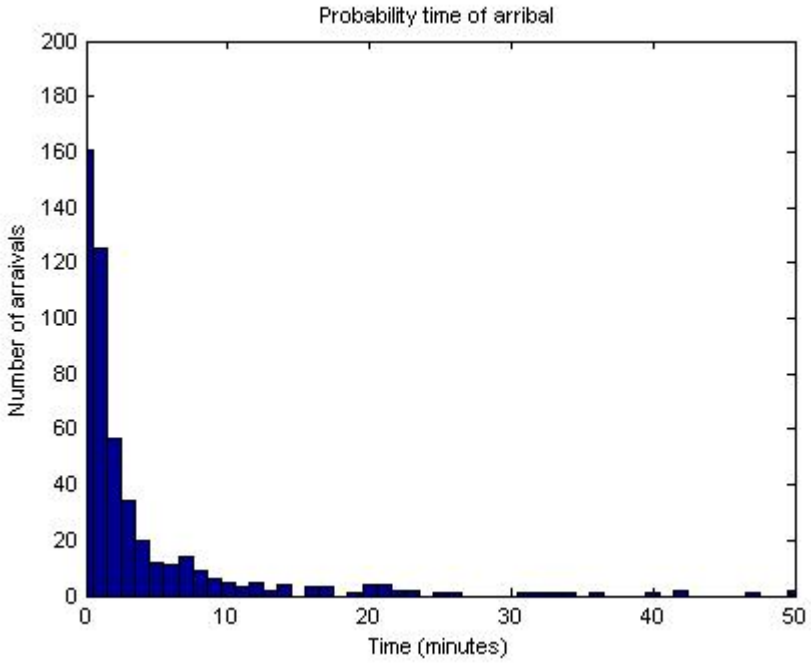


Figure 6.9: Number of arrivals per time for a distance of 200 μm

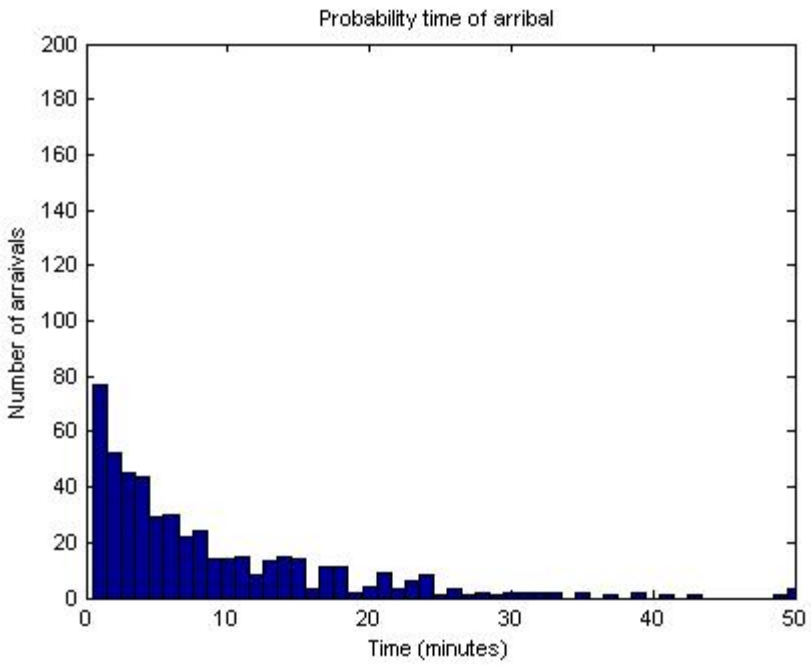


Figure 6.10: Number of arrivals per time for a distance of 700 µm

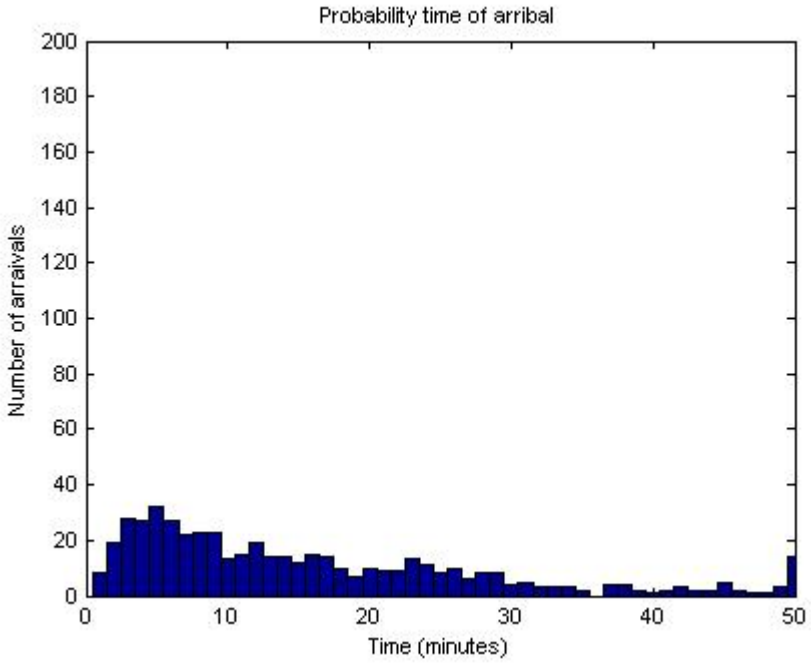


Figure 6.11: Number of arrivals per time for a distance of 1200 µm

# Chapter 7

# Automaton Model of a Flagellated Bacterium for Nano-Machine Design

In the near future, research on nanotechnology will enable the creation of small and simple devices on the nano-scale that will be able to carry out simple tasks. These devices called nano-machines will be programmed as automata and may require communication among them [52].

In this chapter, we propose the design of a nano-machine that will carry the transport of information among nodes of a NanoNetwork. In order to design the communicating nano-machine we have followed the process shown in Figure 7.1.

First, a flagellated bacterium is modeled using automata theory, which is introduced in Section 7.1 (More information regarding automata and automata theory can be found in [24]). This theory is used in order to characterize a bacterium as finite states machine, indeed, as probabilistic finite states automaton, which is done in Section 7.2. We aim that the bacterium automaton model will enable the ICT community to understand the biological processes that occur naturally in biology. Then, the automaton model of the bacterium is improved, in Section 7.3, in order to optimize the features of a flagellated Bacterium. The improved automaton is programmed such a way that the propagation time is minimized. Finally, the scheme of the communicating nano-machine is presented.

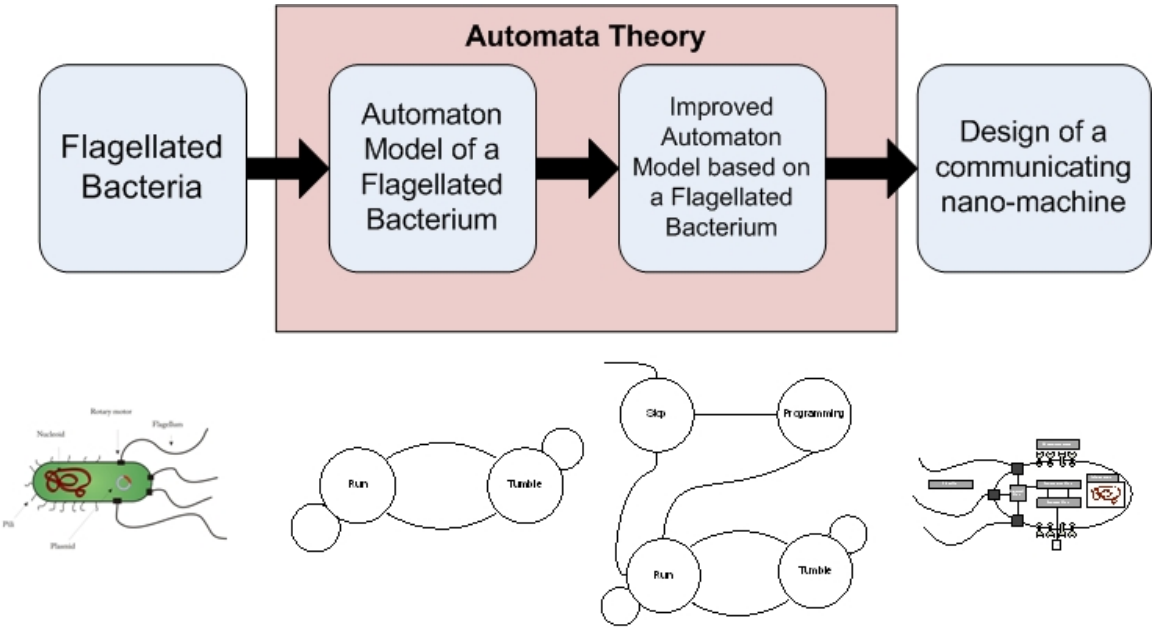


Figure 7.1: Design of a communicating nano-machine

## 7.1 Basics of Language and Automata Theory

Let Σ be a finite and non-empty alphabet which elements are called symbols. Finite sequences of symbols are called words. Let $\Sigma^*$ be the set of all the possible words in Σ, where the empty word is defined by Λ. A language is a subset of $\Sigma^*$. Hence, an automaton is a device which is able to recognize and comprehend a certain language and behave accordingly with the reading of the input symbol and the internal state.

**Definition 7.1:** A *deterministic finite state automaton* is a system $A = \{Q, \Sigma, q_0, \tau, F\}$, where Q is a finite set of the possible internal states of the automaton A, Σ is a finite alphabet, $q_0$ is the initial state, τ is the transition function ($\tau: Q \times \Sigma \rightarrow Q$) and F is a subset of Q, the set of final or acceptance states.

The automaton reads the input, which will be a symbol of Σ, and computes the next state $q'$ as a function of the input, say $a$, and the present state $q$ using the transition function, thus, $q' = \tau\,(a, q)$. Then, the automaton moves to state $q'$ and reads the new input symbol of the system, $b$, and again computes the next state, $q''$, as a function of τ, $q'' = \tau\,(b, q')$.

The automaton is called deterministic because for every input signal of Σ and for every possible state $q \in Q$ the function τ gives one and only one possible next state $q'$. However, sometimes is more practical to relax this behavior, so enabling the automaton to either have some transitions not defined or more than one transaction defined. The non-deterministic automaton allows this behavior by defining τ as a relation instead of as a function [24].

**Definition 7.2**: A *non-deterministic finite stat*e *automaton* is a system $\mathrm{B} = \{\mathrm{Q}, \Sigma, \mathrm{q}_0, \delta, \mathrm{F}\}$, where Q is a finite set of the possible internal states of the automaton B, Σ is a finite alphabet, $\mathrm{q}_0$is the initial state, δ is the transition function : $\mathrm{Q} \times \Sigma \rightarrow \mathrm{P(Q)}$ , where P(Q) denotes the power set of Q, the set of all possible subsets of Q, and F is a set of final or acceptance states.

In a non-deterministic automaton $\delta$ is not required to be a function from $\mathrm{Q} \times \Sigma$ to Q as it was for the Deterministic Finite State automaton, but a general description that associates, a certain subset of Q, the subset of possible future states, for every input symbol from $\Sigma \cup \Lambda$ and present state $q \in Q$. Notice that now the empty set Λ is allowed as input signal and that given a certain input signal and state a finite number of different states are possible. The Probabilistic finite state automaton is a particular case of non-deterministic automaton that decides which will be the next state accordingly to certain transitions probabilities.

**Definition 7.3** : A *probabilistic finite state automaton* is a system $\mathrm{C} = \{Q, \Sigma, \delta, \pi, F\}$, where Q is a finite set of the possible internal states of the automaton $C$, Σ is a finite alphabet, $\delta$ is the transition function $\delta$: $\mathrm{Q} \times \Sigma \times \mathrm{Q} \rightarrow [0,1]$, π is the probability of the starting in each of the states $\pi : \mathrm{Q} \rightarrow [0,1]$ and F is a set of final or acceptance states.

Let $P_{qq'}(a) = \delta(q, a, q')$ be the probability to move from state $q$ to state $q'$ when the symbol $a$ is read. A probabilistic finite state automaton must verify equations (7.1) and (7.2):

$$\sum_{\mathrm{q} \in \mathrm{Q}} \pi(\mathrm{q}) = 1 \tag{7.1}$$

$$\sum_{\mathrm{q}' \in \mathrm{Q}} P_{qq'}(a) = 1 \tag{7.2}$$

Therefore, the probability of observing the sequence of states $s = q_1, q_2, q_3, q_4, q_5$ when the symbols read are $r = a, a, b, b$ is given by:

$$\mathrm{P(s)} = \pi(q_1)\, P_{q_1 q_2}(a)\, P_{q_2 q_3}(a)\, P_{q_3 q_4}(b)\, P_{q_4 q_5}(b) \tag{7.3}$$

## 7.2 Automaton Model of a Flagellated Bacterium

The behavior of a bacterium, as explained in Chapter 5 from a biological perspective, matches perfectly a probabilistic finite state automaton since the changes between the running and tumbling states are probabilistic and its probability density functions have been modeled, as explained in Section 5.4.2. The probabilistic finite state automaton that models a flagellated bacterium is defined by $\theta = \{Q, \Sigma, \delta, \pi, F, O\}$:

- **States (Q):** E. coli bacterium clearly has two internal states either to run or to tumble. Hence, a bacterium can be modeled as a two state probabilistic automaton.
- **Alphabet (Σ):** The input in the system, the variable that the bacterium can read, is the concentration of attractant particles on the environment.
- **Transition Function ($\boldsymbol{\delta}$):** The bacterium changes from run to tumble or vice versa according to the concentration it senses from the environment. Hence, the future state $q'$ depends both on the input and the current state $q$. Where, $\lambda(t)$ is the mean run length computed by low-filtering the concentration as explained in Section 5.4.4. A summary of the probabilities of each of the possible state transactions is given in Table 7.1, where it can be seen that Equation (7.2) is satisfied.

| State transition probabilities $\boldsymbol{P_{qq'}(c)}$ | $\boldsymbol{q' = Run}$ | $\boldsymbol{q' = Tumble}$ |
|---|---|---|
| $\boldsymbol{q = Run}$ | $P_{qq'}$=1-$\frac{1}{\lambda(t)} e^{-t/\lambda(t)}$ | $P_{qq'}$=$\frac{1}{\lambda(t)} e^{-t/\lambda(t)}$ |
| $\boldsymbol{q = Tumble}$ | $P_{qq'}$=$\frac{1}{0.1\ sec} e^{-t/0.1}$ | $P_{qq'}$=1-$\frac{1}{0.1\ sec} e^{-t/0.1sec}$ |

Table 7.1: State Transition Probabilities of the bacterium automaton model.

- **Initial State Probability (π):** In the beginning the bacterium is initially running or tumbling with probabilities $\pi(q_1 = Run)$ and $\pi(q_2 = Tumble)$. These probabilities

must satisfy Equation (7.2). In our simulations we assumed these probabilities as $\pi(q_1 = Run) = 1$ and $\pi(q_2 = Tumble) = 0$.

- **Acceptance States (*F*):** The acceptance states or final states are the empty set $\Lambda$, the bacterium will keep *living* until some external fact damages the automaton.
- **Output (O):** There are two outputs in the automaton of the bacterium, the velocity and the direction at which the bacterium is moving. The values are given in Table 7.2. On the one hand, when the bacterium is in the running state it moves at constant velocity and the changes in direction are given by the rotational diffusion $\phi$, as explained in Section 5.4.1. On the other hand, when the bacterium is tumbling, the velocity is $v = 0\ \mu m/sec$, thus, the only change in direction that must be taken into account is the overall change between runs which is given by $\gamma$ as explained in Section 5.4.3.

| **Outputs** | **Running State** | **Tumbling State** |
|---|---|---|
| **Velocity** | $v = 20\ \mu m/sec$ | $v = 0\ \mu m/sec$ |
| **Angle** | $\theta_{n+1} = \theta_n + \phi$ | $\theta_{RUNn+1} = \theta_{RUNn} + \gamma$ |

Table 7.2: Outputs of the bacterium automaton model.

Finally, the entire bacterium automaton model is given in Figure 7.2.

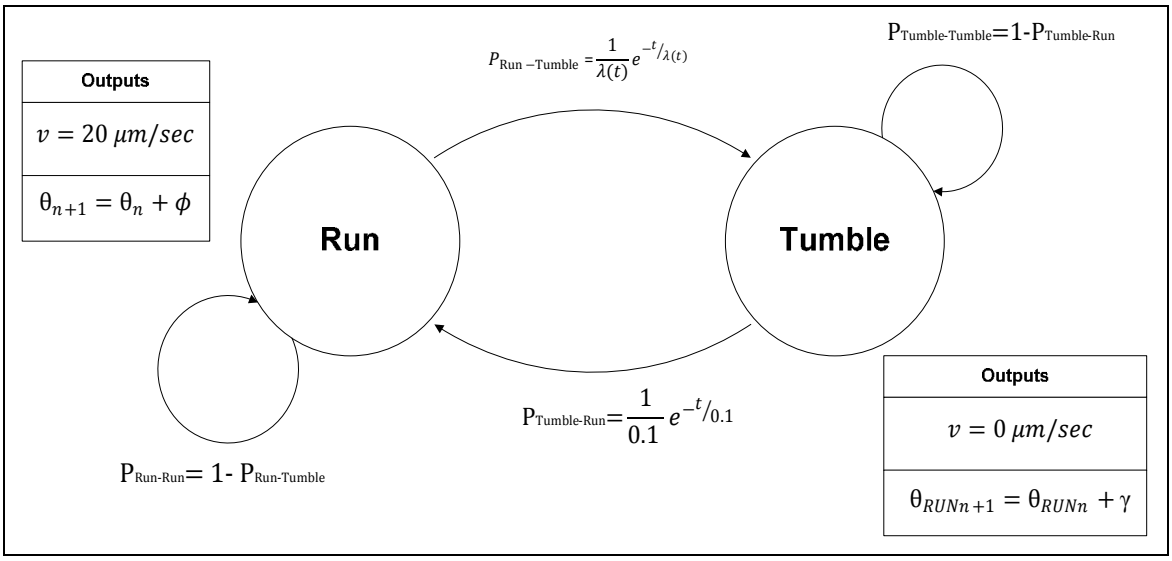


Figure 7.2: Automaton model of E. coli bacterium

## 7.3 Design of an Improved Automaton Model based on a Flagellated Bacterium

The automaton model proposed in this section is an improvement of the automaton model of the flagellated bacterium presented in the previous section. This automaton can be used in order to transport any type of cargo between two points in the nano-scale. We are mainly concerned in the transport of information that can be stored either as DNA molecules or in any other format. This automaton will carry out the same tasks that bacterium does, but in a smarter and more efficient way. For instance, in the simulations developed in Chapter 5, we observe that usually the bacterium stops and changes its direction when it is going to the correct direction. This produces an unnecessary increase in the propagation time and hence a degradation of the system capacity.

The improved automaton is able to minimize the propagation time by doing some signal processing of the sensed concentration $c(t)$. This signal processing will not only allow the reduction of the propagation time, but also the creation of different communication channels. These channels are created by modulating the released concentration in a certain frequency that will be tuned by the communicating nano-machine.

The entire automaton model is given in Section 7.3.1, where, the signal processing carried out internally by the automaton is presented in Section 7.3.2.

### 7.3.1 Improved Automaton Model

The improved automaton is defined by $\vartheta = \{Q, \Sigma, \delta, \pi, F, O\}$ :

- **States (Q):** Since the proposed automaton is based on the automaton of a flagellated bacterium, the automaton has the *run* and *tumble* states. Moreover, this automaton has two more states, namely, *stop* and *programming*. The stop state is used in order to keep the machine attached to a certain node until it receives a task. When this task is received the automaton moves to the programming state, where the node sends to the device the information that must be transmitted and the address of the receiver's node.

- **Alphabet (Σ):** The system has two input signals, $c(t)$ and $b(t)$ . The first input $c(t)$ is the concentration of attractant particles on the environment. From where, the device is able to extract the frequency of the signal and localize the receiver. A second signal, $b(t)$, is created by the nodes using a different type of molecules to transmit information to the device. This signal, e.g., calcium signaling, is transmitted in small amounts and is used when the device is close to the node to transmit control information. The information sent through the private control channel $b(t)$ triggers internal reactions in the device.

- **Transition Function ($\delta$):** When the device is in the running state and is able to receive a certain sequence through the control channel, $b(t) = s_1$, it means that it has reached the receiver and that it must stop. Then the machine remains attached to the node until it receives a sequence, $b(t) = s_2$, which means that the node has new information to be transmitted. The signal $b(t) = s_2$ triggers a change on the state of the machine from Stop to Programming. In the programming state the node transmits to the machine through $b(t)$ all the information regarding the new communication. When all the information has been transmitted, the node sends another specific sequence, $b(t) = s_3$, and then the device changes to the run state and start moving towards the receiver. Notice that all these changes of state are deterministic and depend on specific sequences of the input signal $b(t)$. Where, the changes between runs and tumbles are still probabilistic. We

assume that the probability of a change from tumble to run is distributed in a similar way than in the automaton of the bacterium (Section 7.2), thus, the time required by the automaton to change the direction is in the same order of magnitude that the time required for a bacterium. Finally, the probability of changing from run to tumble is exponentially distributed with a mean run length z(t). The mean run length takes a new value in every synchronous time of the automaton. This value is computed as a function of both the output y(t) of filtering the previous samples of the concentration, and the analysis of frequency changes over time, thus, $z(t) = f(y(t), \Delta f_s)$, as explained in more detail in Section 7.3.2. The table of states transitions can be found in Table 7.3.

| **State transition probabilities $P_{qq'}(c)$** | $q' = Stop$ | $q' = Programming$ | $q' = Run$ | $q' = Tumble$ |
|---|---|---|---|---|
| $q = Stop$ | $b(t) \neq s_2$ | $b(t) = s_2$ | ----- | ----- |
| $q = Programming$ | ----- | $b(t) \neq s_3$ | $b(t) = s_3$ | ----- |
| $q = Run$ | $b(t) = s_1$ | ----- | $P_{qq'}$=1-$\frac{1}{z(t)} e^{-t/z(t)}$ | $P_{qq'}$=$\frac{1}{z(t)} e^{-t/z(t)}$ |
| $q = Tumble$ | ----- | ----- | $P_{qq'}$=$\frac{1}{0.1\ sec} e^{-t/0.1}$ | $P_{qq'}$=1-$\frac{1}{0.1\ sec} e^{-t/0.1}$ |

Table 7.3: State Transition Probabilities for the communicating nano-device.

- **Initial State Probability (π):** The automaton is initially placed in one node in the stop state waiting for orders from the node. Therefore, $\pi(q_1 = Stop) = 1$, $\pi(q_2 = Programming) = 0$, $\pi(q_3 = Run) = 0$ and $\pi(q_4 = Tumble) = 0$.
- **Acceptance States (*F*):** The acceptance states or final states are the empty set Λ.
- **Output:** As occurred with the automaton of the bacterium, this finite state machine has two possible outputs, which are used to modulate the signal that goes to the rotary motors, the velocity and the direction at which the bacterium is moving. The values are

given in Table 7.4. On the one hand, when the automaton is running it moves at a constant velocity and the changes in direction are given by the rotational diffusion $\phi$, as seen in Section 5.4.1 On the other hand, when the bacterium is tumbling, then the velocity is $v = 0\ \mu m/sec$. Thus, the only change in direction that must be taken into account is the overall change $\alpha$ between runs. This angle is internally calculated by the automaton using equation (7.11). A summary of the outputs in every state is given in Table 7.4

| **Outputs** | **Stop** | **Programming** | **Running** | **Tumbling** |
|---|---|---|---|---|
| **Velocity [ µm/sec ]** | $v = 0$ | $v = 0$ | $v = 20$ | $v = 0$ |
| **Angle [ Rad ]** | $\theta = 0$ | $\theta = 0$ | $\theta_{n+1} = \theta_n + \phi$ | $\theta_{RUNn+1} = \theta_{RUNn} + \alpha$ |

Table 7.4: Outputs of the communicating nano-device automaton.

The proposed automaton model of the communicating nano-machine is presented in Figure 7.3.

### 7.3.2 Analysis of Frequency Changes over Time (Calculation of z(t))

The propagation delay is minimized by means of the signal processing carried out internally by the automaton. The automaton computes the mean run length $z(t)$ as a function of the output $y(t)$ of filtering the sensed concentration and the analysis of frequency changes over time $\Delta f_s$.

$$z(t) = f(y(t), \Delta f_s) \tag{7.4}$$

#### A. Filtering the Concentration

As explained in Section 5.4.4, bacteria filter the sensed concentration with a low pass filter that has a cutoff frequency of $fc = 0.636Hz$. The results of the filtering affect the probability of changes from the run to tumble state. However, for the designed communicating nano-machine this filter is a variable parameter from where is possible to obtain powerful features.

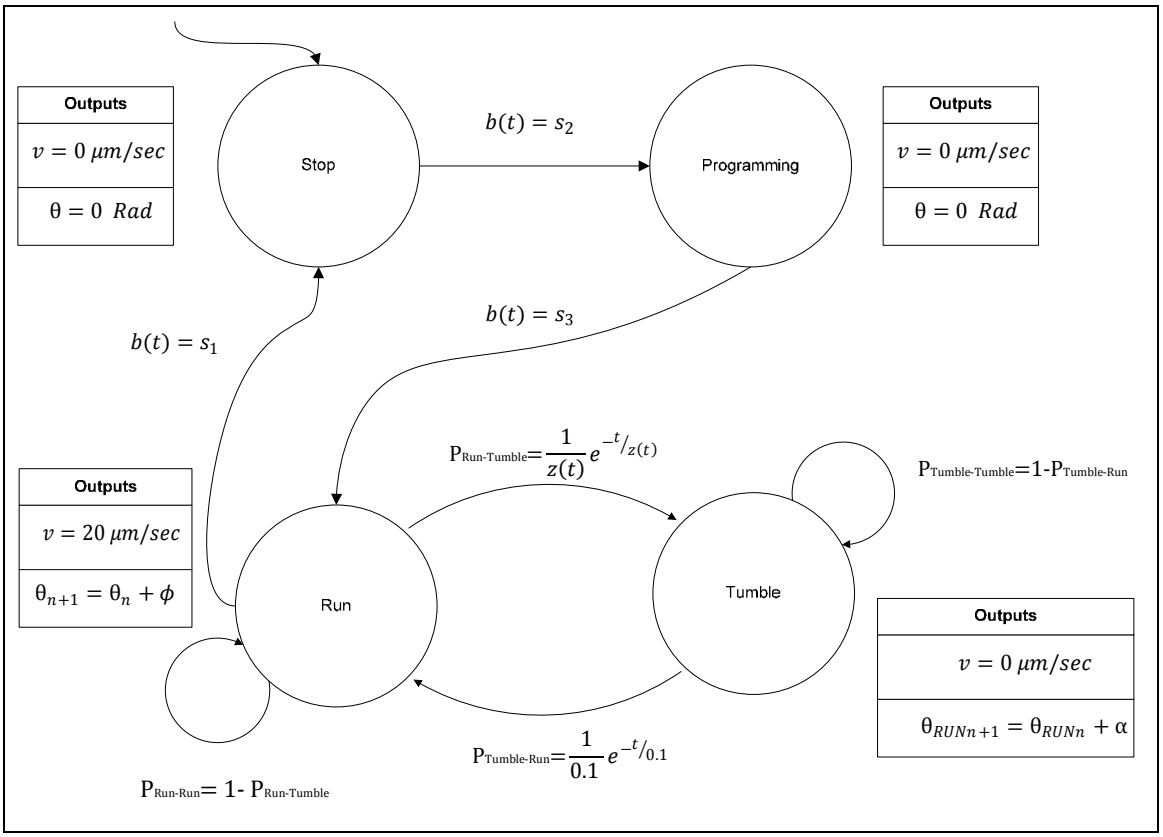


Figure 7.3: Automaton model of the communicating nano-machine

If each receiver is releasing the concentration of attractants using a certain and unique frequency, which is known by the other nodes of the network, then the device can propel itself towards the desired receptor just by changing the impulse response of the band pass filter h(n) to the desired frequency, as shown in Figure 7.4.

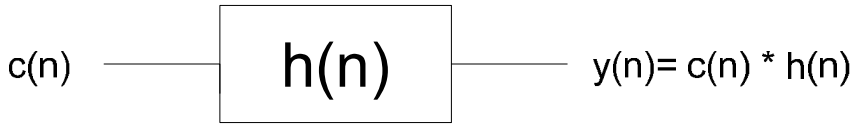


Figure 7.4: Filter of the sensed concentration

## B. Doppler Effect

The frequency received by the device is subject to the Doppler Effect because the device is moving either towards the source of particles, the receiver, or in the opposite direction. Hence,

the device can easily determine whether it is going to the right or the wrong direction just by analyzing sensed frequency:

$$f_s = f_0(1 + \frac{v_\rho}{v_s}) \tag{7.5}$$

where $f_0$ is the frequency at which the receiver is releasing the particles, $v_s$ is the velocity of the signal and $v_\rho$ is the projection of the velocity of the nano-machine in the straight line that leads the machine to the receiver.

The projection of the velocity $v_\rho$ can be expressed as:

$$v_\rho = v_0 \cos \alpha \tag{7.6}$$

where $v_0$ is the velocity at which the device is moving and $\alpha$ is the angle between the current direction and the desired direction, which is distributed between 0 and 180 degrees, as shown in Figure 7.5. Since the nano-machine uses the rotary motors and flagella of bacteria, we assume that it will be able to reach velocities in the same order than bacteria, thus, $v_0 = 20\ \mu m/sec$.

A closed expression for the propagation velocity $v_s$ of a wave of concentration is not trivial to find and it is a research challenge that must be addressed (more information regarding this can be found in [50]). The main difference between wave equation (7.7) and second Fick's law of diffusion (5.6) is that the wave equation relates the Laplacian of the magnitude with the second derivative with respect to the time. This allows the definition of the velocity which relates linearly time and the distance.

$$\frac{\partial^2 u}{\partial t^2} = c^2\, \nabla^2 u \tag{7.7}$$

However, in Fick's law the Laplacian of the magnitude is related only to the first derivative with respect to the time. Therefore, we expect to have an expression of the velocity that is not linear with time or, what is the same, with distance.

$$\frac{\partial c}{\partial t} = D\, \nabla^2 c \tag{7.8}$$

As we have stated previously, it is far from the scope of this work to find a closed expression for the velocity of the wave. However, in order to show the advantages that the use of the Doppler

effect would produce, we have assumed that the velocity of the wave is inversely proportional to the distance from the source (where A is a constant that takes into account the different parameters of the system). We use this assumption because it is known that diffusion is fast for short distances but slow if long distances should be reached.

$$v_s(\rho) = \frac{A}{\rho} \tag{7.9}$$

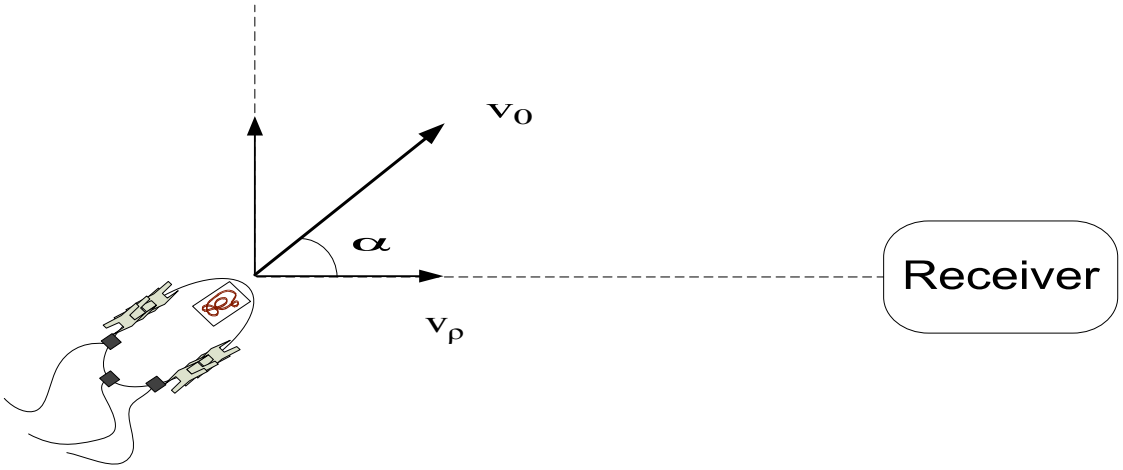


Figure 7.5: Velocity of the communicating nano-machine towards the receiver

Combining equation (7.6) and (7.9) in equation (7.5) , we obtain:

$$f_s(\rho) = f_0\left(1 + \frac{v_0 \cos\alpha}{A}\,\rho\right) \tag{7.10}$$

Notice that in this case, the Doppler frequency not only depends on the velocity at which the receiver is moving, but also on the distance ρ between the emitter and the receiver.

A plot of how the frequency relation $f_s/f_0$ changes as a function of the distance ρ is shown in Figure 7.6. Two possible traces have been plotted by taking the extreme values for the slope of the function. The maximum slope is produced when the nano-machine is moving towards the receiver through the shortest path, thus, the angle α is 0. In this case, the slope of the function takes a value of 5000 $m^{-1}$(Taking A as four times the diffusion coefficient). The minimum value

of the slope is produced when the nano-machines are going exactly to the opposite direction, $\alpha = 180$ , and then the slope is negative with the same value.

As an example, imagine a particular case where the receiver is emitting particles at a frequency $f_0 = 1$ Hz and the nano-machine is correctly tuned at this frequency. Assume that the device is swimming exactly in the best possible direction ($\alpha = 0$) and in a distance of $\rho = 3$ μm . In this case, the machine is moving in the line marked with squares following the arrow (See Figure 7.6). The device knows that if it keeps going in the right direction, the sensed frequency will decrease until $f_0$ is reached. Hence, it has to find the path where it senses the maximum negative slope, while the relation $fs/fo$ is over one. Now imagine that for any reason, e.g., the rotational diffusion, it is moved away from the correct path and its new direction is completely the opposite. The device will sense a jump on the frequency which will move from the 1.015 Hz sensed in the correct direction, to the 0.985 Hz sensed currently. The device knows that it must change the direction, thus, it changes from the run to the tumble state.

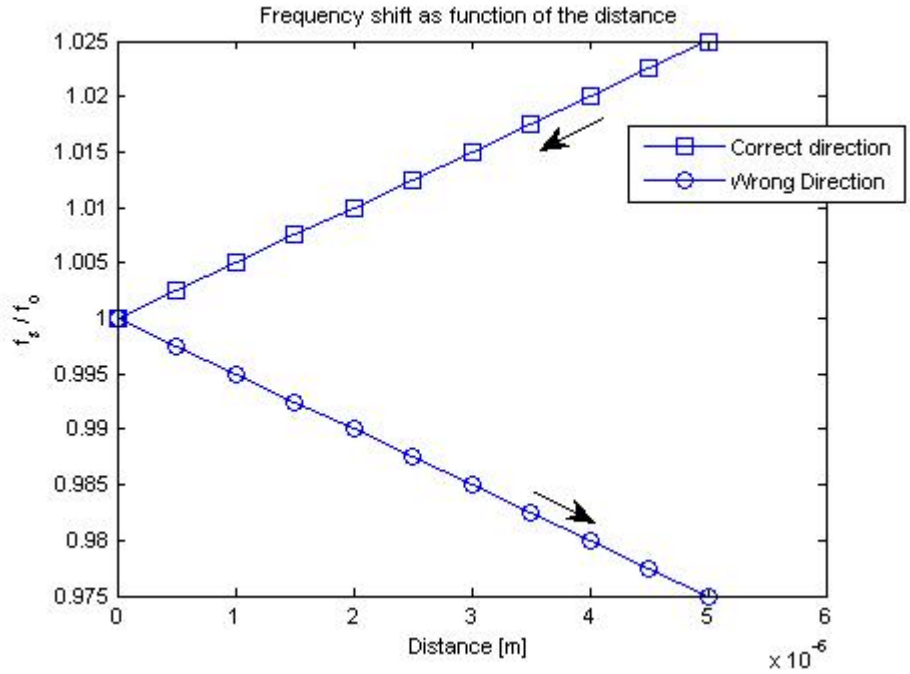


Figure 7.6: Frequency shift as function of the distance

One may wonder how the device will decide the next direction to take among all the possible directions of the space. There exists an easy way for the nano-machine to compute α, hence, the device knows which is the angle that separates its current direction with the best possible direction. This reduces the number of possible changes of direction to just two angles, either to turn α radians to the left or to turn α radians to the right. The α can be computed using equation (7.11). The demonstration of how this expression is reached is in Annex A.

$$\cos\alpha = \begin{cases} \sqrt{\dfrac{-A}{f_0\,\Delta t\,{v_0}^2}\,[f_s(\rho_2) - f_s(\rho_1)]}, & f_s(\rho_i) > f_0 \\ -\sqrt{\dfrac{-A}{f_0\,\Delta t\,{v_0}^2}\,[f_s(\rho_2) - f_s(\rho_1)]}, & f_s(\rho_i) < f_0 \end{cases} \tag{7.11}$$

where it is assumed that the angle α is constant in the interval Δt, thus, that the rotational diffusion does not have a notable influence over the angle for short periods of time.

## 7.4 Design of a Communicating Nano-Machine based on Flagellated Bacterium Automaton Model

By the time that two nano-machines require communication, the resources and knowledge in nanotechnology will be wide. There will exist powerful tools that will allow the creation of nano-machines that will be programmed as automata. In this section, we propose the creation of a nano-robot specially designed to carry messages between nano-machines. This nano-robot will be programmed using the automaton proposed in Section 7.3.

The proposed communicating device is shown in Figure 7.7. We assume that it will be created following the bio-inspired approach (See Section 1.2 C), hence, elements already present in nature will be used as building blocks to crate the nano-machine. Flagella and rotary motors of bacteria will be used in order to give the nano-machine the ability to swim in the forward direction. Whereas, chemoreceptors will allow the nano-machine to sense the concentration of attractants, $c(t)$, present in the environment in every time instant. A different kind of receptor, e.g., ion channels for calcium signaling, will allow the device to sense the control signal $b(t)$. The device has the storage and process units that make the required computations in order to allow the device to behave following the automaton model explained in Section 7.3. Finally, the

process unit transmits the output signals to the control unit that transduce these signal to the biological domain making the rotary motor either to spin or not.

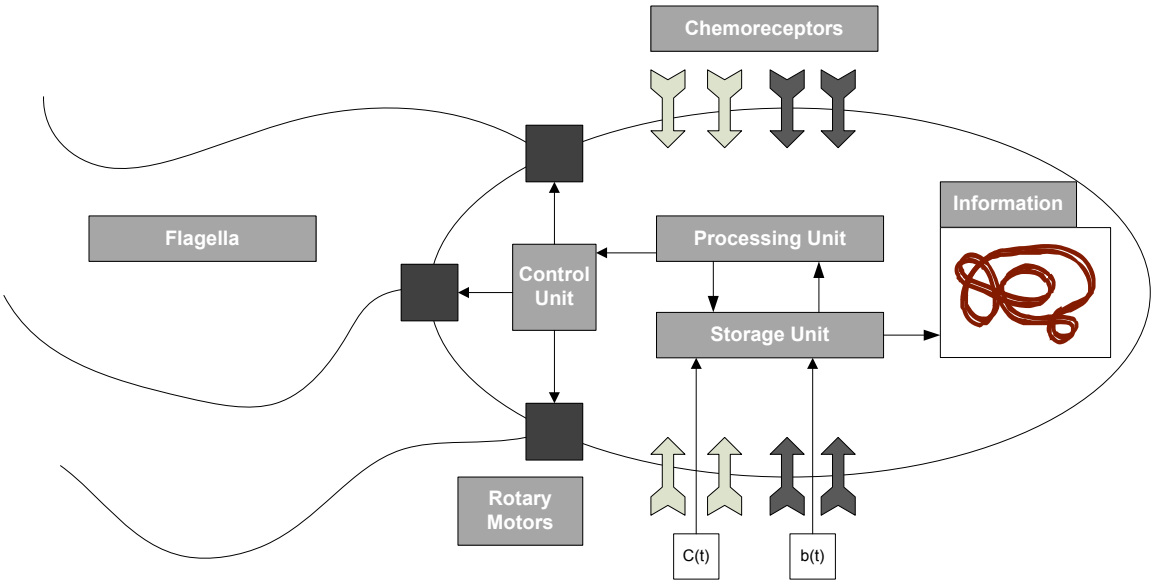


Figure 7.7: A single nano-machine based on a flagellated bacterium.

Hence, as shown in Figure 3.2, the communication process between two nodes of the network is composed by following five steps:

### 7.4.1 Encoding

At the beginning, the communicating machine is attached to the transmitter node in the stop state. When the transmitter has a new communication to be done sends the sequence $b(t) = s_2$ through the control channel. This sequence is detected by the communicating machine which automatically changes to the programming state. Then, the receiver encodes the information that must be sent in the desired format. The information can be expressed as a set of DNA base pairs. In this case, the information can be encoded inside the communicating machine by means of a pilus, in a similar way that the used for bacteria to exchange genetic material (See Section 3.1.4). Otherwise, short-range techniques can be used to transmit the desired information to the communicating nano-machine using the channel $b(t)$.

### 7.4.2 Transmission

The transmitter node sends to the communicating machine the address of the receiver, thus, the frequency at which the receiver is modulating the concentration of attractant particles that is releasing to the environment. The address is used to define the impulse response of the filter $h(n)$. The impulse response is stored in the storage unit and will be used to compute the probability to change from the run to the tumble state, as explained in Section 7.3.2.

Finally, the transmitter node sends the sequence $b(t) = s_3$ to the communicating machine, which triggers a change on the internal state of the machine from programming to run. This internal change is transduced by the control unit to the rotary motors. Hence, the communicating machine starts running towards the receiver, in other words, the information have been transmitted.

### 7.4.3 Propagation

The propagation from the transmitter to the receiver is done by means of an alternation on the running and tumbling states. As happened with bacteria, the communicating machine will arrive to the receiver because of the bias on the run length. The run length when the machine is going in the right direction is longer than the run length when the device is moving in a wrong direction. When the machine is running, it senses the concentration in the environment and stores the observed levels of concentration on the storage unit. Then, the convolution of the concentration $c(n)$ with the impulse response $h(n)$ is done in the process unit. The Doppler Effect is also taken into account in the process unit, which computes $z(t)$ as explained in Section 7.3.2.

This signal $z(t)$ is the mean run length and is used to compute the probability to change from run to tumble. When the device tumbles, a signal is sent to the control unit that transduces that signal to the rotary motors. Then, the machine tumbles for a period of time where the angle suffers a change given by (7.11), and then, the machine starts running again.

### 7.4.4 Reception

Eventually, the communicating machine will arrive close to the receiver and will be able to sense the sequence $b(t) = s_1$ through the control channel. Then, the device moves to the stop state and remains attached to the receiver.

### 7.4.5 Decoding

Once the communicating machine is in the receiver node, it transmits the information to the node. As happened with the encoding, this can be done either by means of a pilus or using short-range techniques, i.e., calcium signaling, in the channel $b(t)$.

The device will remain stopped in the receiver node until this node needs to send a message to another node of the network. And then, the communication process starts over again.

# Chapter 8

# Comparison of Medium-Range Techniques

Both methods show different characteristics and properties that clearly differentiate them. In our opinion, the mechanism to be used must be chosen depending on the environment where the communication is taking place and the communication requirements. The following characteristics will help to determine the selection:

- **Packet size:** When using a flagellated bacterium, the information is introduced in its cytoplasm by means of plasmids, bacteriophages or BACs. BACs allow the encoding of up to 300.000 base pairs of DNA inside the plasmid. Taking into account that the DNA is a quaternary alphabet, this means 600 Kbits. On the other hand, catalytic nanomotors, as Au/Ni/Au/Ni/Pt nanorods, allow encoding up to 64 K bases of DNA, thus 128 Kbits of information on each rod. If rafts of nanorods are built, much more information can be encoded and transported.
- **Diversity:** Bacteria, as a living organism, have spent several billion years developing efficient skills and machinery. For instance, self-reproduction is a process that will be useful when dealing with communication because it is a natural and autonomous way of generating redundancy of the message. Redundancy is obtained both by transmitting several bacteria containing the same information, which does not have any added cost, and by self-reproduction of the carrier bacterium during propagation. Redundancy offers two great advantages. First, a dramatic reduction of the probability of losing a packet. Second, the propagation time is reduced because it is determined by the fastest bacterium.

- **The medium:** Bacteria can be useful when dealing with biomedicine because E. coli is an inoffensive bacterium that lives in the human intestinal tract [5]. However, this bacterium can be dangerous if it is placed outside the intestinal tract, e.g., in the blood torrent. On the other hand, catalytic nanomotors must be introduced in a hydrogen peroxide solution in order to achieve mobility. Therefore, they might be useful for other types of applications, for instance, they could be used as busses to interconnect several parts of DNA computing machines [20].

- **Propagation:** Catalytic nanomotors can be externally directed by magnetic fields, thus the transport of the information can be directed and tracked. If every communication channel is tracked in real time and the magnetic field adjusted depending on the position of the nanorod, really small propagation times could be achieved. However, we have assumed that this will not be feasible, or at least difficult, when there are lots of different communication channels. For this reason, the estimated propagation time does not require an external control of the nanorod, producing long delays. Catalytic nanomotors can also achieve chemotactic behavior by using a raft of nanorods. This produces a decrease in the velocity of the raft when it approaches the target. On the other hand, bacteria move by following a biased random walk model where the preferred direction is the one that leads the bacterium to the receiver. As shown in Figure 8.1, the propagation delay obtained by using flagellated bacteria is between the times obtained using catalytic nanomotors with alignment intervals of 1.2 and 1.8 seconds.

- **Power consumption:** Bacteria do not require external power to move. They just harvest chemical energy in the form of sugars from the environment and use it to power its rotary motors. Catalytic nanomotors also move autonomously with the chemical energy of the environment. However, they require the creation of a magnetic field by the network nodes. As we mentioned in previous chapters, the available power in the nodes is an open research issue that affects directly to the propagation time.

- **Errors:** When using bacteria as communication mechanism, mutations are the main source of errors inside the packet. Mutations are permanent changes in the genome of a certain organism produced by copying errors during cell division process. Hence, the *symbol error probability* is proportional with the *mutation rate* that in bacteria cells is

around $10^{-8}$ errors per base pair per generation [10]. Concerning the catalytic nanomotors, errors will be produced by chemical reactions of the DNA packet with other molecules present in the environment. These chemical interactions can be considered as *additive noise* of the channel.

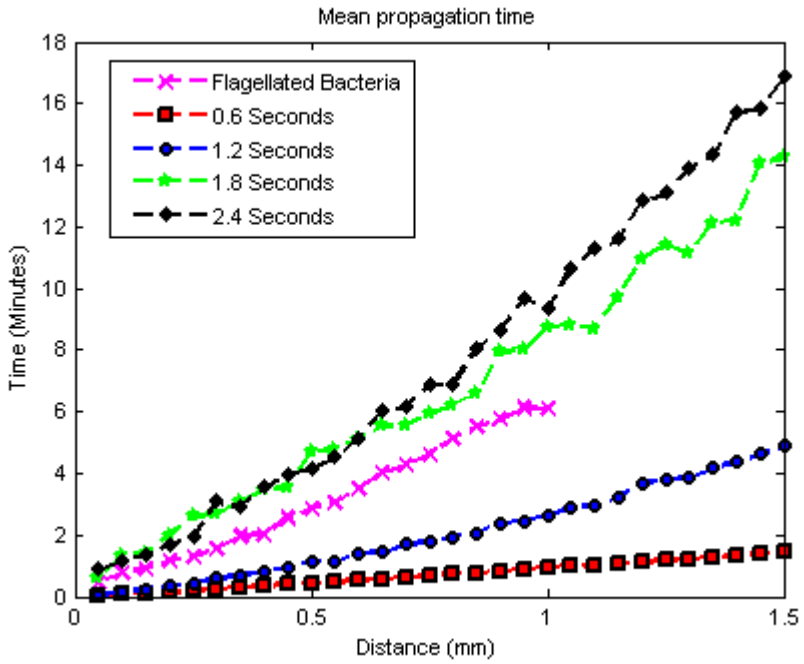


Figure 8.1: Comparison of the propagation time

# Chapter 9

# Open Issues and Conclusions

## 9.1 Open Issues in NanoNetworks

The main challenge by the ICT community in the upcoming years is the development of a NanoNetwork Simulator. This simulator must be able to properly model the NanoNetwork devices (nano-machines and gateways), the molecular communication processes, the network traffic and the noise sources.

In order to achieve this, the first step is the development of physical channel models for the different molecular communication techniques. In [40] a physical channel model for molecular signaling has been developed. This model is valid both for short-range, i.e., calcium signaling, and long-range, i.e., pheromones, techniques. In this Master Thesis, a physical channel model has been developed for medium-range techniques. Hence, the first issue that must be addressed is the development of a physical channel model for Molecular Motors.

The integration of the different models will allow the evaluation of the NanoNetwork architecture and will ease the detection and correction of the bottlenecks of the network. Then, with this simulation tool, it will be possible to analyze different modulation techniques and codification schemes as well as evaluate the network under different traffic loads. This will lead to an expression of the overall channel capacity.

The NanoNetwork simulator must also take into account the noise sources. The noise sources in the nano scale must be identified and classified. For instance, DNA mutations and chemical interactions through the channel produce a degradation of the received information. After the identification of the different source of noise, some detection and correction techniques must be

developed in order to recover the original message and, hence, to minimize the number of errors in the channel.

Moreover, some Channel Access Techniques, Medium Access Control (MAC) protocols and Routing techniques must be developed.

Finally, further research is also required in order to find new communication techniques that allow the transport of information throughout all the parts of the body, for instance through the blood torrent. This will allow the creation of bio-sensor networks able to collect information throughout different parts of the body and take the appropriate measures.

Only by exploiting the required synergies among the biological, technological and ICT research communities, we will be able to obtain novel molecular engineering techniques that will allow the development of such complex and powerful communication networks.

## 9.2 Conclusions

Information and Communication Technologies (ICT) must contribute to the development and intercommunication of new devices in the nano-scale. Several strategies can be followed when dealing with nano-communication. Molecular communication, which is based in the encoding and transmission of the information by means of molecules, seems a good path to follow when communication in the nano-scale is intended. Short-range techniques allow the interconnection of devices in the nano-scale. However, they still have important drawbacks, for instance they are considerably slow when the range between emitter and receiver is bigger than a few μm.

In this work, a molecular network architecture and two new medium-range techniques, namely, Flagellated Bacteria and Catalytic Nanomotors, have been proposed in order to allow the interconnection of devices deployed over different distances. A physical channel model, in terms of propagation delay and probability of losing a packet, has been obtained in order to evaluate the medium-range techniques. The results show that the propagation delays are on the order of magnitude of a few minutes, i.e., Flagellated Bacteria require around 6 minutes to reach a receiver placed at a distance of 1mm from the transmitter, when Catalytic Nanomotors require around 9 minutes (When the alignment interval is 1.8 seconds). These techniques present high propagation delays, but at the same time, they allow the encoding of a lot of information. This fact compensates the high delays leading to the required Bit-Rates by nano-machines. For

instance, when BAC's are used to encode the information the packet size is 600 Kbits. Taking the propagation delay as 6 minutes, the Bit-Rate is:

$$R = \frac{600\ Kbits}{6\ min} = \frac{600\ Kbits}{6\ \cdot 60\ sec} = 1.67\ b/sec$$

Moreover, a communicating nano-machine has been proposed. This nano-machine is programmed as a finite state automaton and it will carry messages among nodes of the NanoNetwork. The finite state automaton of the communicating nano-machine is an improved version of the two-state automaton model of a flagellated bacterium. This will allow the reduction of the propagation time and an increase of the Bit-Rate.

We conclude that the techniques proposed in this work fill in the existing gap between short-range and long-range molecular communication techniques, while being able to fulfill the Bit-Rates requirements of nano-machines.

# Appendix A

## Demonstration of expression of the angle α

As explained in Chapter 7, the sensed frequency $f_s$ is given by:

$$f_s(\rho) = f_0\left(1 + \frac{v_p}{A}\,\rho\right)$$

where $v_\rho$ is the projection of the velocity of the nano-machine in the straight line that leads the machine to the receiver, A is a constant, $\rho$ is the distance that separates the nano-machine and the receiver, and $f_0$ is the frequency at which the receiver is releasing the particles.

Let the machine make the difference between two different samples of the sensed frequency $f_s(\rho_1)$ and $f_s(\rho_2)$. Expressing the distance in the second sample as a function of the distance in the first sample, the velocity and the time between both samples, $\rho_2 = \rho_1 - v_\rho \Delta t$, we obtain that:

$$\frac{A}{f_0}[f_s(\rho_2) - f_s(\rho_1)] = \left[A + v_\rho(\,\rho_1 - v_\rho \Delta t\,)\right] - [A + v_\rho\,\rho_1]$$

$$\frac{A}{f_0}[f_s(\rho_2) - f_s(\rho_1)] = -{v_\rho}^2 \Delta t$$

The projection of the velocity in the radial direction $v_\rho$ can be expressed as the original velocity $v_0 = 20\ \mu m/sec$ multiplied by the cosine of the angle α:

$${v_\rho}^2 = (v_0 \cos\alpha)^2 = \frac{A}{f_0\,\Delta t}[f_s(\rho_2) - f_s(\rho_1)]$$

$$(\cos\alpha)^2 = \frac{-A}{f_0\,\Delta t\,{v_0}^2}[f_s(\rho_2) - f_s(\rho_1)]$$

$$\cos\alpha = \pm\sqrt{\frac{-A}{f_0\,\Delta t\,{v_0}^2}[f_s(\rho_2) - f_s(\rho_1)]}$$

$$\cos\alpha = \begin{cases} \sqrt{\dfrac{-A}{f_0\,\Delta t\,{v_0}^2}\,[f_s(\rho_2) - f_s(\rho_1)]}, & f_s(\rho_i) > f_0 \\ -\sqrt{\dfrac{-A}{f_0\,\Delta t\,{v_0}^2}\,[f_s(\rho_2) - f_s(\rho_1)]}, & f_s(\rho_i) < f_0 \end{cases}$$

Notice that, as shown in Figure 7.6, the difference $[f_s(\rho_2) - f_s(\rho_1)]$ is always negative, making inside of the root positive.

# Appendix B

## Implemented Code for Flagellated Bacteria Simulation

```
function [ seconds] = main( x_des,y_des,SIM_SIZE)

%   This function returns the time(in seconds) required by a bacteria
to go from the
%   emitter placed at X=Y=1mm to a receiver place at x_des,y_des.
%
%   SIM_SIZE is the maximum time that the bacterium has to reach the
receiver.
%   If the bacterium does not reach it, the packet is lost.
% Hence, the max time is SIM_SIZE/DELTA_t seconds


load results_calc_g;
load concen;
%conce returns the vector of concentrations as a function of the
distance
%and deltadeltaS the increase on distance between the elements of the
%vector concen.


%tra(:,1) x position
%tra(:,2) y position
%tra(:,3) angle
%conc concentration
%State is either run (State=0) or tumble (state =1 )



%% Initial conditions
%Conditions
state=0;
t=0;
v=20e-6;
DELTA_t=0.01;
change=0;
count=1;

%initial position of the emitter
tra=zeros(2,3);
tra(1,1)=1e-3;
tra(2,1)=1e-3;
tra(1,2)=1e-3;
tra(2,2)=1e-3;
```

```
ipos=3;
conc=zeros(1,2);
tumbling=zeros(1,2);
deltaS=20e-6;
spline1;
%spline1 returns the impulse response of the bacteria
c=zeros(1,601);


%% Bacteria simulation

for m=3:SIM_SIZE

    % dist is the distance between the reciever and the bacteria
    dist=sqrt((x_des-tra(ipos-1,1))^2+(y_des-tra(ipos-1,2))^2);
    % dist_norm is the distance in terms of steps of 50um, used in the
calculation of alfa
    % where alfa is the tumbling rate
    dist_norm=dist/(50e-6);
    %Stop if it arrives to destination
   if (dist<15e-6)
       break;
   end

    t= t + DELTA_t ;
    if state==0
        %state=0 running

        %Calc concentration

        tumbling(m)=0;
        conc(m)= concen(round(dist/deltadeltaS +1));

            if(m>601)
                c=conc((m-600):m);
            else
                c(602-m:601)=conc(1:m);
            end
            %pruntumble computes the probability that determine if the
% bacterium must  change to the tumble state (cha)
            pruntumble;
            count=count+1;

        if (change==1)
            %change to tumble
            state=1;
            t=0;
            %calculate the new position and angle
            [tra(ipos,1),tra(ipos,2),tra(ipos,3)]=newpos(tra(ipos-
1,1),tra(ipos-1,2),tra(ipos-1,3),v, DELTA_t);
```

```
            %computes the time in tumbling state
            time_tumbling=exprnd(0.1);
        else
            %continue running
            %calculate the new position and angle
            [tra(ipos,1),tra(ipos,2),tra(ipos,3)]=newpos(tra(ipos-
1,1),tra(ipos-1,2),tra(ipos-1,3),v, DELTA_t);

        end
        ipos=ipos+1;
    else
        tumbling(m)=1;
        %state=1 tumbling
        conc(m)= concen(round(dist/deltadeltaS +1));

        if (t>time_tumbling)
            %change to run
            change=0;
            t=0;
            state=0;
            tra(ipos,1)=tra(ipos-1,1);
            tra(ipos,2)=tra(ipos-1,2);
            tra(ipos,3)=changeangle+tra(ipos-1,3);
            ipos=ipos+1;
        else

            %continue stopped

        end
    end
end

iteration=m;
seconds=m*0.01;
minutes=seconds/60;
```

```
function [xx yy angleangle] = newpos( x,y,angle,v,DELTA_t )
%NEWPOS Retutns the new position and angle of the bacteria.
%   The new position (xx,yy) is determined by the angle (angle) the
%   velocity (v), the time increment (DELTA_t) and the previous
position (x,y)
%
%   The new angle (angleangle) is computed by applying Rotational
Difussion
%   to the previous angle (angle)

%   Rotational diffusion
%   Small Random changes in direction due to Brownian motion
%   variance(angle)=2*D*t
%   dt =   sqrt(2*D*DELTA_t)=0.0352
%   where t=deltat=0.01
%   D=0.062;


dt=0.0352;
xx = x+v*cos(angle)*DELTA_t;
yy = y+v*sin(angle)*DELTA_t;
r=dt.*randn(1); %[rad]
angleangle=angle+r; %[rad]


% Edeges of the simulation space
if xx<0
    xx=0;
elseif xx>2e-3
    xx=2e-3;
elseif yy<0
    yy=0;
elseif yy>2e-3
    yy=2e-3;

end
```

# Appendix C

## Implemented Code for Catalytic Nanomotors Simulation

```
function [ seconds] = main( x_des,y_des,SIM_SIZE,alignField)
%   This function returns the time(in seconds) requiered by the
catalytic nanomotor to go from the
%   emitter to the receiver place at x_des,y_des.
%
%   SIM_SIZE is the maximum time that the bacterium has to reach the
receiver.
%   If the  catalytic nanomotor does not reach it, the packet is lost.
%   Hence, the max time is SIM_SIZE/DELTA_t seconds
%   alignField is the alignment interval



%% Initial conditions
%Conditions
% alignField=4; %number of seconds between alignments of the rod and
the field
t=0;
v=20e-6;
DELTA_t=0.1;
anglepath=0;

x_ini=0.1e-3;
y_ini=1e-3;


nalign=alignField/DELTA_t;

%initial position of the emitter
tra=zeros(2,3);
tra(1,1)=x_ini;
tra(2,1)=x_ini;
tra(1,2)=y_ini;
tra(2,2)=y_ini;

%% Nanorod Simulation


for m=3:SIM_SIZE

    %distance between the receiver and the motor
    dist=sqrt((x_des-tra(m-1,1))^2+(y_des-tra(m-1,2))^2);
        %Stop if it arrives to destination
   if (dist<20e-6)
```

```
        break;
    end
    t= t + DELTA_t ;
    align=(mod(m,nalign)==0);
    if align
        % computes the angle of the path
        dy=y_des-tra(m-1,2);
        dx=x_des-tra(m-1,1);
        anglepath=atan(abs(dy)/abs(dx));
        if ((dx<0) && (dy>0))
            anglepath=pi-anglepath;
        elseif  ((dy<0)&&(dx<0))
            anglepath=anglepath+pi;
        elseif ((dy<0) && (dx>0))
            anglepath=2*pi-anglepath;
        end
    end
    %computes the new position
   [tra(m,1),tra(m,2),tra(m,3)]=newpos(tra(m-1,1),tra(m-1,2),tra(m-
1,3),v, DELTA_t, align,anglepath);
end
seconds=t;
minutes=seconds/60;
iteration=m;
```

```
function [xx yy angleangle] = newpos(
x,y,angle,v,DELTA_t,align,anglepath)
%NEWPOS Retutns the new position and angle of the nanorod.
%   The new position (xx,yy) is determined by the angle (angle) the
%   velocity (v), the time increment (DELTA_t) and the previous
position (x,y)
%
%   The new angle (angleangle) is computed by applying the
Directionality
%   factor of the nanorod to the previous angle (angle)

    Direc=0.6; %Directionality without magnetic field

            if (align)
            %     a=stdDirec.*randn(1);
                dif=abs(angle-anglepath);
                if ((dif<pi/2)|| (dif>3*pi/2))
                    angleangle=mod(anglepath,2*pi);
                else
                     angleangle=mod(anglepath+pi,2*pi);
                end

                xx = x+v*cos(angleangle)*DELTA_t;
                yy = y+v*sin(angleangle)*DELTA_t;
            else
                d_desv=acos(Direc)/sqrt(2/DELTA_t);

                a= d_desv.*randn(1);
                xx = x+v*cos(angle)*DELTA_t;
                yy = y+v*sin(angle)*DELTA_t;
                r=dt.*randn(1); %[rad]
                angleangle=mod(angle+a+r,2*pi); %[rad]

            end


    if xx<0
        xx=0;
        angleangle=angle+pi;
    elseif xx>2e-3
        xx=2e-3;
        angleangle=angle+pi;
    elseif yy<0
        yy=0;
        angleangle=angle+pi;
    elseif yy>2e-3
        yy=2e-3;
        angleangle=angle+pi;

    end
```

# Bibliography


[1] L.M. Adleman, "Molecular computation of solutions to combinatorial problems," *Science*, vol. 266, no. 5187, pp. 1021-1024, Nov 1994.

[2] J. Adler, "Chemoreceptors in Bacteria," *Science*, vol. 166, no. 3913, pp. 1588-1597, Dec 1969.

[3] J. Adler, "Chemotaxis in Bacteria," *Annual Review of Biochemistry*, vol. 44, pp. 341-356, 1975.

[4] I.F. Akyildiz, F. Brunetti, and C. Blázquez, "Nanonetworks: A new communication paradigm," *Computer Networks*, vol. 52, no. 12, 2008.

[5] J. Bath and A.J. Turberfield, "DNA nanomachines," *Nature Nanotechnology*, vol. 2, pp. 275-84, May 2007.

[6] H.C. Berg, *E. Coli in Motion: Biological and Medical Physics Biomedical Engineering.*, Elias Greenbaum, Ed.: Springer, 2004.

[7] H.C. Berg, *Random walks in biology*.: Princeton University Press, 1993.

[8] H.C. Berg, "The rotary motor of bacterial flagella," *Annual Review of Biochemistry*, vol. 72, pp. 19-54, 2003.

[9] H.C. Berg and D.A. Brown, "Chemotaxis in Escherichia coli analysed by three-dimensional tracking.," *Nature*, vol. 239, Oct 1972.

[10] F.R. Blattner et al., "The Complete Genome Sequence of Escherichia coli K-12," *Science*, vol. 277, no. 5331, pp. 1453 - 1462, September 19997.

[11] S.M. Block, J.E. Segall, and H.C. Berg, "Impulse Responses in Bacterial Chemotaxis," *Cell*, vol. 31, pp. 215-226, November 1982.

[12] D. Boneh, C. Dunworth, R.J. Lipton, and J. Segall, "On the Computational Power of DNA," *Discrete Applied Mathematics*, vol. 71, pp. 79-94, 1995.

[13] P. Burke, Z. Yu, and S. Li, "Quantitative Theory of Nanowire and Nanotube Antenna Performance," *condmat/0408418*, 2004.

[14] C. Chang, "The highlights in the nano world," *Proceedings of the IEEE 2003*, vol. 91, no.

11, November 2003.

[15] K. Demirok, R. Laocharoensuk, K.M. Manesh, and J. Wang, "Ultrafast Catalytic Alloy Nanomotors," *Angewandte Chemie International Edition*, vol. 47, no. 48, pp. 9349-9351, 2008.

[16] JW Drake, B Charlesworth, D Charlesworth, and JF Crow, "Rates of spontaneous mutation," *Genetics.* , vol. 148, p. 1667–1686, Apr 1998.

[17] K.E. Drexler, *Nanosystems: molecular machinery, manufacturing, and computation*. New York: John Wiley & Sons, 1992.

[18] D.A. Fletcher and J.A. Theriot, "An introduction to cell motility for the physical scientist.," *Phys Biol.*, vol. 1, no. T1-T10, June 2004.

[19] R.A. Freitas, *Nanomedicine, Volume I: Basic Capabilities*.: Landes Biosience, 1999.

[20] H. Goldstein, "The race to the bottom [consumer nanodevice]," *Spectrum, IEEE*, vol. 42, no. 3, pp. 32-39, March 2005.

[21] D.A. Goodenough and D.L. Paul, "Beyond the gap: Functions of unpaired connexon channels," *Nature Reviews, Molecular Cell Biology*, vol. 4, no. 4, pp. 285-294, April 2003.

[22] M. Hazani et al., "DNA-mediated self-assembly of carbon nanotube-based electronic devices," *Chemical Physics Letters*, vol. 391, no. 4-6, pp. 389-392, June 2006.

[23] G.L. Hazelbauer, R.E. Miesibov, and J. Adler, "Escherichia coli mutants defective in chemotaxis toward specific chemicals," *Proceedings of the National Academy of Sciences of the United States of America (PNAS)*, vol. 64, no. 4, pp. 1300-1307, December 1969.

[24] J.E. Hopcroft and J.D. Ullman, *Introduction to automata theory, languages, and computation*. New York, US: ACM SIGACT News, 1979.

[25] R.F. Ismagilov, A. Schwartz, N. Bowden, and G.M. Whitesides, "Autonomous Movement and Self-Assembly," *Angewandte Chemie*, vol. 114, no. 4, pp. 674-676, Feb 2002.

[26] I.S. Johnson, "Human Insulin from Recombinant DNA Technology," *Science, New Series*, vol. 219, no. 4585, pp. 632-637, Feb 1983.

[27] T.R. Kline, W.F. Paxton, T.E. Mallouk, and A. Sen, "Catalytic Nanomotors: Remote-Controlled Autonomous Movement of Striped Metallic Nanorods," *Angewandte Chemie*,

vol. 117, no. 5, pp. 754-756, 2005.

[28] R. Kurzweil. (2001, March) The Law of Accelerating Returns. [Online]. http://www.kurzweilai.net/articles/art0134.html?printable=1

[29] K. Kwok and J. C. Ellenbogen, "Moletronics: future electronics," *Materials Today*, vol. 5, pp. 28-37, Feb 2002.

[30] H. Lee, A.M. Purdon, V. Chu, and R.M. Westervelt, "Controlled assembly of magnetic nanoparticles from magnetotactic bacteria using microelectromagnets arrays," *Nano letters*, vol. 4, no. 5, pp. 995-998, 2004.

[31] G. Lipps, *Plasmids: Current Research and Future Trends*, Georg Lipps, Ed.: Caister Academic Press, 2008.

[32] R.J. Lipton and E.B. Baum, *DNA Based Computers: Proceedings of a Dimacs Workshop April 4, 1995*. Princeton University: AMS Bookstore, 1996.

[33] M. Meyyappan, J Li, J Li, and A. Cassell, "Nanotechnology: An Overview and Integration with MEMS," in *Proceedings of the 19th IEEE International Conference on Micro Electro Mechanical Systems*, Istanbul, 2006, pp. 1-3.

[34] Y. Moritani, S. Hiyama, and T. Suda, "Molecular Communication among Nanomachines Using Vesicles," in *Proceedings NSTI Nanotechnology Conference and Trade Show.*, vol. 2, 2006.

[35] T. Nakano et al., "Molecular communication for nanomachines using intercellular calcium signaling," in *5th IEEE Conference on Nanotechnology*, Irvine, 2005.

[36] D.L. Nelson and M.M. Cox, *Lehninger principles of biochemistry*, 4th ed.: W. H. Freeman and Company, 2005.

[37] W.F. Paxton et al., "Catalytic nanomotors: Autonomous movement of striped nanorods," *Journal of the American Chemical Society*, vol. 126, no. 41, pp. 13424-13431, 2004.

[38] W.F. Paxton, A. Sen, and T.E. Mallouk, "Motility of Catalytic Nanoparticles through Self-Generated Forces," *Chemistry - A European Journal*, vol. 11, no. 22, pp. 6462 - 6470, 2005.

[39] J. Philibert, "One and a half century of diffusion: Fick, Einstein, before and beyond," *Diffusion Fundamentals*, vol. 2, pp. 1.1-1.10, 2005.

[40] M. Pierobon and I.F. Akyildiz, "A Physical Channel Model for Molecular Communication in Nanonetworks," *To appear in IEEE Journal on Selected Areas in Communications (JSAC) on BIO-INSPIRED NETWORKING*, 2008.

[41] E.M. Purcell, "Life at Low Reynolds Number," *American Journal of Physics*, vol. 45, pp. 3-11, 1977.

[42] P. Reimann, "Brownian motors: noisy transport far from equilibrium," Universitaet Augsburg, Accepted for publication in Physics Reports August 2001.

[43] M.C. Roco and W.S. Bainbridge, *Nanotechnology: Societal Implications- Individual Perspectives*. Berlin: National Science Foundation, 2006.

[44] N. Rott, "Note on the History of the Reynolds Number," *Annual Review of Fluid Mechanics*, vol. 22, pp. 1-11, 1990.

[45] A.K. Salem, P.C. Searson, and K.W. Leong, "Multifunctional Nanorods for Gene Delivery," *Nature Materials*, vol. 2, no. 10, pp. 668-671, 2003.

[46] D.J. Schurig et al., "Metamaterial Electromagnetic Cloak at Microwave Frequencies," *Science*, vol. 314, no. 5801, pp. 977 - 980, Nov 2006.

[47] V. Sourjik and H.C. Berg, "Receptor sensitivity in bacterial chemotaxis," *PNAS*, vol. 99, no. 1, pp. 123-127, January 2002.

[48] T. Suda, M. Moore, T. Nakano, R. Egashira, and A. Enomoto, "Exploratory Research on Molecular Communication," in *Genetic and Evolutionary Computation Conference (GECCO)-05,* University of California, Irvine, June 2005.

[49] R.D. Vale, T. Funatsu, D.W. Pierce, and L. Romberg, "Direct observation of single kinesin molecules moving along microtubules," *Nature*, vol. 380, no. 6573, pp. 451-453, Apr 1996.

[50] A.I. Volpert, V.A. Volpert, and V.A. Volpert, *Traveling Wave Solutions of Parabolic Systems*. Providence, Rhode Island: AMS (American Mathematical Society ), 1994.

[51] Y. Wang et al., "Bipolar Electrochemical Mechanism for the Propulsion of Catalytic Nanomotors in Hydrogen Peroxide Solutions," *Langmuir*, vol. 5, no. 22, pp. 10451-10456, December 2006.

[52] J. Wiederman and L. Petru, "Communicating Mobile Nano-Machines and Their Computational Power," Institute of Computer Science. Academy of Sciences of the Czech

Republic, Prague, Technical Report, 2008.

[53] T.D. Wyatt, *Pheromones and Animal Behavior: Communication by Smell and Taste*, T.D Wyatt, Ed., 2003.